

## APPENDIX F

### Exercises

#### 1. Chapter 1: Objectives and Methods of Solid Mechanics

##### 1.1. Defining a problem in solid mechanics

1.1.1. For each of the following applications, outline *briefly*:

- What would you calculate if you were asked to model the component for a design application?
  - What level of detail is required in modeling the geometry of the solid?
  - How would you model loading applied to the solid?
  - Would you conduct a static or dynamic analysis? Is it necessary to account for thermal stresses? Is it necessary to account for temperature variation as a function of time?
  - What constitutive law would you use to model the material behavior?
- 1.1.1.1. A load cell intended to model forces applied to a specimen in a tensile testing machine
  - 1.1.1.2. The seat-belt assembly in a vehicle
  - 1.1.1.3. The solar panels on a communications satellite.
  - 1.1.1.4. A compressor blade in a gas turbine engine
  - 1.1.1.5. A MEMS optical switch
  - 1.1.1.6. An artificial knee joint
  - 1.1.1.7. A solder joint on a printed circuit board
  - 1.1.1.8. An entire printed circuit board assembly
  - 1.1.1.9. The metal interconnects inside a microelectronic circuit

1.2. What is the difference between a linear elastic stress-strain law and a hyperelastic stress-strain law? Give examples of representative applications for both material models.

1.3. What is the difference between a rate-dependent (viscoplastic) and rate independent plastic constitutive law? Give examples of representative applications for both material models.

1.4. Choose a recent publication describing an application of theoretical or computational solid mechanics from one of the following journals: Journal of the Mechanics and Physics of Solids; International Journal of Solids and Structures; Modeling and Simulation in Materials Science and Engineering; European Journal of Mechanics A; Computer methods in Applied Mechanics and Engineering. Write a short summary of the paper stating: (i) the goal of the paper; (ii) the problem that was solved, including idealizations and assumptions involved in the analysis; (iii) the method of analysis; and (iv) the main results; and (v) the conclusions of the study

## 2. Chapter 2: Governing Equations

### 2.1. Mathematical Description of Shape Changes in Solids

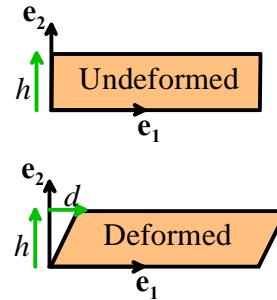
2.1.1. A thin film of material is deformed in simple shear during a plate impact experiment, as shown in the figure.

2.1.1.1. Write down expressions for the displacement field in the film, in terms of  $x_1, x_2$ ,  $d$  and  $h$ , expressing your answer as components in the basis shown.

2.1.1.2. Calculate the Lagrange strain tensor associated with the deformation, expressing your answer as components in the basis shown.

2.1.1.3. Calculate the infinitesimal strain tensor for the deformation, expressing your answer as components in the basis shown.

2.1.1.4. Find the principal values of the infinitesimal strain tensor, in terms of  $d$  and  $h$



2.1.2. Find a displacement field corresponding to a uniform infinitesimal strain field  $\varepsilon_{ij}$ . (Don't make this hard – in particular do not use the complicated approach described in Section 2.1.20. Instead, think about what kind of function, when differentiated, gives a constant). Is the displacement unique?

2.1.3. Find a formula for the displacement field that generates *zero* infinitesimal strain.

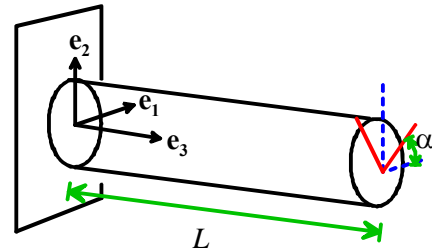
2.1.4. Find a displacement field that corresponds to a uniform Lagrange strain tensor  $E_{ij}$ . Is the displacement unique? Find a formula for the most general displacement field that generates a uniform Lagrange strain.

2.1.5. The displacement field in a homogeneous, isotropic circular shaft twisted through angle  $\alpha$  at one end is given by

$$u_1 = x_1 \left[ \cos \left( \frac{\alpha x_3}{L} \right) - 1 \right] - x_2 \sin \left( \frac{\alpha x_3}{L} \right)$$

$$u_2 = x_1 \sin \left( \frac{\alpha x_3}{L} \right) + x_2 \left[ \cos \left( \frac{\alpha x_3}{L} \right) - 1 \right]$$

$$u_3 = 0$$



2.1.5.1. Calculate the matrix of components of the deformation gradient tensor

2.1.5.2. Calculate the matrix of components of the Lagrange strain tensor. Is the strain tensor a function of  $x_3$ ? Why?

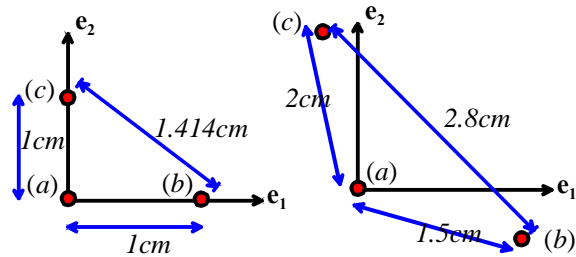
2.1.5.3. Find an expression for the increase in length of a material fiber of initial length  $dl$ , which is on the outer surface of the cylinder and initially oriented in the  $\mathbf{e}_3$  direction.

2.1.5.4. Show that material fibers initially oriented in the  $\mathbf{e}_1$  and  $\mathbf{e}_2$  directions do not change their length.

2.1.5.5. Calculate the principal values and directions of the Lagrange strain tensor at the point  $x_1 = a$ ,  $x_2 = 0$ ,  $x_3 = 0$ . Hence, deduce the orientations of the material fibers that have the greatest and smallest increase in length.

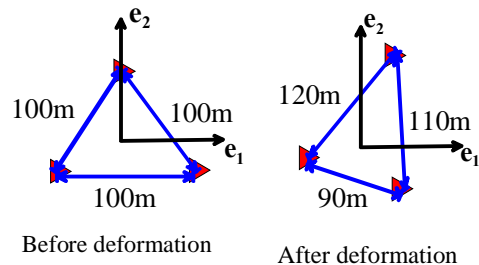
- 2.1.5.6. Calculate the components of the infinitesimal strain tensor. Show that, for small values of  $\alpha$ , the infinitesimal strain tensor is identical to the Lagrange strain tensor, but for finite rotations the two measures of deformation differ.
- 2.1.5.7. Use the infinitesimal strain tensor to obtain estimates for the lengths of material fibers initially oriented with the three basis vectors. Where is the error in this estimate greatest? How large can  $\alpha$  be before the error in this estimate reaches 10%?

2.1.6. To measure the in-plane deformation of a sheet of metal during a forming process, your managers place three small hardness indentations on the sheet. Using a travelling microscope, they determine that the initial lengths of the sides of the triangle formed by the three indents are 1cm, 1cm, 1.414cm, as shown in the picture below. After deformation, the sides have lengths 1.5cm, 2.0cm and 2.8cm. Your managers would like to use this information to determine the in-plane components of the Lagrange strain tensor. Unfortunately, being business economics graduates, they are unable to do this.



- 2.1.6.1. Explain how the measurements can be used to determine  $E_{11}$ ,  $E_{22}$ ,  $E_{12}$  and do the calculation.
- 2.1.6.2. Is it possible to determine the deformation gradient from the measurements provided? Why? If not, what additional measurements would be required to determine the deformation gradient?

2.1.7. To track the deformation in a slowly moving glacier, three survey stations are installed in the shape of an equilateral triangle, spaced 100m apart, as shown in the picture. After a suitable period of time, the spacing between the three stations is measured again, and found to be 90m, 110m and 120m, as shown in the figure. Assuming that the deformation of the glacier is homogeneous over the region spanned by the survey stations, please compute the components of the Lagrange strain tensor associated with this deformation, expressing your answer as components in the basis shown.



- 2.1.8. Compose a limerick that will help you to remember the distinction between engineering shear strains and the formal (mathematical) definition of shear strain
- 2.1.9. A rigid body motion is a nonzero displacement field that does not distort any infinitesimal volume element within a solid. Thus, a rigid body displacement induces no strain, and hence no stress, in the solid. The deformation corresponding to a 3D rigid rotation about an axis through the origin is

$$\mathbf{y} = \mathbf{R} \cdot \mathbf{x} \quad \text{or} \quad y_i = R_{ij}x_j$$

where  $\mathbf{R}$  must satisfy  $\mathbf{R} \cdot \mathbf{R}^T = \mathbf{R}^T \cdot \mathbf{R} = \mathbf{I}$ ,  $\det(\mathbf{R}) > 0$ .

- 2.1.9.1. Show that the Lagrange strain associated with this deformation is zero.
- 2.1.9.2. As a specific example, consider the deformation

$$\begin{bmatrix} y_1 \\ y_2 \\ y_3 \end{bmatrix} = \begin{bmatrix} \cos \theta & -\sin \theta & 0 \\ \sin \theta & \cos \theta & 0 \\ 0 & 0 & 1 \end{bmatrix} \begin{bmatrix} x_1 \\ x_2 \\ x_3 \end{bmatrix}$$

This is the displacement field caused by rotating a solid through an angle  $\theta$  about the  $\mathbf{e}_3$  axis. Find the deformation gradient for this displacement field, and show that the deformation gradient tensor is orthogonal, as predicted above. Show also that the infinitesimal strain tensor for this displacement field is not generally zero, but is of order  $\theta^2$  if  $\theta$  is small.

- 2.1.9.3. If the displacements are small, we can find a simpler representation for a rigid body displacement. Consider a deformation of the form

$$y_i = \epsilon_{ijk} \omega_j x_k$$

Here  $\boldsymbol{\omega}$  is a vector with magnitude  $\ll 1$ , which represents an infinitesimal rotation about an axis parallel to  $\boldsymbol{\omega}$ . Show that the infinitesimal strain tensor associated with this displacement is always zero. Show further that the Lagrange strain associated with this displacement field is

$$E_{ij} = \frac{1}{2} (\delta_{ij} \omega_k \omega_k - \omega_i \omega_j)$$

This is not, in general, zero. It is small if all  $\omega_k \ll 1$ .

- 2.1.10. The formula for the deformation due to a rotation through an angle  $\theta$  about an axis parallel to a unit vector  $\mathbf{n}$  that passes through the origin is

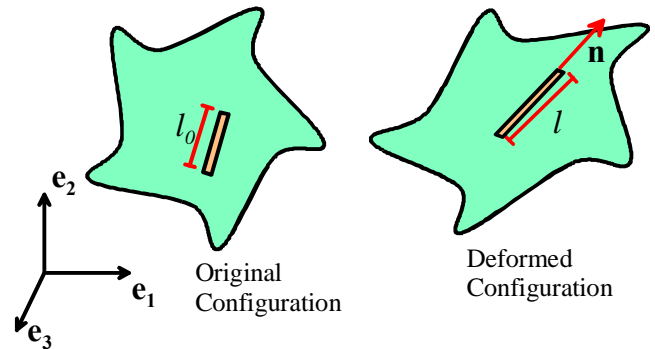
$$y_i = [\cos \theta \delta_{ij} + (1 - \cos \theta) n_i n_j + \sin \theta \epsilon_{ikj} n_k] x_j$$

- 2.1.10.1. Calculate the components of corresponding deformation gradient  
 2.1.10.2. Verify that the deformation gradient satisfies  $F_{ik} F_{jk} = F_{ki} F_{kj} = \delta_{ij}$   
 2.1.10.3. Find the components of the *inverse* of the deformation gradient  
 2.1.10.4. Verify that both the Lagrange strain tensor and the Eulerian strain tensor are zero for this deformation. What does this tell you about the distortion of the material?  
 2.1.10.5. Calculate the Jacobian of the deformation gradient. What does this tell you about volume changes associated with the deformation?

- 2.1.11. In Section 2.1.6 it was stated that the Eulerian strain tensor  $E_{ij}^*$  can be used to relate the length of a material fiber in a deformable solid before and after deformation, using the formula

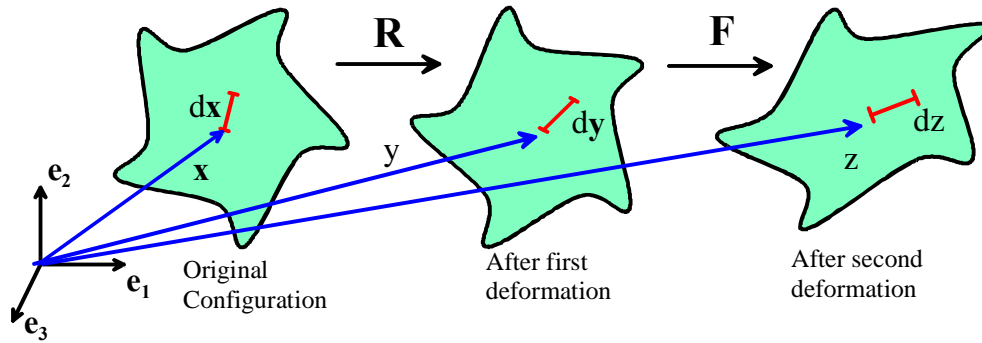
$$\frac{l^2 - l_0^2}{2l^2} = E_{ij}^* n_i n_j$$

where  $n_i$  are the components of a unit vector parallel to the material fiber after deformation. Derive this result.



- 2.1.12. Suppose that you have measured the Lagrange strain tensor for a deformation, and wish to calculate the Eulerian strain tensor. On purely physical grounds, do you think this is possible, without calculating the deformation gradient? If so, find a formula relating Lagrange strain  $E_{ij}$  to Eulerian strain  $E_{ij}^*$ .
- 2.1.13. Repeat problem 2.1.6, but instead of calculating the Lagrange strain tensor, find the components of the Eulerian strain tensor  $E_{ij}^*$  (you can do this directly, or use the results of problem 2.1.12, or both)
- 2.1.14. Repeat problem 2.1.7, but instead of calculating the Lagrange strain tensor, find the components of the Eulerian strain tensor  $E_{ij}^*$  (you can do this directly, or use the results for problem 2.1.12, or both)
- 2.1.15. The Lagrange strain tensor can be used to calculate the change in angle between any two material fibers in a solid as the solid is deformed. In this problem you will calculate the formula that can be used to do this. To this end, consider two infinitesimal material fibers in the undeformed solid, which are characterized by vectors with components  $dx_i^{(1)} = l_1 m_i^{(1)}$  and  $dx_i^{(2)} = l_2 m_i^{(2)}$ , where  $\mathbf{m}^{(1)}$  and  $\mathbf{m}^{(2)}$  are two unit vectors. Recall that the angle  $\theta_0$  between  $\mathbf{m}^{(1)}$  and  $\mathbf{m}^{(2)}$  before deformation can be calculated from  $\cos \theta_0 = m_i^{(1)} m_i^{(2)}$ . Let  $dy_i^{(1)}$  and  $dy_i^{(2)}$  represent the two material fibers after deformation. Show that the angle between  $dy_i^{(1)}$  and  $dy_i^{(2)}$  can be calculated from the formula

$$\cos \theta_1 = \frac{2E_{ij} m_i^{(1)} m_j^{(2)} + \cos \theta_0}{\sqrt{1 + 2E_{ij} m_i^{(1)} m_j^{(1)}} \sqrt{1 + 2E_{ij} m_i^{(2)} m_j^{(2)}}}$$



- 2.1.16. Suppose that a solid is subjected to a sequence of two homogeneous deformations (i) a rigid rotation  $\mathbf{R}$ , followed by (ii) an arbitrary homogeneous deformation  $\mathbf{F}$ . Taking the original configuration as reference, find formulas for the following deformation measures for the final configuration of the solid, in terms of  $\mathbf{F}$  and  $\mathbf{R}$ :
- 2.1.16.1. The deformation gradient
  - 2.1.16.2. The Left and Right Cauchy-Green deformation tensors
  - 2.1.16.3. The Lagrange strain
  - 2.1.16.4. The Eulerian strain.
- 2.1.17. Repeat problem 2.1.16, but this time assume that the sequence of the two deformations is reversed, i.e. the solid is first subjected to an arbitrary homogeneous deformation  $\mathbf{F}$ , and is subsequently subjected to a rigid rotation  $\mathbf{R}$ .

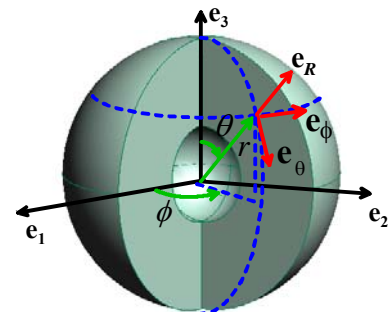
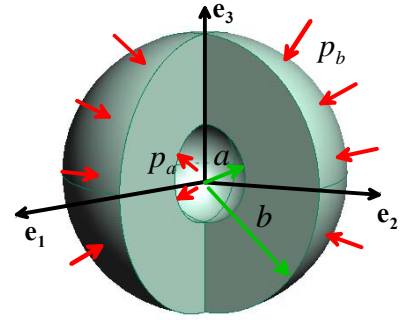
- 2.1.18. A spherical shell (see the figure) is made from an incompressible material. In its undeformed state, the inner and outer radii of the shell are  $A, B$ . After deformation, the new values are  $a, b$ . The deformation in the shell can be described (in Cartesian components) by the equation

$$y_i = \left( R^3 + a^3 - A^3 \right)^{1/3} \frac{x_i}{R} \quad R = \sqrt{x_k x_k}$$

- 2.1.18.1. Calculate the components of the deformation gradient tensor  
 2.1.18.2. Verify that the deformation is volume preserving  
 2.1.18.3. Find the deformed length of an infinitesimal radial line that has initial length  $l_0$ , expressed as a function of  $R$   
 2.1.18.4. Find the deformed length of an infinitesimal circumferential line that has initial length  $l_0$ , expressed as a function of  $R$   
 2.1.18.5. Using the results of 2.1.18.3, 2.1.18.4, find the principal stretches for the deformation.  
 2.1.18.6. Find the *inverse* of the deformation gradient, expressed as a function of  $y_i$ . It is best to do this by working out a formula that enables you to calculate  $x_i$  in terms of  $y_i$  and  $r = \sqrt{y_i y_i}$  and differentiate the result rather than to attempt to invert the result of 10.1.
- 2.1.19. Suppose that the spherical shell described in Problem 2.1.18 is continuously expanding (visualize a balloon being inflated). The rate of expansion can be characterized by the velocity  $v_a = da/dt$  of the surface that lies at  $R=A$  in the undeformed cylinder.
- 2.1.19.1. Calculate the velocity field  $v_i = dy_i/dt$  in the sphere as a function of  $x_i$   
 2.1.19.2. Calculate the velocity field as a function of  $y_i$  (there is a long, obvious way to do this and a quick, subtle way)  
 2.1.19.3. Calculate the time derivative of the deformation gradient tensor calculated in 2.1.18.1.  
 2.1.19.4. Calculate the components of the velocity gradient  $L_{ij} = \frac{\partial v_i}{\partial y_j}$  by differentiating the result of 2.1.19.1  
 2.1.19.5. Calculate the components of the velocity gradient using the results of 2.1.19.3 and 2.1.18.6  
 2.1.19.6. Calculate the stretch rate tensor  $D_{ij}$ . Verify that the result represents a volume preserving stretch rate field.
- 2.1.20. Repeat Problem 2.1.18.1, 2.1.18.6 and all of 2.1.19, but this time solve the problem using spherical-polar coordinates, using the various formulas for vector and tensor operations given in Appendix E. In this case, you may assume that a point with position  $\mathbf{x} = R\mathbf{e}_R$  in the undeformed solid has position vector

$$\mathbf{y} = \left( R^3 + a^3 - A^3 \right)^{1/3} \mathbf{e}_R$$

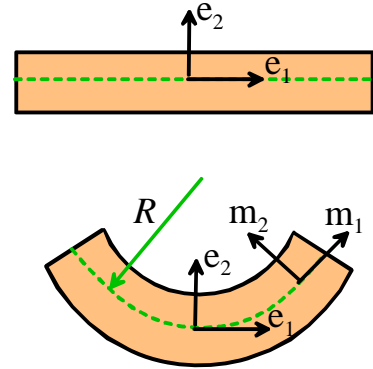
after deformation.



2.1.21. An initially straight beam is bent into a circle with radius  $R$  as shown in the figure. Material fibers that are perpendicular to the axis of the undeformed beam are assumed to remain perpendicular to the axis after deformation, and the beam's thickness and the length of its axis are assumed to be unchanged. Under these conditions the deformation can be described as

$$y_1 = (R - x_2) \sin(x_1 / R) \quad y_2 = R - (R - x_2) \cos(x_1 / R)$$

where, as usual  $\mathbf{x}$  is the position of a material particle in the undeformed beam, and  $\mathbf{y}$  is the position of the same particle after deformation.

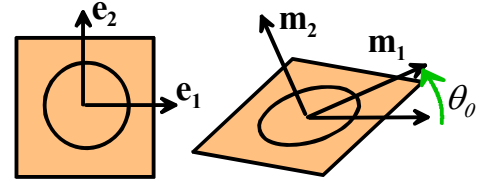


- 2.1.21.1. Calculate the deformation gradient field in the beam, expressing your answer as a function of  $x_1, x_2$ , and as components in the basis  $\{\mathbf{e}_1, \mathbf{e}_2, \mathbf{e}_3\}$  shown.
- 2.1.21.2. Calculate the Lagrange strain field in the beam.
- 2.1.21.3. Calculate the infinitesimal strain field in the beam.
- 2.1.21.4. Compare the values of Lagrange strain and infinitesimal strain for two points that lie at  $(x_1 = 0, x_2 = h)$  and  $(x_1 = L, x_2 = 0)$ . Explain briefly the physical origin of the difference between the two strain measures at each point. Recommend maximum allowable values of  $h/R$  and  $L/R$  for use of the infinitesimal strain measure in modeling beam deflections.
- 2.1.21.5. Calculate the deformed length of an infinitesimal material fiber that has length  $l_0$  and orientation  $\mathbf{e}_1$  in the undeformed beam. Express your answer as a function of  $x_2$ .
- 2.1.21.6. Calculate the change in length of an infinitesimal material fiber that has length  $l_0$  and orientation  $\mathbf{e}_2$  in the undeformed beam.
- 2.1.21.7. Show that the two material fibers described in 2.1.21.5 and 2.1.21.6 remain mutually perpendicular after deformation. Is this true for *all* material fibers that are mutually perpendicular in the undeformed solid?
- 2.1.21.8. Find the components in the basis  $\{\mathbf{e}_1, \mathbf{e}_2, \mathbf{e}_3\}$  of the Left and Right stretch tensors  $\mathbf{U}$  and  $\mathbf{V}$  as well as the rotation tensor  $\mathbf{R}$  for this deformation. You should be able to write down  $\mathbf{U}$  and  $\mathbf{R}$  by inspection, without needing to wade through the laborious general process outlined in Section 2.1.13. The results can then be used to calculate  $\mathbf{V}$ .
- 2.1.21.9. Find the principal directions of  $\mathbf{U}$  as well as the principal stretches. You should be able to write these down using your physical intuition without doing any tedious calculations.
- 2.1.21.10. Let  $\{\mathbf{m}_1, \mathbf{m}_2, \mathbf{m}_3\}$  be a basis in which  $\mathbf{m}_1$  is parallel to the axis of the deformed beam, as shown in the figure. Write down the components of each of the unit vectors  $\mathbf{m}_i$  in the basis  $\{\mathbf{e}_1, \mathbf{e}_2, \mathbf{e}_3\}$ . Hence, compute the transformation matrix  $Q_{ij} = \mathbf{m}_i \cdot \mathbf{e}_j$  that is used to transform tensor components from  $\{\mathbf{e}_1, \mathbf{e}_2, \mathbf{e}_3\}$  to  $\{\mathbf{m}_1, \mathbf{m}_2, \mathbf{m}_3\}$ .
- 2.1.21.11. Find the components of the deformation gradient tensor, Lagrange strain tensor, as well as  $\mathbf{U}$ ,  $\mathbf{V}$  and  $\mathbf{R}$  in the basis  $\{\mathbf{m}_1, \mathbf{m}_2, \mathbf{m}_3\}$ .
- 2.1.21.12. Find the principal directions of  $\mathbf{V}$  expressed as components in the basis  $\{\mathbf{m}_1, \mathbf{m}_2, \mathbf{m}_3\}$ . Again, you should be able to simply write down this result.

- 2.1.22. A sheet of material is subjected to a two dimensional homogeneous deformation of the form

$$y_1 = A_{11}x_1 + A_{12}x_2 \quad y_2 = A_{21}x_1 + A_{22}x_2$$

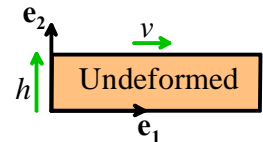
where  $A_{ij}$  are constants. Suppose that a circle of unit radius is drawn on the undeformed sheet. This circle is distorted to a smooth curve on the deformed sheet. Show that the distorted circle is an ellipse, with semi-axes that are parallel to the principal directions of the left stretch tensor  $\mathbf{V}$ , and that the lengths of the semi-axes of the ellipse are equal to the principal stretches for the deformation. There are many different ways to approach this calculation – some are very involved. The simplest way is probably to assume that the principal directions of  $\mathbf{V}$  subtend an angle  $\theta_0$  to the  $\{\mathbf{e}_1, \mathbf{e}_2\}$  basis as shown in the figure, write the polar decomposition  $\mathbf{A} = \mathbf{V} \cdot \mathbf{R}$  in terms of principal stretches  $\lambda_1, \lambda_2$  and  $\theta_0$ , and then show that  $\mathbf{y} = \mathbf{V} \cdot \mathbf{R} \cdot \mathbf{x}$  (where  $\mathbf{x}$  is on the unit circle) describes an ellipse.



- 2.1.23. A solid is subjected to a rigid rotation so that a unit vector  $\mathbf{a}$  in the undeformed solid is rotated to a new orientation  $\mathbf{b}$ . Find a rotation tensor  $\mathbf{R}$  that is consistent with this deformation, in terms of the components of  $\mathbf{a}$  and  $\mathbf{b}$ . Is the rotation tensor unique? If not, find the most general formula for the rotation tensor.

- 2.1.24. In a plate impact experiment, a thin film of material with thickness  $h$  is subjected to a homogeneous shear deformation by displacing the upper surface of the film horizontally with a speed  $v$ .

- 2.1.24.1. Write down the velocity field in the film
- 2.1.24.2. Calculate the velocity gradient, the stretch rate and the spin rate
- 2.1.24.3. Calculate the instantaneous angular velocity of a material fiber parallel to the  $\mathbf{e}_2$  direction in the film
- 2.1.24.4. Calculate the instantaneous angular velocity of a material fiber parallel to  $(\mathbf{e}_1 + \mathbf{e}_2)/\sqrt{2}$
- 2.1.24.5. Calculate the stretch rates for the material fibers in 22.3 and 22.4
- 2.1.24.6. What is the direction of the material fiber with the greatest angular velocity? What is the direction of the material fiber with the greatest stretch rate?



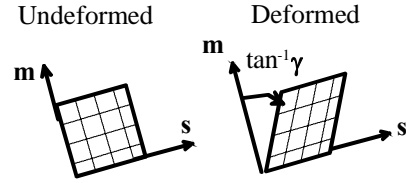
- 2.1.25. The velocity field  $\mathbf{v}$  due to a rigid rotation about an axis through the origin can be characterized by a skew tensor  $\mathbf{W}$  or an angular velocity vector  $\boldsymbol{\omega}$  defined so that

$$\mathbf{v} = \mathbf{W} \cdot \mathbf{x} \quad \mathbf{v} = \boldsymbol{\omega} \times \mathbf{x}$$

Find a formula relating the components of  $\mathbf{W}$  and  $\boldsymbol{\omega}$ . (One way to approach this problem is to calculate a formula for  $\mathbf{W}$  by taking the time derivative of Rodriguez formula – see Sect 2.1.1).



- 2.1.26. A single crystal deforms by shearing on a single active slip system as illustrated in the figure. The crystal is loaded so that the slip direction  $\mathbf{s}$  and normal to the slip plane  $\mathbf{m}$  maintain a constant direction during the deformation



- 2.1.26.1. Show that the deformation gradient can be expressed in terms of the components of the slip direction  $\mathbf{s}$  and the normal to the slip plane  $\mathbf{m}$  as

$F_{ij} = \delta_{ij} + \gamma s_i m_j$  where  $\gamma$  denotes the shear, as illustrated in the figure.

- 2.1.26.2. Suppose shearing proceeds at some rate  $\dot{\gamma}$ . At the instant when  $\gamma = 0$ , calculate (i) the velocity gradient tensor; (ii) the stretch rate tensor and (iii) the spin tensor associated with the deformation.

- 2.1.27. The properties of many rubbers and foams are specified by functions of the following invariants of the left Cauchy-Green deformation tensor  $B_{ij} = F_{ik} F_{jk}$ .

$$I_1 = \text{trace}(\mathbf{B}) = B_{kk}$$

$$I_2 = \frac{1}{2} (I_1^2 - \mathbf{B} \cdot \mathbf{B}) = \frac{1}{2} (I_1^2 - B_{ik} B_{ki})$$

$$I_3 = \det \mathbf{B} = J^2$$

Invariants of a tensor are defined in Appendix B – they are functions of the components of a tensor that are independent of the choice of basis.

- 2.1.27.1. Verify that  $I_1, I_2, I_3$  are invariants. The simplest way to do this is to show that  $I_1, I_2, I_3$  are unchanged during a change of basis.

- 2.1.27.2. In order to calculate stress-strain relations for these materials, it is necessary to evaluate derivatives of the invariants. Show that

$$\frac{\partial I_1}{\partial F_{ij}} = 2F_{ij}, \quad \frac{\partial I_2}{\partial F_{ij}} = 2(I_1 F_{ij} - B_{ik} F_{kj}), \quad \frac{\partial I_3}{\partial F_{ij}} = 2I_3 F_{ji}^{-1}$$

- 2.1.28. The infinitesimal strain field in a long cylinder containing a hole at its center is given by

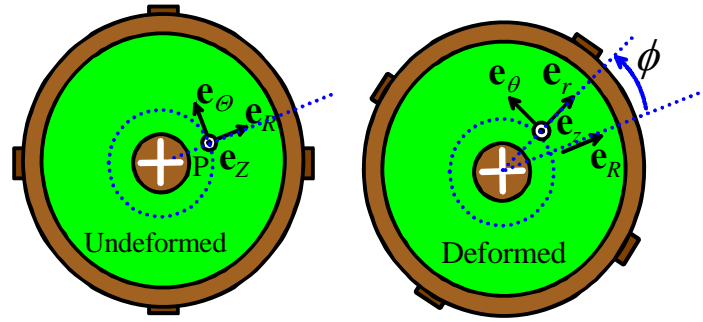
$$\varepsilon_{31} = -bx_2/r \quad \varepsilon_{31} = bx_1/r \quad r = \sqrt{x_1^2 + x_2^2}$$

- 2.1.28.1. Show that the strain field satisfies the equations of compatibility.

- 2.1.28.2. Show that the strain field is consistent with a displacement field of the form  $u_3 = \theta$ , where

$\theta = b \tan^{-1} x_2 / x_1$ . Note that although the strain field is compatible, the displacement field is *multiple valued* – i.e. the displacements are not equal at  $\theta = 2\pi$  and  $\theta = 0$ , which supposedly represent the same point in the solid. Surprisingly, displacement fields like this do exist in solids – they are caused by dislocations in a crystal. These are discussed in more detail in Sections 5.3.4

2.1.29. The figure shows a test designed to measure the response of a polymer to large shear strains. The sample is a hollow cylinder with internal radius  $a_0$  and external radius  $a_1$ . The inside diameter is bonded to a fixed rigid cylinder. The external diameter is bonded inside a rigid tube, which is rotated through an angle  $\alpha(t)$ . Assume that the specimen deforms as indicated in the figure, i.e. (a) cylindrical sections remain cylindrical; (b) no point in the specimen moves in the axial or radial directions; (c) that a cylindrical element of material at radius  $R$  rotates through angle  $\phi(R, t)$  about the axis of the specimen. Take the undeformed configuration as reference. Let  $(R, \Theta, Z)$  denote the cylindrical-polar coordinates of a material point in the reference configuration, and let  $\{\mathbf{e}_R, \mathbf{e}_\Theta, \mathbf{e}_Z\}$  be cylindrical-polar basis vectors at  $(R, \Theta, Z)$ . Let  $(r, \theta, z)$  denote the coordinates of this point in the deformed configuration, and let  $\{\mathbf{e}_r, \mathbf{e}_\theta, \mathbf{e}_z\}$  by cylindrical-polar basis vectors located at  $(r, \theta, z)$ .



(a) cylindrical sections remain cylindrical; (b) no point in the specimen moves in the axial or radial directions; (c) that a cylindrical element of material at radius  $R$  rotates through angle  $\phi(R, t)$  about the axis of the specimen. Take the undeformed configuration as reference. Let  $(R, \Theta, Z)$  denote the cylindrical-polar coordinates of a material point in the reference configuration, and let  $\{\mathbf{e}_R, \mathbf{e}_\Theta, \mathbf{e}_Z\}$  be cylindrical-polar basis vectors at  $(R, \Theta, Z)$ . Let  $(r, \theta, z)$  denote the coordinates of this point in the deformed configuration, and let  $\{\mathbf{e}_r, \mathbf{e}_\theta, \mathbf{e}_z\}$  by cylindrical-polar basis vectors located at  $(r, \theta, z)$ .

- 2.1.29.1. Write down expressions for  $(r, \theta, z)$  in terms of  $(R, \Theta, Z)$  (this constitutes the deformation mapping)
- 2.1.29.2. Let P denote the material point at  $(R, \Theta, Z)$  in the reference configuration. Write down the reference position vector  $\mathbf{X}$  of P, expressing your answer as components in the basis  $\{\mathbf{e}_R, \mathbf{e}_\Theta, \mathbf{e}_Z\}$ .
- 2.1.29.3. Write down the deformed position vector  $\mathbf{x}$  of P, expressing your answer in terms of  $(R, \Theta, Z)$  and basis vectors  $\{\mathbf{e}_R, \mathbf{e}_\Theta, \mathbf{e}_Z\}$ .
- 2.1.29.4. Find the components of the deformation gradient tensor  $\mathbf{F}$  in  $\{\mathbf{e}_R, \mathbf{e}_\Theta, \mathbf{e}_Z\}$ . (Recall that the gradient operator in cylindrical-polar coordinates is  $\nabla = (\mathbf{e}_R \frac{\partial}{\partial R} + \mathbf{e}_\Theta \frac{1}{R} \frac{\partial}{\partial \Theta} + \mathbf{e}_Z \frac{\partial}{\partial Z})$ ; recall also that  $\frac{\partial \mathbf{e}_R}{\partial \Theta} = \mathbf{e}_\Theta$ ;  $\frac{\partial \mathbf{e}_\Theta}{\partial \Theta} = -\mathbf{e}_R$ )
- 2.1.29.5. Show that the deformation gradient can be decomposed into a sequence  $\mathbf{F} = \mathbf{R} \cdot \mathbf{S}$  of a simple shear  $\mathbf{S}$  followed by a rigid rotation through angle  $\phi$  about the  $\mathbf{e}_Z$  direction  $\mathbf{R}$ . In this case the simple shear deformation will have the form

$$\mathbf{S} = \mathbf{e}_R \mathbf{e}_R + \mathbf{e}_\Theta \mathbf{e}_\Theta + \mathbf{e}_Z \mathbf{e}_Z + k \mathbf{e}_\Theta \mathbf{e}_R$$

where  $k$  is to be determined.

- 2.1.29.6. Find the components of  $\mathbf{F}$  in  $\{\mathbf{e}_r, \mathbf{e}_\theta, \mathbf{e}_z\}$ .
- 2.1.29.7. Verify that the deformation is volume preserving (i.e. check the value of  $J = \det(\mathbf{F})$ )
- 2.1.29.8. Find the components of the right Cauchy-Green deformation tensors in  $\{\mathbf{e}_R, \mathbf{e}_\Theta, \mathbf{e}_Z\}$
- 2.1.29.9. Find the components of the left Cauchy-Green deformation tensor in  $\{\mathbf{e}_r, \mathbf{e}_\theta, \mathbf{e}_z\}$
- 2.1.29.10. Find  $\mathbf{F}^{-1}$  in  $\{\mathbf{e}_R, \mathbf{e}_\Theta, \mathbf{e}_Z\}$ .
- 2.1.29.11. Find the principal values of the stretch tensor  $\mathbf{U}$
- 2.1.29.12. Write down the velocity field  $\mathbf{v}$  in terms of  $(r, \theta, z)$  in the basis  $\{\mathbf{e}_r, \mathbf{e}_\theta, \mathbf{e}_z\}$
- 2.1.29.13. Calculate the spatial velocity gradient  $\mathbf{L}$  in the basis  $\{\mathbf{e}_r, \mathbf{e}_\theta, \mathbf{e}_z\}$

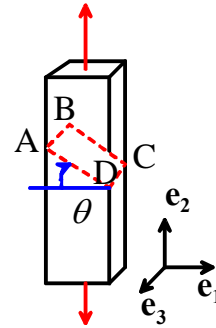
## 2.2. Mathematical Description of internal forces in solids in Solids

2.2.1. A rectangular bar is loaded in a state of uniaxial tension, as shown in the figure.

2.2.1.1. Write down the components of the stress tensor in the bar, using the basis vectors shown.

2.2.1.2. Calculate the components of the normal vector to the plane ABCD shown, and hence deduce the components of the traction vector acting on this plane, expressing your answer as components in the basis shown, in terms of  $\theta$

2.2.1.3. Compute the normal and tangential tractions acting on the plane shown.

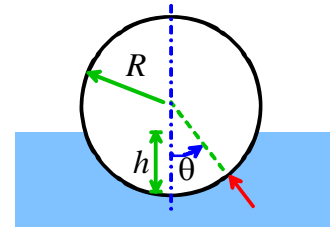


2.2.2. Consider a state of hydrostatic stress  $\sigma_{ij} = p\delta_{ij}$ . Show that the traction vector acting on any internal plane in the solid (or, more likely, fluid!) has magnitude  $p$  and direction normal to the plane.

2.2.3. A cylinder of radius  $R$  is partially immersed in a static fluid.

2.2.3.1. Recall that the pressure at a depth  $d$  in a fluid has magnitude  $\rho g d$ . Write down an expression for the horizontal and vertical components of traction acting on the surface of the cylinder in terms of  $\theta$ .

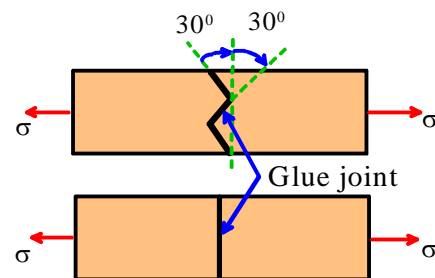
2.2.3.2. Hence compute the resultant force exerted by the fluid on the cylinder.



2.2.4. The figure shows two designs for a glue joint. The glue will fail if the stress acting normal to the joint exceeds 60 MPa, or if the shear stress acting parallel to the plane of the joint exceeds 300 MPa.

2.2.4.1. Calculate the normal and shear stress acting on each joint, in terms of the applied stress  $\sigma$

2.2.4.2. Hence, calculate the value of  $\sigma$  that will cause each joint to fail.



2.2.5. For the Cauchy stress tensor with components

$$\begin{bmatrix} 100 & 250 & 0 \\ 250 & 200 & 0 \\ 0 & 0 & 300 \end{bmatrix}$$

compute

2.2.5.1. The traction vector acting on an internal material plane with normal  $\mathbf{n} = \frac{1}{\sqrt{2}}\mathbf{e}_1 - \frac{1}{\sqrt{2}}\mathbf{e}_2$

2.2.5.2. The principal stresses

2.2.5.3. The hydrostatic stress

2.2.5.4. The deviatoric stress tensor

2.2.5.5. The Von-Mises equivalent stress

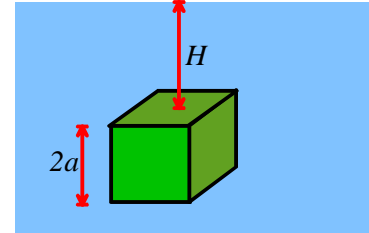
2.2.6. Show that the hydrostatic stress  $\sigma_{kk}$  is invariant under a change of basis – i.e. if  $\sigma_{ij}^{\mathbf{e}}$  and  $\sigma_{ij}^{\mathbf{m}}$  denote the components of stress in bases  $\{\mathbf{e}_1, \mathbf{e}_2, \mathbf{e}_3\}$  and  $\{\mathbf{m}_1, \mathbf{m}_2, \mathbf{m}_3\}$ , respectively, show that  $\sigma_{kk}^{\mathbf{e}} = \sigma_{kk}^{\mathbf{m}}$ .

2.2.7. A rigid, cubic solid is immersed in a fluid with mass density  $\rho$ .

Recall that a stationary fluid exerts a compressive pressure of magnitude  $\rho gh$  at depth  $h$ .

2.2.7.1. Write down expressions for the traction vector exerted by the fluid on each face of the cube. You might find it convenient to take the origin for your coordinate system at the center of the cube, and take basis vectors  $\{\mathbf{e}_1, \mathbf{e}_2, \mathbf{e}_3\}$  perpendicular to the cube faces.

2.2.7.2. Calculate the resultant force due to the tractions acting on the cube, and show that the vertical force is equal and opposite to the weight of fluid displaced by the cube.



2.2.8. Show that the result of problem 2.2.7 applies to any arbitrarily shaped solid immersed below the surface of a fluid, i.e. prove that the resultant force acting on an immersed solid with volume  $V$  is

$$\mathbf{P}_i = \rho g V \delta_{i3}, \text{ where it is assumed that } \mathbf{e}_3 \text{ is vertical. To do this}$$

2.2.8.1. Let  $n_j$  denote the components of a unit vector normal to the surface of the immersed solid

2.2.8.2. Write down a formula for the traction (as a vector) exerted by the fluid on the immersed solid

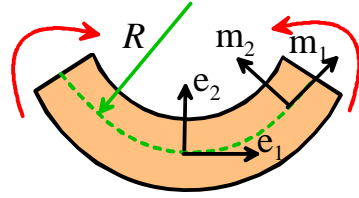
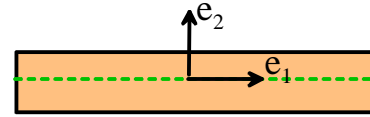
2.2.8.3. Integrate the traction to calculate the resultant force, and manipulate the result obtain the required formula.

2.2.9. A component contains a feature with a 90 degree corner as shown in the picture. The surfaces that meet at the corner are not subjected to any loading.

- 2.2.10. In this problem we consider further the beam bending calculation discussed in Problem 2.1.21. Suppose that the beam is made from a material in which the Material Stress tensor is related to the Lagrange strain tensor by

$$\Sigma_{ij} = 2\mu E_{ij}$$

(this can be regarded as representing an elastic material with zero Poisson's ratio and shear modulus  $\mu$ )



- 2.2.10.1. Calculate the distribution of material stress in the bar, expressing your answer as components in the  $\{\mathbf{e}_1, \mathbf{e}_2, \mathbf{e}_3\}$  basis
- 2.2.10.2. Calculate the distribution of nominal stress in the bar expressing your answer as components in the  $\{\mathbf{e}_1, \mathbf{e}_2, \mathbf{e}_3\}$  basis
- 2.2.10.3. Calculate the distribution of Cauchy stress in the bar expressing your answer as components in the  $\{\mathbf{e}_1, \mathbf{e}_2, \mathbf{e}_3\}$  basis
- 2.2.10.4. Repeat 15.1-15.3 but express the stresses as components in the  $\{\mathbf{m}_1, \mathbf{m}_2, \mathbf{m}_3\}$  basis
- 2.2.10.5. Calculate the distribution of traction on a surface in the beam that has normal  $\mathbf{e}_1$  in the undeformed beam. Give expressions for the tractions in both  $\{\mathbf{e}_1, \mathbf{e}_2, \mathbf{e}_3\}$  and  $\{\mathbf{m}_1, \mathbf{m}_2, \mathbf{m}_3\}$
- 2.2.10.6. Show that the surfaces of the beam that have positions  $x_2 = \pm h/2$  in the undeformed beam are traction free after deformation
- 2.2.10.7. Calculate the resultant moment acting on the ends of the beam.
- 2.2.11. A solid is subjected to some loading that induces a Cauchy stress  $\sigma_{ij}^{(0)}$  at some point in the solid. The solid and the loading frame are then rotated together so that the entire solid (as well as the loading frame) is subjected to a rigid rotation  $R_{ij}$ . This causes the components of the Cauchy stress tensor to change to new values  $\sigma_{ij}^{(1)}$ . The goal of this problem is to calculate a formula relating  $\sigma_{ij}^{(0)}$ ,  $\sigma_{ij}^{(1)}$  and  $R_{ij}$ .
- 2.2.11.1. Let  $n_i^{(0)}$  be a unit vector normal to an internal material plane in the solid before rotation. After rotation, this vector (which rotates with the solid) is  $n_i^{(1)}$ . Write down the formula relating  $n_i^{(0)}$  and  $n_i^{(1)}$
- 2.2.11.2. Let  $T_i^{(0)}$  be the internal traction vector that acts on a material plane with normal  $n_i^{(0)}$  in the solid before application of the rigid rotation. Let  $T_i^{(1)}$  be the traction acting on the same material plane after rotation. Write down the formula relating  $T_i^{(0)}$  and  $T_i^{(1)}$
- 2.2.11.3. Finally, using the definition of Cauchy stress, find the relationship between  $\sigma_{ij}^{(0)}$ ,  $\sigma_{ij}^{(1)}$  and  $R_{ij}$ .
- 2.2.12. Repeat problem 2.2.11, but instead, calculate a relationship between the components of Nominal stress  $S_{ij}^{(0)}$  and  $S_{ij}^{(1)}$  before and after the rigid rotation.

- 2.2.13. Repeat problem 2.2.11, but instead, calculate a relationship between the components of material stress  $\Sigma_{ij}^{(0)}$  and  $\Sigma_{ij}^{(1)}$  before and after the rigid rotation.

### 2.3. Equations of motion and equilibrium for deformable solids

- 2.3.1. A prismatic concrete column of mass density  $\rho$  supports its own weight, as shown in the figure. (Assume that the solid is subjected to a uniform gravitational body force of magnitude  $g$  per unit mass).

- 2.3.1.1. Show that the stress distribution

$$\sigma_{22} = -\rho g(H - x_2)$$

satisfies the equations of static equilibrium

$$\frac{\partial \sigma_{ij}}{\partial x_i} + \rho b_j = 0$$

and also satisfies the boundary conditions  $\sigma_{ij}n_i = 0$

on all free boundaries.

- 2.3.1.2. Show that the traction vector acting on a plane with normal  $\mathbf{n} = \sin \theta \mathbf{e}_1 + \cos \theta \mathbf{e}_2$  at a height  $x_2$  is given by

$$\mathbf{T} = -\rho g(H - x_2) \cos \theta \mathbf{e}_2$$

- 2.3.1.3. Deduce that the normal component of traction acting on the plane is

$$T_n = -\rho g(H - x_2) \cos^2 \theta$$

- 2.3.1.4. show also that the tangential component of traction acting on the plane is

$$\mathbf{T}_t = \rho g(H - x_2) \sin \theta \cos \theta (\cos \theta \mathbf{e}_1 - \sin \theta \mathbf{e}_2)$$

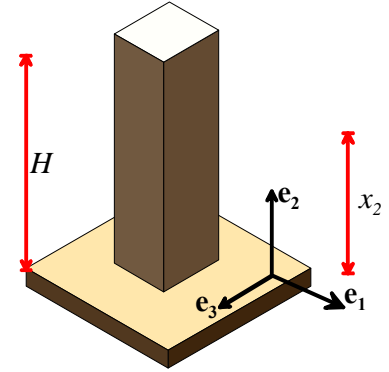
(the easiest way to do this is to note that  $\mathbf{T} = T_n \mathbf{n} + \mathbf{T}_t$  and solve for the tangential traction).

- 2.3.1.5. Suppose that the concrete contains a large number of randomly oriented microcracks. A crack which lies at an angle  $\theta$  to the horizontal will propagate if

$$|\mathbf{T}_t| + \mu T_n > \tau_0$$

where  $\mu$  is the friction coefficient between the faces of the crack and  $\tau_0$  is a critical shear stress that is related to the size of the microcracks and the fracture toughness of the concrete, and is therefore a material property.

- 2.3.1.6. Assume that  $\mu = 1$ . Find the orientation of the microcrack that is most likely to propagate. Hence, find an expression for the maximum possible height of the column, in terms of



- 2.3.2. Is the stress field given below in static equilibrium? If not, find the acceleration or body force density required to satisfy linear momentum balance

$$\begin{aligned} \sigma_{11} &= Cx_1x_2 & \sigma_{12} &= \sigma_{21} = C(a^2 - x_2^2) \\ \sigma_{33} &= \sigma_{23} = \sigma_{13} = 0 \end{aligned}$$

- 2.3.3. Let  $\phi$  be a twice differentiable, scalar function of position. Derive a plane stress field from  $\phi$  by setting

$$\sigma_{11} = \frac{\partial^2 \phi}{\partial x_2^2} \quad \sigma_{22} = \frac{\partial^2 \phi}{\partial x_1^2} \quad \sigma_{12} = \sigma_{21} = -\frac{\partial^2 \phi}{\partial x_1 \partial x_2}$$

Show that this stress field satisfies the equations of stress equilibrium with zero body force.

## 2.3.4. The stress field

$$\sigma_{ij} = \frac{-3P_k x_k x_i x_j}{4\pi R^5} \quad R = \sqrt{x_k x_k}$$

represents the stress in an infinite, incompressible elastic solid that is subjected to a point force with components  $P_k$  acting at the origin (you can visualize a point force as a very large body force which is concentrated in a very small region around the origin).

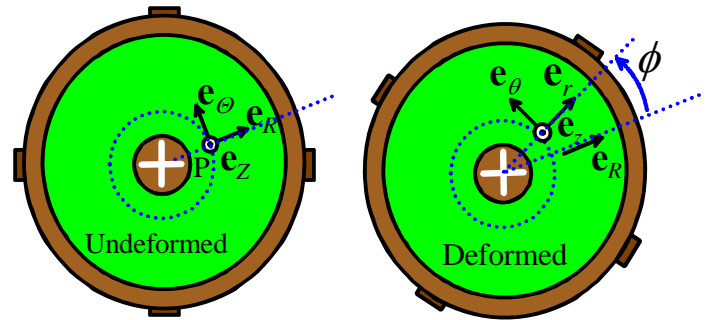
2.3.4.1. Verify that the stress field is in static equilibrium

2.3.4.2. Consider a spherical region of material centered at the origin. This region is subjected to (1) the body force acting at the origin; and (2) a force exerted by the stress field on the outer surface of the sphere. Calculate the resultant force exerted on the outer surface of the sphere by the stress, and show that it is equal in magnitude and opposite in direction to the body force.

2.3.5. In this problem, we consider the internal forces in the polymer specimen described in Problem 2.1.29 of the previous section. Suppose that the specimen is homogeneous, has mass density  $\rho$  in the reference configuration, and may be idealized as a viscous fluid, in which the Kirchhoff stress is related to stretch rate by

$$\boldsymbol{\tau} = \mu \mathbf{D} + p \mathbf{I}$$

where  $p$  is an indeterminate hydrostatic pressure and  $\mu$  is the viscosity.



2.3.5.1. Find expressions for the Cauchy stress tensor, expressing your answer as components in  $\{\mathbf{e}_r, \mathbf{e}_\theta, \mathbf{e}_z\}$

2.3.5.2. Assume steady, quasi-static deformation (neglect accelerations). Express the equations of equilibrium in terms of  $\phi(r, t)$

2.3.5.3. Solve the equilibrium equation, together with appropriate boundary conditions, to calculate  $\phi(r, t)$

2.3.5.4. Find the torque necessary to rotate the external cylinder

2.3.5.5. Calculate the rate of mechanical work done on the sample

2.3.5.6. Calculate an expression for the rate of heat generation inside the fluid as a function of  $r$

2.3.5.7. Calculate the acceleration of a material particle in the fluid

2.3.5.8. Estimate the rotation rate  $\dot{\alpha}$  where inertia begins to play a significant role in determining the state of stress in the fluid

## 2.4. Work done by stresses; the principle of virtual work

- 2.4.1. A solid with volume  $V$  is subjected to a distribution of traction  $t_i$  on its surface. Assume that the solid is in static equilibrium. By considering a virtual velocity of the form  $\delta v_i = A_{ij} y_j$ , where  $A_{ij}$  is a constant symmetric tensor, use the principle of virtual work to show that the average stress in a solid can be computed from the shape of the solid and the tractions acting on its surface using the expression

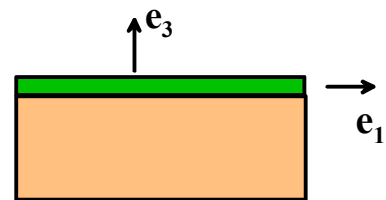
$$\frac{1}{V} \int_V \sigma_{ij} dV = \frac{1}{V} \int_S \frac{1}{2} (t_i y_j + t_j y_i) dA$$

## 3. Chapter 3: Constitutive Models: Relations between Stress and Strain

### 3.1. General Requirements for Constitutive Equations

### 3.2. Linear Elastic Constitutive Equations

- 3.2.1. Using the table of values given in Section 3.2.4, find values of bulk modulus, Lamé modulus, and shear modulus for steel, aluminum and rubber
- 3.2.2. A specimen of an isotropic, linear elastic material with Young's modulus  $E$  and is placed inside a rigid box that prevents the material from stretching in any direction. This means that the strains in the specimen are zero. The specimen is then heated to increase its temperature by  $\Delta T$ . Find a formula for the stress in the specimen. Find a formula for the strain energy density. How much strain energy would be stored in a  $1\text{cm}^3$  sample of steel if its temperature were increased by  $100^\circ\text{C}$ ? Compare the strain energy with the heat required to change the temperature by  $100^\circ\text{C}$  – the specific heat capacity of steel is about  $470\text{ J}/(\text{kg}\cdot^\circ\text{C})$
- 3.2.3. A specimen of an isotropic, linear elastic solid is free of stress, and is heated to increase its temperature by  $\Delta T$ . Find expressions for the strain and displacement fields in the solid.
- 3.2.4. A thin isotropic, linear elastic thin film with Young's modulus  $E$ , Poisson's ratio  $\nu$  and thermal expansion coefficient  $\alpha$  is bonded to a stiff substrate. The film is stress free at some initial temperature, and then heated to increase its temperature by  $T$ . The substrate prevents the film from stretching in its own plane, so that  $\varepsilon_{11} = \varepsilon_{22} = \varepsilon_{12} = 0$ , while the surface is traction free, so that the film deforms in a state of plane stress. Calculate the stresses in the film in terms of material properties and temperature, and deduce an expression for the strain energy density in the film.





3.2.5. A cubic material may be characterized either by its moduli as

$$\begin{bmatrix} \sigma_{11} \\ \sigma_{22} \\ \sigma_{33} \\ \sigma_{12} \\ \sigma_{13} \\ \sigma_{23} \end{bmatrix} = \begin{bmatrix} c_{11} & c_{12} & c_{12} & 0 & 0 & 0 \\ & c_{11} & c_{12} & 0 & 0 & 0 \\ & & c_{11} & 0 & 0 & 0 \\ & sym & & c_{44} & 0 & 0 \\ & & & 0 & c_{44} & 0 \\ & & & 0 & 0 & c_{44} \end{bmatrix} \begin{bmatrix} \varepsilon_{11} \\ \varepsilon_{22} \\ \varepsilon_{33} \\ 2\varepsilon_{12} \\ 2\varepsilon_{13} \\ 2\varepsilon_{23} \end{bmatrix}$$

or by the engineering constants

$$\begin{bmatrix} \varepsilon_{11} \\ \varepsilon_{22} \\ \varepsilon_{33} \\ 2\varepsilon_{12} \\ 2\varepsilon_{13} \\ 2\varepsilon_{23} \end{bmatrix} = \begin{bmatrix} 1/E & -\nu/E & -\nu/E & 0 & 0 & 0 \\ -\nu/E & 1/E & -\nu/E & 0 & 0 & 0 \\ -\nu/E & -\nu/E & 1/E & 0 & 0 & 0 \\ 0 & 0 & 0 & 1/\mu & 0 & 0 \\ 0 & 0 & 0 & 0 & 1/\mu & 0 \\ 0 & 0 & 0 & 0 & 0 & 1/\mu \end{bmatrix} \begin{bmatrix} \sigma_{11} \\ \sigma_{22} \\ \sigma_{33} \\ \sigma_{12} \\ \sigma_{13} \\ \sigma_{23} \end{bmatrix}$$

Calculate formulas relating  $c_{ij}$  to  $E, \nu$  and  $\mu$ , and deduce an expression for the anisotropy factor  $A = 2\mu(1+\nu)/E$

3.2.6. Suppose that the stress-strain relation for a linear elastic solid is expressed in matrix form as  $[\sigma] = [C][\varepsilon]$ , where  $[\sigma]$ ,  $[\varepsilon]$  and  $[C]$  represent the stress and strain vectors and the matrix of elastic constants defined in Section ????. Show that the material has a positive definite strain energy density ( $U > 0 \quad \forall [\varepsilon] \neq 0$ ) if and only if the eigenvalues of  $[C]$  are all positive.

3.2.7. Let  $[\sigma]$ ,  $[\varepsilon]$  and  $[C]$  represent the stress and strain vectors and the matrix of elastic constants in the isotropic linear elastic constitutive equation

$$\begin{bmatrix} \sigma_{11} \\ \sigma_{22} \\ \sigma_{33} \\ \sigma_{23} \\ \sigma_{13} \\ \sigma_{12} \end{bmatrix} = \frac{E}{(1+\nu)(1-2\nu)} \begin{bmatrix} 1-\nu & \nu & \nu & 0 & 0 & 0 \\ \nu & 1-\nu & \nu & 0 & 0 & 0 \\ \nu & \nu & 1-\nu & 0 & 0 & 0 \\ 0 & 0 & 0 & \frac{(1-2\nu)}{2} & 0 & 0 \\ 0 & 0 & 0 & 0 & \frac{(1-2\nu)}{2} & 0 \\ 0 & 0 & 0 & 0 & 0 & \frac{(1-2\nu)}{2} \end{bmatrix} \begin{bmatrix} \varepsilon_{11} \\ \varepsilon_{22} \\ \varepsilon_{33} \\ 2\varepsilon_{23} \\ 2\varepsilon_{13} \\ 2\varepsilon_{12} \end{bmatrix} - \frac{E\alpha\Delta T}{1-2\nu} \begin{bmatrix} 1 \\ 1 \\ 1 \\ 0 \\ 0 \\ 0 \end{bmatrix}$$

3.2.7.1. Calculate the eigenvalues of the stiffness matrix  $[C]$  for an isotropic solid in terms of Young's modulus and Poisson's ratio. Hence, show that the eigenvalues are positive (a necessary requirement for the material to be stable – see problem ??) if and only if  $-1 < \nu < 1/2$  and  $E > 0$ .

3.2.7.2. Find the eigenvectors of  $[C]$  and sketch the deformations associated with these eigenvectors.

- 3.2.8. Let  $[\sigma]$ ,  $[\varepsilon]$  and  $[C]$  represent the stress and strain vectors and the matrix of elastic constants in the isotropic linear elastic constitutive equation for a cubic crystal

$$\begin{bmatrix} \sigma_{11} \\ \sigma_{22} \\ \sigma_{33} \\ \sigma_{23} \\ \sigma_{12} \\ \sigma_{13} \end{bmatrix} = \begin{bmatrix} c_{11} & c_{12} & c_{12} & 0 & 0 & 0 \\ & c_{11} & c_{12} & 0 & 0 & 0 \\ & & c_{11} & 0 & 0 & 0 \\ & sym & & c_{44} & 0 & 0 \\ & & & 0 & c_{44} & 0 \\ & & & 0 & 0 & c_{44} \end{bmatrix} \begin{bmatrix} \varepsilon_{11} \\ \varepsilon_{22} \\ \varepsilon_{33} \\ 2\varepsilon_{23} \\ 2\varepsilon_{12} \\ 2\varepsilon_{13} \end{bmatrix}$$

Calculate the eigenvalues of the stiffness matrix  $[C]$  and hence find expressions for the admissible ranges of  $c_{11}, c_{12}, c_{44}$  for the eigenvalues to be positive.

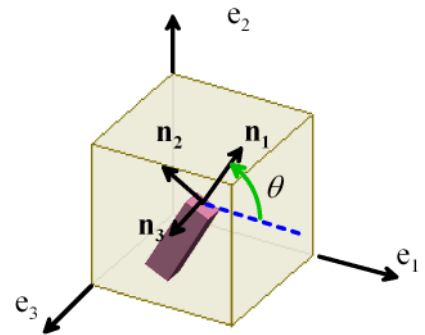
- 3.2.9. Let  $C_{ijkl}^{(e)}$  denote the components of the elasticity tensor in a basis  $\{\mathbf{e}_1, \mathbf{e}_2, \mathbf{e}_3\}$ . Let  $\{\mathbf{m}_1, \mathbf{m}_2, \mathbf{m}_3\}$  be a second basis, and define  $\Omega_{ij} = \mathbf{m}_i \cdot \mathbf{e}_j$ . Recall that the components of the stress and strain tensor in  $\{\mathbf{e}_1, \mathbf{e}_2, \mathbf{e}_3\}$  and  $\{\mathbf{m}_1, \mathbf{m}_2, \mathbf{m}_3\}$  are related by  $\sigma_{ij}^{(m)} = \Omega_{ik} \sigma_{kl}^{(e)} \Omega_{jl}$   $\varepsilon_{ij}^{(m)} = \Omega_{ik} \varepsilon_{kl}^{(e)} \Omega_{jl}$ . Use this result, together with the elastic constitutive equation, to show that the components of the elasticity tensor in  $\{\mathbf{m}_1, \mathbf{m}_2, \mathbf{m}_3\}$  can be calculated from

$$C_{ijkl}^{(m)} = \Omega_{ip} \Omega_{jq} C_{pqrs}^{(e)} \Omega_{kr} \Omega_{ls}$$

- 3.2.10. Consider a cube-shaped specimen of an *anisotropic*, linear elastic material. The tensor of elastic moduli and the thermal expansion coefficient for the solid (expressed as components in an arbitrary basis) are  $C_{ijkl}^{(e)}, \alpha_{ij}^{(e)}$ . The solid is placed inside a rigid box that prevents the material from stretching in any direction. This means that the strains in the specimen are zero. The specimen is then heated to increase its temperature by  $\Delta T$ . Find a formula for the strain energy density, and show that the result is independent of the orientation of the material with respect to the box.

- 3.2.11. The figure shows a cubic crystal. Basis vectors  $\{\mathbf{e}_1, \mathbf{e}_2, \mathbf{e}_3\}$  are aligned perpendicular to the faces of the cubic unit cell. A tensile specimen is cut from the cube – the axis of the specimen lies in the  $\{\mathbf{e}_1, \mathbf{e}_2\}$  plane and is oriented at an angle  $\theta$  to the  $\mathbf{e}_1$  direction. The specimen is then loaded in uniaxial tension  $\sigma_{nn}$  parallel to its axis. This means that the stress components in the basis  $\{\mathbf{n}_1, \mathbf{n}_2, \mathbf{n}_3\}$  shown in the picture

are  $\begin{bmatrix} \sigma_{nn} & 0 & 0 \\ 0 & 0 & 0 \\ 0 & 0 & 0 \end{bmatrix}$



- 3.2.11.1. Use the basis change formulas for tensors to calculate the components of stress in the  $\{\mathbf{e}_1, \mathbf{e}_2, \mathbf{e}_3\}$  basis in terms of  $\theta$ .

Use the stress-strain equations in Section 3.1.16 to find the strain components in the  $\{\mathbf{e}_1, \mathbf{e}_2, \mathbf{e}_3\}$  basis, in terms of the engineering constants  $E, \nu, \mu$  for the cubic crystal. You need only calculate  $\varepsilon_{11}, \varepsilon_{22}, \varepsilon_{12}$ .

- 3.2.11.2. Use the basis change formulas again to calculate the strain components in the  $\{\mathbf{n}_1, \mathbf{n}_2, \mathbf{n}_3\}$  basis oriented with the specimen. Again, you need only calculate  $\varepsilon_{11}, \varepsilon_{22}, \varepsilon_{12}$ . Check your answer by setting  $\mu = E/2(1+\nu)$  - this makes the crystal isotropic, and you should recover the isotropic solution.
- 3.2.11.3. Define the effective axial Young's modulus of the tensile specimen as  $E(\theta) = \sigma_{nn} / \varepsilon_{nn}$ , where  $\varepsilon_{nn} = \mathbf{n} \cdot \boldsymbol{\varepsilon} \cdot \mathbf{n}$  is the strain component parallel to the  $\mathbf{n}_1$  direction. Find a formula for  $E(\theta)$  in terms of  $E, \nu, \mu$ .
- 3.2.11.4. Using data for copper, plot a graph of  $E(\theta)$  against  $\theta$ . For copper, what is the orientation that maximizes the longitudinal stiffness of the specimen? Which orientation minimizes the stiffness?

### 3.3. Hypoelasticity

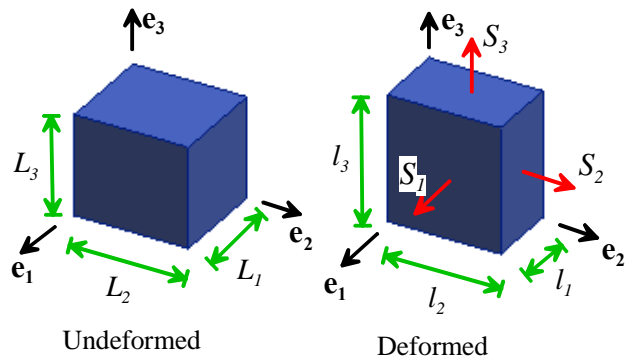
### 3.4. Generalized Hooke's law: Materials subjected to small strains and large rotations

### 3.5. Hyperelasticity

- 3.5.1. Derive the stress-strain relations for an incompressible, Neo-Hookean material subjected to

- 3.5.1.1. Uniaxial tension
- 3.5.1.2. Equibiaxial tension
- 3.5.1.3. Pure shear

Derive expressions for the Cauchy stress, the Nominal stress, and the Material stress tensors (the solutions for nominal stress are listed in the table in Section 3.5.6). You should use the following procedure: (i) assume that the specimen experiences the length changes listed in 3.5.6; (ii) use the formulas in Section 3.5.5 to compute the Cauchy stress, leaving the hydrostatic part of the stress  $p$  as an unknown; (iii) Determine the hydrostatic stress from the boundary conditions (e.g. for uniaxial tensile parallel to  $\mathbf{e}_1$  you know  $\sigma_{22} = \sigma_{33} = 0$ ; for equibiaxial tension or pure shear in the  $\mathbf{e}_1, \mathbf{e}_2$  plane you know that  $\sigma_{33} = 0$ )



- 3.5.2. Repeat problem 3.5.1 for an incompressible Mooney-Rivlin material.
- 3.5.3. Repeat problem 3.5.1 for an incompressible Arruda-Boyce material
- 3.5.4. Repeat problem 3.5.1 for an incompressible Ogden material.
- 3.5.5. Using the results listed in the table in Section 3.5.6, and the material properties listed in Section 3.5.7, plot graphs showing the nominal stress as a function of stretch ratio  $\lambda$  for each of (a) a Neo-Hookean material; (b) a Mooney-Rivlin material; (c) the Arruda-Boyce material and (c) the Ogden material when subjected to uniaxial tension, biaxial tension, and pure shear (for the latter case, plot the largest tensile stress  $S_1$ ).

3.5.6. A foam specimen is idealized as an Ogden-Storakers foam with strain energy density

$$\tilde{U} = \frac{2\mu}{\alpha^2} \left( \lambda_1^\alpha + \lambda_2^\alpha + \lambda_3^\alpha - 3 + \frac{1}{\beta} (J^{-\alpha\beta} - 1) \right)$$

where  $\mu, \alpha$  and  $\beta$  are material properties. Calculate:

- 3.5.6.1. The Cauchy stress in a specimen subjected to a pure volume change with principal stretches  $\lambda_1 = \lambda_2 = \lambda_3 = \lambda$
- 3.5.6.2. The Cauchy stress in a specimen subjected to volume preserving uniaxial extension
- 3.5.6.3. The Cauchy stress in a specimen subjected to uniaxial tension, as a function of the tensile stretch ratio  $\lambda_1$ . (To solve this problem you will need to assume that the solid is subjected to principal stretches  $\lambda_1$  parallel to  $\mathbf{e}_1$ , and stretches  $\lambda_2$  parallel to  $\mathbf{e}_2$  and  $\mathbf{e}_3$ . You will need to determine  $\lambda_2$  from the condition that  $\sigma_{22} = \sigma_{33} = 0$  in a uniaxial tensile test.

3.5.7. Suppose that a hyperelastic solid is characterized by a strain energy density  $\bar{U}(\bar{I}_1, \bar{I}_2, J)$  where

$$\bar{I}_1 = \frac{B_{kk}}{J^{2/3}} \quad \bar{I}_2 = \frac{1}{2} \left( \bar{I}_1^2 - \frac{B_{ik}B_{ki}}{J^{4/3}} \right) \quad J = \sqrt{\det \mathbf{B}}$$

are invariants of the Left Cauchy-Green deformation tensor  $B_{ij} = F_{ik}F_{jk}$ . Suppose that the solid is subjected to an infinitesimal strain, so that  $\mathbf{B}$  can be approximated as  $B_{ij} \approx \delta_{ij} + \varepsilon_{ij}$ , where  $\varepsilon_{ij}$  is a symmetric infinitesimal strain tensor. Linearize the constitutive equations for  $\varepsilon_{ij} \ll 1$ , and show that the relationship between Cauchy stress  $\sigma_{ij}$  and infinitesimal strain  $\varepsilon_{ij}$  is equivalent to the isotropic linear elastic constitutive equation. Give formulas for the bulk modulus and shear modulus for the equivalent solid in terms of the derivatives of  $\bar{U}$ .

3.5.8. The constitutive law for a hyperelastic solid is derived from a strain energy potential  $U(I_1, I_2, I_3)$ , where

$$I_1 = \text{trace}(\mathbf{B}) = B_{kk} \quad I_2 = \frac{1}{2} (I_1^2 - \mathbf{B} \cdot \mathbf{B}) = \frac{1}{2} (I_1^2 - B_{ik}B_{ki}) \quad I_3 = \det \mathbf{B} = J^2$$

are the invariants of the Left Cauchy-Green deformation tensor  $\mathbf{B} = \mathbf{F} \cdot \mathbf{F}^T$   $B_{ij} = F_{ik}F_{jk}$ .

- 3.5.8.1. Calculate the Cauchy stress induced in the solid when it is subjected to a rigid rotation, followed by an arbitrary homogeneous deformation. Hence, demonstrate that the constitutive law is isotropic.
- 3.5.8.2. Apply the simple check described in Section 3.1 to test whether the constitutive law is objective.

3.5.9. The strain energy density of a hyperelastic solid is sometimes specified as a function of the *right* Cauchy-Green deformation tensor  $C_{ij} = F_{ki}F_{kj}$ , instead of  $B_{ij}$  as described in Section 3.5. (This procedure must be used if the material is anisotropic, for example)

3.5.9.1. Suppose that the strain energy density has the general form  $W(C_{ij})$ . Derive formulas for the Material stress, Nominal stress and Cauchy stress in the solid as functions of  $F_{ij}$ ,  $C_{ij}$  and  $\partial W / \partial C_{ij}$

3.5.9.2. Apply the simple check described in Section 3.1 to demonstrate that the resulting stress-strain relation is objective.

3.5.9.3. Calculate the Cauchy stress induced in the solid when it is subjected to a rigid rotation, followed by an arbitrary homogeneous deformation. Hence, demonstrate that the constitutive law is not, in general, isotropic.

3.5.9.4. Suppose that the constitutive law is simplified further by writing the strain energy density as a function of the *invariants* of  $\mathbf{C}$ , i.e.  $W(C_{ij}) = U(I_1, I_2, I_3)$ , where

$$I_1 = C_{kk} \quad I_2 = \frac{1}{2} \left( I_1^2 - C_{ik}C_{ki} \right) \quad I_3 = \det \mathbf{C} = J^2$$

Derive expressions relating the Cauchy stress components to  $\partial U / \partial I_j$ .

3.5.9.5. Demonstrate that the simplified constitutive law described in 8.4 characterizes an isotropic solid.

### 3.6. Viscoelasticity

3.6.1. A cantilever beam of length  $L$  and rectangular cross section  $a \times a$  is made from an incompressible viscoelastic material with constitutive law

$$S_{ij}(t) = \int_0^t 2\mu_r(t-t') \frac{de_{ij}}{dt'} dt'$$

where  $S_{ij}$  and  $e_{ij}$  are the components of deviatoric stress and strain, and the relaxation modulus has the form

$$\mu_r(\tau) = \mu_\infty + \mu_1 \exp(-\tau / t_1^\mu)$$

where  $\mu_\infty$ ,  $\mu_1$  and  $t_1$  are material constants. Making the usual approximations associated with beam theory, find an expression for the deflection of the end of the beam as a function of time. (You don't need to derive beam theory from scratch – any quick way to get to the solution is fine)

3.6.2. Find some experimental data for the relaxation modulus (or creep compliance, if you prefer) of a polymer (most texts on polymers have such data; alternatively you can use the e-search skills that Mark Skelton demonstrated earlier)

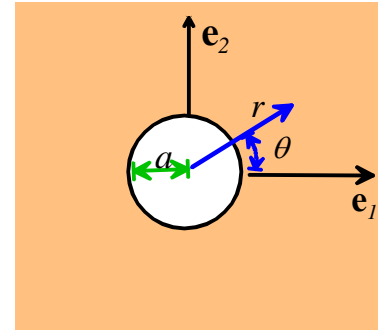
### 3.7. Small-strain metal plasticity

3.7.1. The stress state induced by stretching a large plate containing a cylindrical hole of radius  $a$  at the origin is given by

$$\sigma_{11} = \sigma_0 \left( 1 + \left( \frac{3a^4}{2r^4} - \frac{a^2}{r^2} \right) \cos 4\theta - \frac{3a^2}{2r^2} \cos 2\theta \right)$$

$$\sigma_{22} = \sigma_0 \left( \left( \frac{a^2}{r^2} - \frac{3a^4}{2r^4} \right) \cos 4\theta - \frac{a^2}{2r^2} \cos 2\theta \right)$$

$$\sigma_{12} = \sigma_0 \left( \left( \frac{3a^4}{2r^4} - \frac{a^2}{r^2} \right) \sin 4\theta - \frac{a^2}{2r^2} \sin 2\theta \right)$$



Here,  $\sigma_0$  is the stress in the plate far from the hole. (Stress components not listed are all zero)

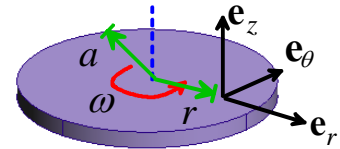
3.7.1.1. Plot contours of von-Mises equivalent stress (normalized by  $\sigma_0$ ) as a function of  $r/a$  and  $\theta$ , for a material with  $\nu = 0.3$ . Hence identify the point in the solid that first reaches yield.

3.7.1.2. Assume that the material has a yield stress  $Y$ . Calculate the critical value of  $\sigma_0/Y$  that will just cause the plate to reach yield.

3.7.2. The stress state (expressed in cylindrical-polar coordinates) in a thin disk with mass density  $\rho_0$  that spins with angular velocity  $\omega$  can be shown to be

$$\sigma_{rr} = (3 + \nu) \frac{\rho_0 \omega^2}{8} \{ a^2 - r^2 \}$$

$$\sigma_{\theta\theta} = \frac{\rho_0 \omega^2}{8} \{ (3 + \nu) a^2 - (3\nu + 1) r^2 \}$$



Assume that the disk is made from an elastic-plastic material with yield stress  $Y$  and  $\nu = 1/3$ .

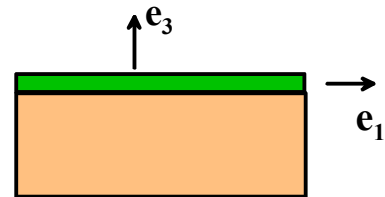
3.7.2.1. Find a formula for the critical angular velocity that will cause the disk to yield, assuming Von-Mises yield criterion. Where is the critical point in the disk where plastic flow first starts?

3.7.2.2. Find a formula for the critical angular velocity that will cause the disk to yield, using the Tresca yield criterion. Where is the critical point in the disk where plastic flow first starts?

3.7.2.3. Using parameters representative of steel, estimate how much kinetic energy can be stored in a disk with a 0.5m radius and 0.1m thickness.

3.7.2.4. Recommend the best choice of material for the flywheel in a flywheel energy storage system.

3.7.3. An isotropic, elastic-perfectly plastic thin film with Young's Modulus  $E$ , Poisson's ratio  $\nu$ , yield stress in uniaxial tension  $Y$  and thermal expansion coefficient  $\alpha$  is bonded to a stiff substrate. It is stress free at some initial temperature and then heated. The substrate prevents the film from stretching in its own plane, so that  $\varepsilon_{11} = \varepsilon_{22} = \varepsilon_{12} = 0$ , while the surface is traction free, so that the film deforms in a state of plane stress. Calculate



the critical temperature change  $\Delta T_y$  that will cause the film to yield, using (a) the Von Mises yield criterion and (b) the Tresca yield criterion.

- 3.7.4. Assume that the thin film described in the preceding problem shows so little strain hardening behavior that it can be idealized as an elastic-perfectly plastic solid, with uniaxial tensile yield stress  $Y$ . Suppose the film is stress free at some initial temperature, and then heated to a temperature  $\beta\Delta T_y$ , where  $\Delta T_y$  is the yield temperature calculated in the preceding problem, and  $\beta > 1$ .

3.7.4.1. Find the stress in the film at this temperature.

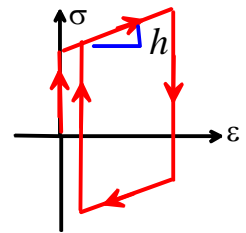
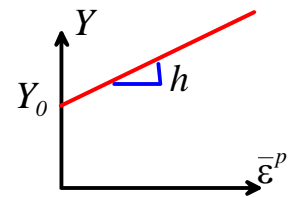
3.7.4.2. The film is then cooled back to its original temperature. Find the stress in the film after cooling.

- 3.7.5. Suppose that the thin film described in the preceding problem is made from an elastic, isotropically hardening plastic material with a Mises yield surface, and yield stress-v-plastic strain as shown in the figure. The film is initially stress free, and then heated to a temperature  $\beta\Delta T_y$ , where  $\Delta T_y$  is the yield temperature calculated in problem 1, and  $\beta > 1$ .

3.7.5.1. Find a formula for the stress in the film at this temperature.

3.7.5.2. The film is then cooled back to its original temperature. Find the stress in the film after cooling.

3.7.5.3. The film is cooled further by a temperature change  $\Delta T < 0$ . Calculate the critical value of  $\Delta T$  that will cause the film to reach yield again.



Kinematic hardening

- 3.7.6. Suppose that the thin film described in the preceding problem is made from an elastic, *linear kinematically* hardening plastic material with a Mises yield surface, and yield stress-v-plastic strain as shown in the figure. The stress is initially stress free, and then heated to a temperature  $\beta\Delta T_y$ , where  $\Delta T_y$  is the yield temperature calculated in problem 1, and  $\beta > 1$ .

3.7.6.1. Find a formula for the stress in the film at this temperature.

3.7.6.2. The film is then cooled back to its original temperature. Find the stress in the film after cooling.

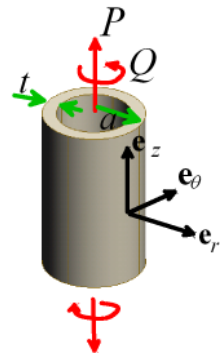
3.7.6.3. The film is cooled further by a temperature change  $\Delta T < 0$ . Calculate the critical value of  $\Delta T$  that will cause the film to reach yield again.

- 3.7.7. A thin-walled tube of mean radius  $a$  and wall thickness  $t \ll a$  is subjected to an axial load  $P$  which exceeds the initial yield load by 10% (i.e.  $P = 1.1P_y$ ). The axial load is then removed, and a torque  $Q$  is applied to the tube. You may assume that the axial load induce a uniaxial stress  $\sigma_{zz} = P/(2\pi at)$  while the torque induces a shear stress  $\sigma_{z\theta} = Q/(2\pi a^2 t)$ . Find the magnitude of  $Q$  to cause further plastic flow, assuming that the solid is

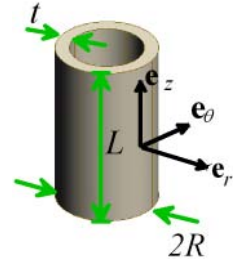
3.7.7.1. an isotropically hardening solid with a Mises yield surface

3.7.7.2. a linear kinematically hardening solid with a Mises yield surface

Express your answer in terms of  $P_y$  and appropriate geometrical terms, and assume infinitesimal deformation.



3.7.8. A cylindrical, thin-walled pressure vessel with initial radius  $R$ , length  $L$  and wall thickness  $t \ll R$  is subjected to internal pressure  $p$ . The vessel is made from an isotropic elastic-plastic solid with Young's modulus  $E$ , Poisson's ratio  $\nu$ , and its yield stress varies with accumulated plastic strain  $\varepsilon_e$  as  $Y = Y_0 + h\varepsilon_e$ . Recall that the stresses in a thin-walled pressurized tube are related to the internal pressure by  $\sigma_{zz} = pR/(2t)$ ,  $\sigma_{\theta\theta} = pR/t$



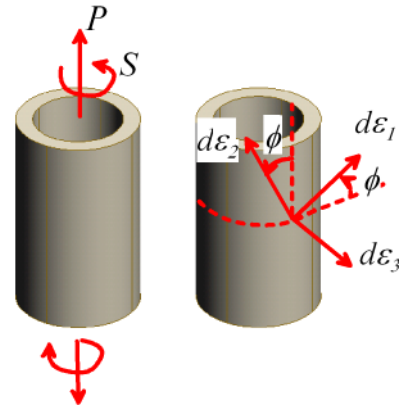
3.7.8.1. Calculate the critical value of internal pressure required to initiate yield in the solid

3.7.8.2. Find a formula for the strain increment  $d\varepsilon_{rr}, d\varepsilon_{\theta\theta}, d\varepsilon_{zz}$  resulting from an increment in pressure  $dp$

3.7.8.3. Suppose that the pressure is increased 10% above the initial yield value. Find a formula for the change in radius, length and wall thickness of the vessel. Assume small strains.

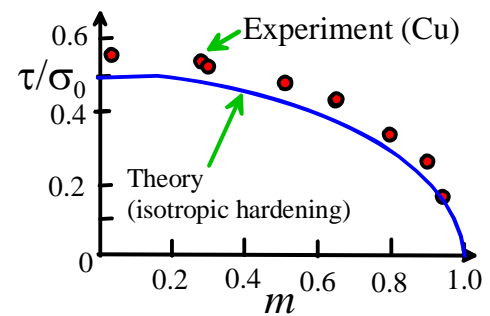
3.7.9. Write a simple program that will compute the history of stress resulting from an arbitrary history of strain applied to an isotropic, elastic-plastic von-Mises solid. Assume that the yield stress is related to the accumulated effective strain by  $Y = Y_0(1 + \bar{\varepsilon}^p / \varepsilon_0)^n$ , where  $Y_0$ ,  $\varepsilon_0$  and  $n$  are material constants. Check your code by using it to compute the stress resulting from a volume preserving uniaxial strain  $\varepsilon_{11} = \lambda$ ,  $\varepsilon_{22} = \varepsilon_{33} = -\lambda/2$ , and compare the predictions of your code with the analytical solution. Try one other cycle of strain of your choice.

3.7.10. In a classic paper, Taylor, G. I., and Quinney, I., 1932, "The Plastic Distortion of Metals," Philos. Trans. R. Soc. London, Ser. A, 230, pp. 323–362 described a series of experiments designed to investigate the plastic deformation of various ductile metals. Among other things, they compared their experimental measurements with the predictions of the von-Mises and Tresca yield criteria and their associated flow rules. They used the apparatus shown in the figure. Thin walled cylindrical tubes were first subjected to an axial stress  $\sigma_{zz} = \sigma_0$ . The stress was sufficient to extend the tubes plastically. The axial stress was then reduced to a magnitude  $m\sigma_0$ , with  $0 < m < 1$ , and a progressively increasing torque was applied to the tube so as to induce a shear stress  $\sigma_{z\theta} = \tau$  in the solid. The twist, extension and internal volume of the tube were recorded as the torque was applied. In this problem you will compare their experimental results with the predictions of plasticity theory. Assume that the material is made from an isotropically hardening *rigid* plastic solid, with a Von Mises yield surface, and yield stress-v-plastic strain given by  $Y = Y_0 + h\bar{\varepsilon}^p$ .



3.7.10.1. One set of experimental results is illustrated in the figure to the right. The figure shows the ratio  $\tau/\sigma_0$  required to initiate yield in the tube during torsional loading as a function of  $m$ . Show that

$$\text{theory predicts that } \tau/\sigma_0 = \sqrt{(1-m^2)}/\sqrt{3}$$

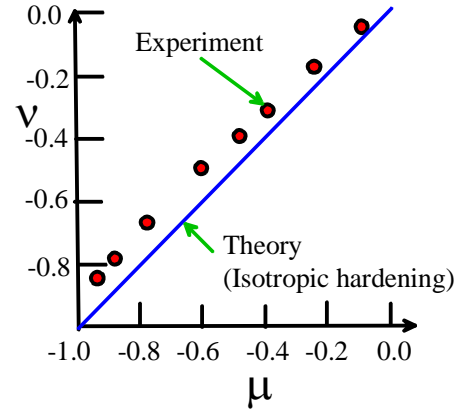




- 3.7.10.2. Compute the magnitudes of the principal stresses  $(\sigma_1, \sigma_2, \sigma_3)$  at the point of yielding under combined axial and torsional loads in terms of  $\sigma_0$  and  $m$ .
- 3.7.10.3. Suppose that, for a given axial stress  $\sigma_{zz} = m\sigma_0$ , the shear stress  $\tau$  is first brought to the critical value required to initiate yield in the solid, and is then increased by an infinitesimal increment  $d\tau$ . Find expressions for the resulting plastic strain increments  $d\varepsilon_{zz}, d\varepsilon_{\theta\theta}, d\varepsilon_{rr}, d\varepsilon_{r\theta}$ , in terms of  $m, \sigma_0, h$  and  $d\tau$ .
- 3.7.10.4. Hence, deduce expressions for the magnitudes of the principal strains increments  $(d\varepsilon_1, d\varepsilon_2, d\varepsilon_3)$  resulting from the stress increment  $d\tau$ .
- 3.7.10.5. Using the results of 11.2 and 11.6, calculate the so-called “Lode parameters,” defined as

$$\nu = 2 \frac{(d\varepsilon_2 - d\varepsilon_3)}{(d\varepsilon_1 - d\varepsilon_3)} - 1 \quad \mu = 2 \frac{(\sigma_2 - \sigma_3)}{(\sigma_1 - \sigma_3)} - 1$$

and show that the theory predicts  $\nu = \mu$



- 3.7.11. The Taylor/Quinney experiments show that the constitutive equations for an isotropically hardening Von-Mises solid predict behavior that matches reasonably well with experimental observations, but there is a clear systematic error between theory and experiment. In this problem, you will compare the predictions of a *linear kinematic hardening* law with experiment. Assume that the solid has a yield function and hardening law given by

$$f = \sqrt{\frac{3}{2}}(S_{ij} - \alpha_{ij})(S_{ij} - \alpha_{ij}) - Y_0 = 0 \quad d\alpha_{ij} = \frac{2}{3}c d\varepsilon_{ij}^p$$

- 3.7.11.1. Assume that during the initial tensile test, the axial stress  $\sigma_{zz} = \sigma_0$  in the specimens reached a magnitude  $\sigma_0 = \beta Y_0$ , where  $Y_0$  is the initial tensile yield stress of the solid and  $\beta > 1$  is a scalar multiplier. Assume that the axial stress was then reduced to  $m\sigma_0$  and a progressively increasing shear stress was applied to the solid. Show that the critical value of  $\tau/\sigma_0$  at which plastic deformation begins is given by

$$\frac{\tau}{\sigma_0} = \frac{1}{\sqrt{3}} \left\{ \frac{1}{\beta^2} - (m - 1 + \beta^{-1})^2 \right\}^{1/2}$$

Plot  $\tau/\sigma_0$  against  $m$  for various values of  $\beta$ .

- 3.7.11.2. Suppose that, for a given axial stress  $\sigma_{zz} = m\sigma_0$ , the shear stress is first brought to the critical value required to initiate yield in the solid, and is then increased by an infinitesimal increment  $d\tau$ . Find expressions for the resulting plastic strain increments, in terms of  $m, \beta, c, Y_0$  and  $d\tau$ .
- 3.7.11.3. Hence, deduce the magnitudes of the principal strains in the specimen  $(d\varepsilon_1, d\varepsilon_2, d\varepsilon_3)$ .
- 3.7.11.4. Compute the magnitudes of the principal stresses  $(\sigma_1, \sigma_2, \sigma_3)$  at the point of yielding under combined axial and torsional loads in terms of  $m, \beta$ , and  $Y_0$ .
- 3.7.11.5. Finally, find expressions for Lode's parameters

$$\nu = 2 \frac{(d\varepsilon_2 - d\varepsilon_3)}{(d\varepsilon_1 - d\varepsilon_3)} - 1 \quad \mu = 2 \frac{(\sigma_2 - \sigma_3)}{(\sigma_1 - \sigma_3)} - 1$$

3.7.11.6. Plot  $\nu$  versus  $\mu$  for various values of  $\beta$ , and compare your predictions with Taylor and Quinney's measurements.

3.7.12. An elastic- nonlinear kinematic hardening solid has Young's modulus  $E$ , Poisson's ratio  $\nu$ , a Von-Mises yield surface

$$f(\sigma_{ij}, \alpha_{ij}) = \sqrt{\frac{3}{2} (S_{ij} - \alpha_{ij})(S_{ij} - \alpha_{ij})} - Y = 0$$

where  $Y$  is the initial yield stress of the solid, and a hardening law given by

$$d\alpha_{ij} = \frac{2}{3} c d\varepsilon_{ij}^p - \gamma \alpha_{ij} d\bar{\varepsilon}^p$$

where  $c$  and  $\gamma$  are material properties. In the undeformed solid,  $\alpha_{ij} = 0$ . Calculate the formulas relating the total strain increment  $d\varepsilon_{ij}$  to the state of stress  $\sigma_{ij}$ , the state variables  $\alpha_{ij}$  and the increment in stress  $d\sigma_{ij}$  applied to the solid

3.7.13. Consider a *rigid* nonlinear kinematic hardening solid, with yield surface and hardening law described in the preceding problem.

3.7.13.1. Show that the constitutive law implies that  $\alpha_{kk} = 0$

3.7.13.2. Show that under uniaxial loading with  $\sigma_{11} = \sigma$ ,  $\alpha_{22} = \alpha_{33} = -\alpha_{11}/2$

3.7.13.3. Suppose the material is subjected to a monotonically increasing uniaxial tensile stress  $\sigma_{11} = \sigma$ . Show that the uniaxial stress-strain curve has the form  $\sigma = Y + (c/\gamma)[1 - \exp(-\gamma\varepsilon)]$  (it is simplest to calculate  $\alpha_{ij}$  as a function of the strain and then use the yield criterion to find the stress)

3.7.14. Suppose that a solid contains a large number of randomly oriented slip planes, so that it begins to yield when the resolved shear stress on *any* plane in the solid reaches a critical magnitude  $k$ .

3.7.14.1. Suppose that the material is subjected to principal stresses  $\sigma_1, \sigma_2, \sigma_3$ . Find a formula for the maximum resolved shear stress in the solid, and by means of appropriate sketches, identify the planes that will begin to slip.

3.7.14.2. Draw the yield locus for this material.

3.7.15. Consider a rate independent plastic material with yield criterion  $f(\sigma_{ij}) = 0$ . Assume that (i) the constitutive law for the material has an associated flow rule, so that the plastic strain increment is related to the yield criterion by  $d\varepsilon_{ij}^p = d\bar{\varepsilon}^p \partial f / \partial \sigma_{ij}$ ; and (ii) the yield surface is convex, so that

$$f[\sigma_{ij}^* + \beta(\sigma_{ij} - \sigma_{ij}^*)] - f[\sigma_{ij}^*] \geq 0$$

for all stress states  $\sigma_{ij}$  and  $\sigma_{ij}^*$  satisfying  $f(\sigma_{ij}) = 0$  and  $f(\sigma_{ij}^*) \leq 0$  and  $0 \leq \beta \leq 1$ . Show that the material obeys the principle of maximum plastic resistance.

3.7.16. The yield strength of a frictional material (such as sand) depends on hydrostatic pressure. A simple model of yield and plastic flow in such a material is proposed as follows:

$$\text{Yield criterion } F(\sigma_{ij}) = f(\sigma_{ij}) + \mu\sigma_{kk} = 0 \quad f(\sigma_{ij}) = \sqrt{\frac{3}{2} S_{ij} S_{ij}}$$

$$\text{Flow rule } d\varepsilon_{ij}^p = d\bar{\varepsilon}^p \frac{\partial f}{\partial \sigma_{ij}}$$

Where  $\mu$  is a material constant (some measure of the friction between the sand grains).

- 3.7.16.1. Sketch the yield surface for this material in principal stress space (note that the material looks like a Mises solid whose yield stress increases with hydrostatic pressure. You will need to sketch the full 3D surface, not just the projection that is used for pressure independent surfaces)
- 3.7.16.2. Sketch a vector indicating the direction of plastic flow for some point on the yield surface drawn in part (3.8.3.1)
- 3.7.16.3. By finding a counter-example, demonstrate that this material does not satisfy the principle of maximum plastic resistance

$$(\sigma_{ij} - \sigma_{ij}^*) d\varepsilon_{ij}^p \geq 0$$

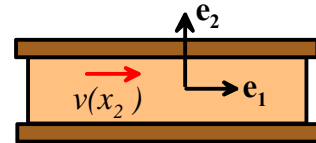
(you can do this graphically, or by finding two specific stress states that violate the condition)

- 3.7.16.4. Demonstrate that the material is not stable in the sense of Drucker – i.e. find a cycle of loading for which the work done by the traction increment through the displacement increment is non-zero.
- 3.7.16.5. What modification would be required to the constitutive law to make it satisfy the PMPR and Drucker stability? How does the physical response of the stable material differ from the original model (think about compaction under combined shear and pressure).

### 3.8. Viscoplasticity

### 3.9. Large strain, rate dependent plasticity

- 3.9.1. The figure shows a thin film of material that is deformed plastically during a pressure-shear plate impact experiment. The goal of this problem is to derive the equations governing the velocity and stress fields in the specimen. Assume that:



- The film deforms in simple shear, and that the velocity  $\mathbf{v} = v(x_2, t)\mathbf{e}_1$  and Kirchoff stress fields  $\boldsymbol{\tau} = q(x_2, t)(\mathbf{e}_1 \otimes \mathbf{e}_2 + \mathbf{e}_2 \otimes \mathbf{e}_1) + p(x_2, t)(\mathbf{e}_1 \otimes \mathbf{e}_1 + \mathbf{e}_2 \otimes \mathbf{e}_2)$  are independent of  $x_1$
  - The material has mass density  $\rho$  and isotropic elastic response, with shear modulus  $\mu$  and Poisson's ratio  $\nu$
  - The film can be idealized as a finite strain viscoplastic solid with power-law Mises flow potential, as described in Section 3.9. Assume that the plastic spin is zero.
- 3.9.1.1. Calculate the velocity gradient tensor  $\mathbf{L}$ , the stretch rate tensor  $\mathbf{D}$  and spin tensor  $\mathbf{W}$  for the deformation, expressing your answer as components in the  $\mathbf{e}_1, \mathbf{e}_2$  basis shown in the figure
  - 3.9.1.2. Find an expression for the plastic stretch rate, in terms of the stress and material properties
  - 3.9.1.3. Use the elastic stress rate-stretch rate relation  $\tau_{ij} = C_{ijkl} D_{kl}^e$  (i) to show that  $p = \text{constant}$  and (ii) to obtain an expression for the time derivative of the shear stress  $q$  in terms of  $v(x_2)$ ,  $\tau$  and appropriate material properties
  - 3.9.1.4. Write down the linear momentum balance equation in terms of  $\tau$  and  $v$ .

3.9.1.5. How would the governing equations change if  $\mathbf{W}^P = \mathbf{W}$  ?

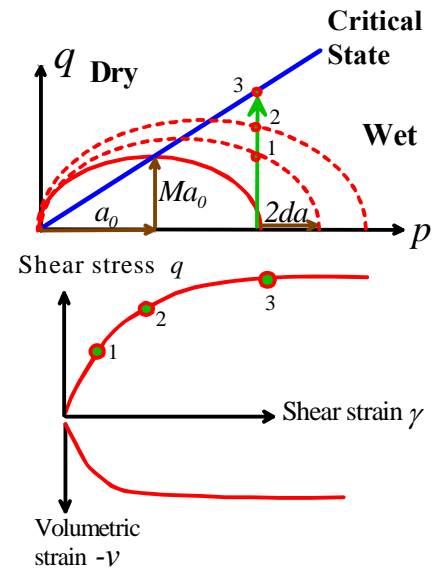
### 3.10. Crystal Plasticity

### 3.11. Critical State Models for Soils

3.11.1. A drained specimen of a soil can be idealized as Cam-clay, using the constitutive equations listed in Section 3.11. At time  $t=0$  the soil has a strength  $a_0$ . The specimen is subjected to a monotonically increasing hydrostatic stress  $p$ , and the volumetric strain  $\Delta V/V = \varepsilon_{kk}$  is measured. Calculate a relationship between the pressure and volumetric strain, in terms of the initial strength of the soil  $a_0$  and the hardening rate  $c$ .

3.11.2. An undrained specimen of a soil can be idealized as Cam-clay, using the constitutive equations listed in Section 3.11. The elastic constants of the soil are characterized by its bulk modulus  $K$  and Poisson's ratio  $\nu$ , while its plastic properties are characterized by  $M$  and  $c$ . The fluid has a bulk modulus  $K_w$ . At time  $t=0$  the soil has a cavity volume fraction  $n_0$  and strength  $a_0$ , and  $p_s = p_w = 0$ . The specimen is subjected to a monotonically increasing hydrostatic pressure  $p$ , and is then unloaded. The volumetric strain  $\Delta V/V = \varepsilon_{kk}$  is measured. Assume that both elastic and plastic strains are small. Show that the relationship between the normalized pressure  $p/a_0$  and normalized volumetric strain  $K\varepsilon_{kk}/a_0$  is a function of only three dimensionless material properties:  $\alpha = K_w/n_0a_0c$ ,  $\beta = K/a_0c$  and  $\gamma = n_0c$ . Plot the dimensionless pressure-volume curves (showing both the elastic and plastic parts of the loading cycle for a few representative values of  $\alpha$ ,  $\beta$  and  $\gamma$ .

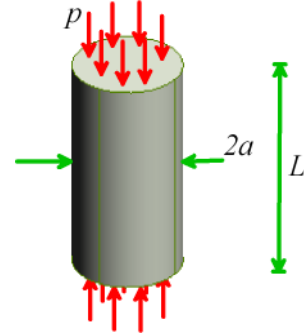
3.11.3. A drained specimen of Cam-clay is first subjected to a monotonically increasing confining pressure  $p$ , with maximum value  $p > a_0$ . The confining pressure is then held constant, and the specimen is subjected to a monotonically increasing shear stress  $q$ . Calculate the volumetric strain  $\varepsilon_{kk}^p$  and the shear strain  $\varepsilon_{12}^p$  during the shear loading as a function of  $q$  and appropriate material properties, and plot the resulting shear stress-shear strain and volumetric strain-shear strain curves as indicated in the figure.



## 4. Solutions to simple boundary and initial value problems

### 4.1. Axially and Spherically Symmetric Solutions for Linear Elastic Solids

4.1.1. A solid cylindrical bar with radius  $a$  and length  $L$  is subjected to a uniform pressure  $p$  on its ends. The bar is made from a linear elastic solid with Young's modulus  $E$  and Poisson's ratio  $\nu$ .



4.1.1.1. Write down the components of the stress in the bar. Show that the stress satisfies the equation of static equilibrium, and the boundary conditions  $\sigma_{ij}n_i = t_j$  on all its surfaces. Express your answer as components in a Cartesian basis  $\{\mathbf{e}_1, \mathbf{e}_2, \mathbf{e}_3\}$  with  $\mathbf{e}_1$  parallel to the axis of the cylinder.

4.1.1.2. Find the strain in the bar (neglect temperature changes)

4.1.1.3. Find the displacement field in the bar

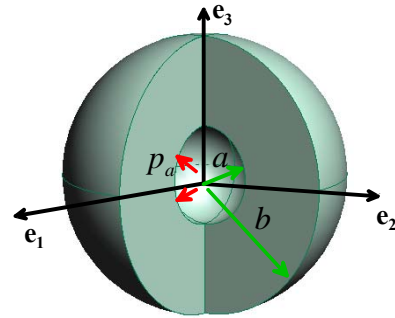
4.1.1.4. Calculate a formula for the change in length of the bar

4.1.1.5. Find a formula for the stiffness of the bar (stiffness = force/extension)

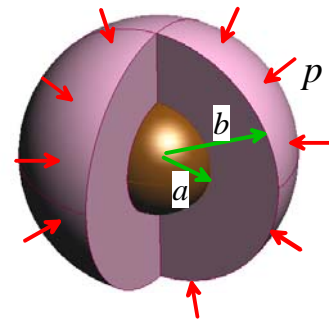
4.1.1.6. Find the change in volume of the bar

4.1.1.7. Calculate the total strain energy in the bar.

4.1.2. Elementary calculations predict that the stresses in a internally pressurized thin-walled sphere with radius  $R$  and wall thickness  $t \ll R$  are  $\sigma_{\theta\theta} \approx \sigma_{\phi\phi} \approx pR/2t$ ,  $\sigma_{rr} \approx p/2$ . Compare this estimate with the exact solution in Section 4.1.4. To do this, set  $a = R[1 - t/(2R)]$ ,  $b = R[1 + t/(2R)]$  and expand the formulas for the stresses as a Taylor series in  $t/R$ . Suggest an appropriate range of  $t/R$  for the thin-walled approximation to be accurate.



4.1.3. A baseball can be idealized as a small rubber core with radius  $a$ , surrounded by a shell of yarn with outer radius  $b$ . As a first approximation, assume that the yarn can be idealized as a linear elastic solid with Young's modulus  $E_s$  and Poisson's ratio  $\nu_s$ , while the core can be idealized as an incompressible material. Suppose that ball is subjected to a uniform pressure  $p$  on its outer surface. Note that, if the core is incompressible, its outer radius cannot change, and therefore the radial displacement  $u_R = 0$  at  $R = a$ . Calculate the full displacement and stress fields in the yarn in terms of  $p$  and relevant geometric variables and material properties.



4.1.4. Reconsider problem 3, but this time assume that the core is to be idealized as a linear elastic solid with Young's modulus  $E_c$  and Poisson's ratio  $\nu_c$ . Give expressions for the displacement and stress fields in both the core and the outer shell.

4.1.5. Suppose that an elastic sphere, with outer radius  $a + \Delta$ , and with Young's modulus  $E$  and Poisson's ratio  $\nu$  is inserted into a spherical shell with identical elastic properties, but with inner radius  $a$  and outer radius  $b$ . Assume that  $\Delta \ll a$  so that the deformation can be analyzed using linear elasticity theory. Calculate the stress and displacement fields in both the core and the outer shell.

4.1.6. A spherical planet with outer radius  $a$  has a radial variation in its density that can be described as

$$\rho(R) = \rho_0 a^2 / (a^2 + R^2)$$

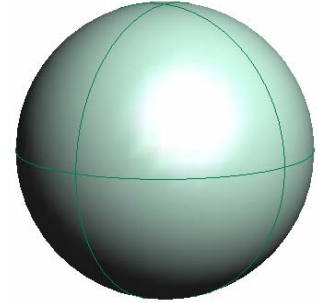
As a result, the interior of the solid is subjected to a radial body force field

$$\mathbf{b} = -\frac{ga}{R(1 - \pi/4)} \left( 1 - \frac{a}{R} \tan^{-1} \frac{R}{a} \right) \mathbf{e}_r$$

where  $g$  is the acceleration due to gravity at the surface of the sphere.

Assume that the planet can be idealized as a linear elastic solid with

Young's modulus  $E$  and Poisson's ratio  $\nu$ . Calculate the displacement and stress fields in the solid.



4.1.7. A solid, spherical nuclear fuel pellet with outer radius  $a$  is subjected to a uniform internal distribution of heat due to a nuclear reaction. The heating induces a steady-state temperature field

$$T(r) = (T_a - T_0) \frac{r^2}{a^2} + T_0$$

where  $T_0$  and  $T_a$  are the temperatures at the center and outer surface of the pellet, respectively.

Assume that the pellet can be idealized as a linear elastic solid with Young's modulus  $E$ , Poisson's ratio  $\nu$  and thermal expansion coefficient  $\alpha$ . Calculate the distribution of stress in the pellet.

4.1.8. A long cylindrical pipe with inner radius  $a$  and outer radius  $b$  has hot fluid with temperature  $T_a$  flowing through it. The outer surface of the pipe has temperature  $T_b$ . The inner and outer surfaces of the pipe are traction free. Assume plane strain deformation, with  $\varepsilon_{zz} = 0$ . In addition, assume that the temperature distribution in the pipe is given by

$$T(r) = \frac{T_a \log(r/b) - T_b \log(r/a)}{\log(a/b)}$$

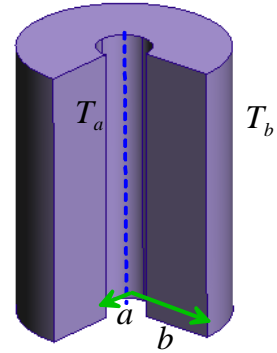
4.1.8.1. Calculate the stress components  $\sigma_{rr}, \sigma_{\theta\theta}, \sigma_{zz}$  in the pipe.

4.1.8.2. Find a formula for the variation of Von-Mises stress

$$\sigma_e = \sqrt{\frac{1}{2} \left\{ (\sigma_1 - \sigma_2)^2 + (\sigma_1 - \sigma_3)^2 + (\sigma_2 - \sigma_3)^2 \right\}}$$

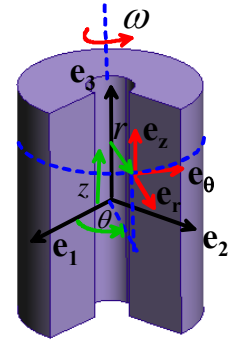
in the tube. Where does the maximum value occur?

4.1.8.3. The tube will yield if the von Mises stress reaches the yield stress of the material. Calculate the critical temperature difference  $T_a - T_b$  that will cause yield in a mild steel pipe.



## 4.2. Axially and spherically symmetric solutions to quasi-static elastic-plastic problems

4.2.1. The figure shows a long hollow cylindrical shaft with inner radius  $a$  and outer radius  $b$ , which spins with angular speed  $\omega$  about its axis. Assume that the disk is made from an elastic-perfectly plastic material with yield stress  $Y$  and density  $\rho$ . The goal of this problem is to calculate the critical angular speed that will cause the cylinder to collapse (the point of plastic collapse occurs when the entire cylinder reaches yield).



Plane strain

4.2.1.1. Using the cylindrical-polar basis shown, list any stress or strain components that must be zero. Assume plane strain deformation.

4.2.1.2. Write down the boundary conditions that the stress field must satisfy at  $r=a$  and  $r=b$

4.2.1.3. Write down the linear momentum balance equation in terms of the stress components, the angular velocity and the disk's density. Use polar coordinates and assume axial symmetry.

4.2.1.4. Using the plastic flow rule, show that  $\sigma_{zz} = (\sigma_{rr} + \sigma_{\theta\theta})/2$  if the cylinder deforms plastically under plane strain conditions

4.2.1.5. Using Von-Mises yield criterion, show that the radial and hoop stress must satisfy  $|\sigma_{\theta\theta} - \sigma_{rr}| = 2Y/\sqrt{3}$

4.2.1.6. Hence, show that the radial stress must satisfy the equation

$$\frac{d\sigma_{rr}}{dr} = -\rho r \omega^2 + \frac{2}{\sqrt{3}} \frac{Y}{r}$$

4.2.1.7. Finally, calculate the critical angular speed that will cause plastic collapse.

4.2.2. Consider a spherical pressure vessel subjected to cyclic internal pressure, as described in Section 4.2.4. Show that a cyclic plastic zone can only develop in the vessel if  $b/a$  exceeds a critical magnitude. Give a formula for the critical value of  $b/a$ , and find a (numerical, if necessary) solution for  $b/a$ .

4.2.3. A long cylindrical pipe with internal bore  $a$  and outer diameter  $b$  is made from an elastic-perfectly plastic solid, with Young's modulus  $E$ , Poisson's ratio  $\nu$  and uniaxial tensile yield stress  $Y$  is subjected to internal pressure. The (approximate) solution for a cylinder that is subjected to a monotonically increasing pressure is given in Section 4.2.6. The goal of this problem is to extend the solution to investigate the behavior of a cylinder that is subjected to *cyclic* pressure.

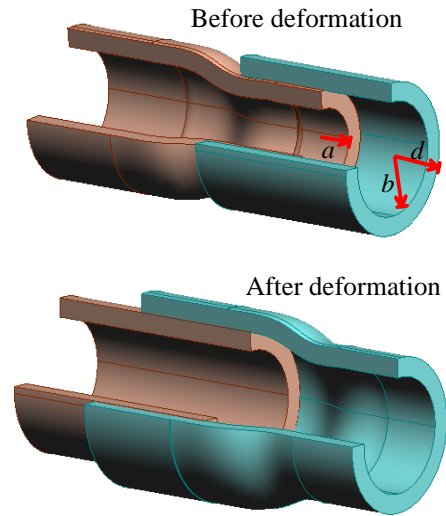
4.2.3.1. Suppose that the internal pressure is first increased to a value that lies in the range  $(1 - a^2/b^2) < \sqrt{3}p_a/Y < 2\log(b/a)$ , and then returned to zero. Assume that the solid unloads elastically (so the *change* in stress during unloading can be calculated using the elastic solution). Calculate the residual stress in the cylinder after unloading.

4.2.3.2. Hence, determine the critical internal pressure at which the residual stresses cause the cylinder to yield after unloading

4.2.3.3. Find the stress and displacement in the cylinder at the instant maximum pressure, and after subsequent unloading, for internal pressures exceeding the value calculated in 4.2.3.2.



4.2.4. The following technique is sometimes used to connect tubular components down oil wells. As manufactured, the smaller of the two tubes has inner and outer radii  $(a, b)$ , while the larger has inner and outer radii  $(b, d)$ , so that the end of the smaller tube can simply be inserted into the larger tube. An over-sized die is then pulled through the bore of the inner of the two tubes. The radius of the die is chosen so that both cylinders are fully plastically deformed as the die passes through the region where the two cylinders overlap. As a result, a state of residual stress is developed at the coupling, which clamps the two tubes together. Assume that the tubes are elastic-perfectly plastic solids with Young's modulus  $E$ , Poisson's ratio  $\nu$  and yield stress in uniaxial tension  $Y$ .

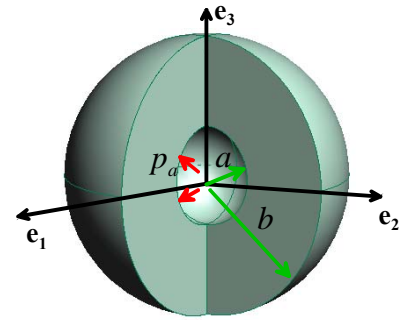


- 4.2.4.1. Use the solution given in Section 4.2.6 to calculate the radius of the die that will cause both cylinders to yield throughout their wall-thickness (i.e. the radius of the plastic zone must reach  $d$ ).
- 4.2.4.2. The die effectively subjects to the inner bore of the smaller tube to a cycle of pressure. Use the solution to the preceding problem to calculate the residual stress distribution in the region where the two tubes overlap (neglect end effects and assume plane strain deformation)
- 4.2.4.3. For  $d/a = 1.5$ , calculate the value of  $b$  that gives the strongest coupling.

4.2.5. A spherical pressure vessel is subjected to internal pressure  $p_a$  and is free of traction on its outer surface. The vessel deforms by creep, and may be idealized as an elastic-power law viscoplastic solid with flow potential

$$g(\sigma_e) = \dot{\epsilon}_0 \left( \frac{\sigma_e}{Y} \right)^m$$

where  $Y, m, \dot{\epsilon}_0$  are material properties and  $\sigma_e$  is the Von-Mises equivalent stress. Calculate the steady-state stress and strain rate fields in the solid, and deduce an formula for the rate of expansion of the inner bore of the vessel. Note that at steady state, the stress is constant, and so the elastic strain rate must vanish.



### 4.3. Spherically and axially symmetric solutions to quasi-static large strain elasticity problems

- 4.3.1. Consider the pressurized hyperelastic spherical shell described in Section 4.3.3. For simplicity, assume that the shell is made from an incompressible neo-Hookean material (recall that the Neo-Hookean constitutive equation is the special case  $\mu_2 = 0$  in the Mooney-Rivlin material). Calculate the total strain energy of the sphere, in terms of relevant geometric and material parameters. Hence, derive



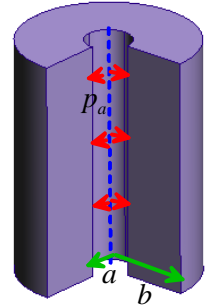
an expression for the total potential energy of the system (assume that the interior and exterior are subjected to constant pressure). Show that the relationship between the internal pressure and the geometrical parameters  $\alpha = a/A$ ,  $\beta = b/B$  can be obtained by minimizing the potential energy of the system.

4.3.2. Consider an internally pressurized hollow rubber cylinder, as shown in the picture. Assume that

- Before deformation, the cylinder has inner radius  $A$  and outer radius  $B$
- After deformation, the cylinder has inner radius  $a$  and outer radius  $b$
- The solid is made from an incompressible Mooney-Rivlin solid, with strain energy potential

$$U = \frac{\mu_1}{2}(I_1 - 3) + \frac{\mu_2}{2}(I_2 - 3)$$

- No body forces act on the cylinder; the inner surface  $r=a$  is subjected to pressure  $p_a$ ; while the outer surface  $r=b$  is free of stress.
- Assume plane strain deformation.



Assume that a material particle that has radial position  $R$  before deformation moves to a position  $r=f(R)$  after the cylinder is loaded.

- 4.3.2.1. Express the incompressibility condition  $\det(\mathbf{F})=1$  in terms of  $f(R)$
- 4.3.2.2. Integrate the incompressibility condition to calculate  $r$  in terms of  $R, A$  and  $a$ , and also calculate the inverse expression that relates  $R$  to  $A, a$  and  $r$ .
- 4.3.2.3. Calculate the components of the left Cauchy-Green deformation tensor  $B_{rr}, B_{\theta\theta}$
- 4.3.2.4. Find an expression for the Cauchy stress components  $\sigma_{rr}, \sigma_{\theta\theta}$  in the cylinder in terms of  $B_{rr}, B_{\theta\theta}$  and an indeterminate hydrostatic stress  $p$ .
- 4.3.2.5. Use 3.4 and the equilibrium equation to derive an expression for the radial stress  $\sigma_{rr}$  in the cylinder. Use the boundary conditions to find a relationship between the applied pressure and  $\alpha = a/A$ ,  $\beta = b/B$ .
- 4.3.2.6. Plot a graph showing the variation of normalized pressure  $p_a B^2 / (\mu_1 + \mu_2)(B^2 - A^2)$  as a function of the normalized displacement of the inner bore of the cylinder  $a/A - 1$ . Compare the nonlinear elastic solution with the equivalent linear elastic solution.

4.3.3. A long rubber tube has internal radius  $A$  and external radius  $B$ . The tube can be idealized as an incompressible neo-Hookean material with material constant  $\mu_1$ . The tube is turned inside-out, so that the surface that lies at  $R=A$  in the undeformed configuration moves to  $r=a$  in the deformed solid, while the surface that lies at  $R=B$  moves to  $r=b$ . Note that  $B > A$ , and  $a > b$ . To approximate the deformation, assume that

- planes that lie perpendicular to  $\mathbf{e}_z$  in the undeformed solid remain perpendicular to  $\mathbf{e}_z$  after deformation
- The axial stretch  $\lambda_{zz}$  in the tube is constant

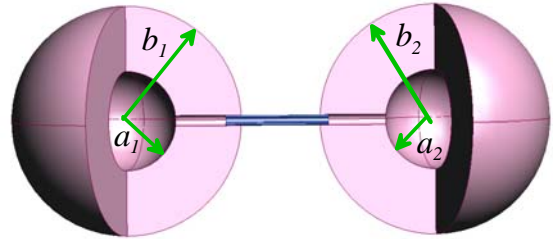
It is straightforward to show that the deformation mapping can be described as

$$\begin{aligned} r &= \sqrt{a^2 + (B^2 - R^2)/\lambda_{zz}} & R &= \sqrt{B^2 + (a^2 - r^2)\lambda_{zz}} \\ z &= -\lambda_{zz}Z & Z &= -z/\lambda_{zz} \end{aligned}$$

- 4.3.3.1. Calculate the deformation gradient, expressing your answer in terms of  $R$ , as components in the  $\{\mathbf{e}_r, \mathbf{e}_\theta, \mathbf{e}_z\}$  basis. Verify that the deformation preserves volume.
- 4.3.3.2. Calculate the components of the left Cauchy-Green deformation tensor  $B_{rr}, B_{\theta\theta}, B_{zz}$

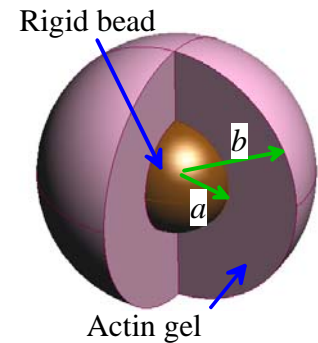
- 4.3.3.3. Find an expression for the Cauchy stress components  $\sigma_{rr}, \sigma_{\theta\theta}, \sigma_{zz}$  in the cylinder in terms of  $B_{rr}, B_{\theta\theta}$  and an indeterminate hydrostatic stress  $p$ .
- 4.3.3.4. Use 4.3 and the equilibrium equation and boundary conditions to calculate an expressions for the Cauchy stress components.
- 4.3.3.5. Finally, use the condition that the resultant force acting on any cross-section of the tube must vanish to obtain an equation for the axial stretch  $\lambda_{zz}$ . Does the tube get longer or shorter when it is inverted?

- 4.3.4. Two spherical, hyperelastic shells are connected by a thin tube, as shown in the picture. When stress free, both spheres have internal radius  $A$  and external radius  $B$ . The material in each sphere can be idealized as an incompressible, neo-Hookean solid, with material constant  $\mu_1$ . Suppose that the two



spheres together contain a volume  $V \geq 8\pi A^3/3$  of an incompressible fluid. As a result, the two spheres have deformed internal and external radii  $(a_1, b_1)$ ,  $(a_2, b_2)$  as shown in the picture. Investigate the possible equilibrium configurations for the system, as functions of the dimensionless fluid volume  $\omega = V/(8\pi A^3/3) - 1$  and  $B/A$ . To display your results, plot a graph showing the equilibrium values of  $\alpha_1 = a_1/A$  as a function of  $\omega$ , for various values of  $B/A$ . You should find that for small values of  $\omega$  there is only a single stable equilibrium configuration. For  $\omega$  exceeding a critical value, there are three possible equilibrium configurations: two in which one sphere is larger than the other (these are stable), and a third in which the two spheres have the same size (this is unstable).

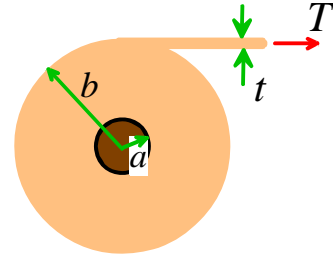
- 4.3.5. In a model experiment intended to duplicate the propulsion mechanism of the lysteria bacterium, a spherical bead with radius  $a$  is coated with an enzyme known as an “Arp2/3 activator.” When suspended in a solution of actin, the enzyme causes the actin to polymerize at the surface of the bead. The polymerization reaction causes a spherical gel of a dense actin network to form around the bead. New gel is continuously formed at the bead/gel interface, forcing the rest of the gel to expand radially around the bead. The actin gel is a long-chain polymer and consequently can be idealized as a rubber-like incompressible neo-Hookean material. Experiments show that after reaching a critical radius the actin gel loses spherical symmetry and occasionally will fracture. Stresses in the actin network are believed to drive both processes. In this problem you will calculate the stress state in the growing, spherical, actin gel.



- 4.3.5.1. Note that this is an unusual boundary value problem in solid mechanics, because a compatible reference configuration cannot be identified for the solid. Nevertheless, it is possible to write down a deformation gradient field that characterizes the change in shape of infinitesimal volume elements in the gel. To this end: (a) write down the length of a circumferential line at the surface of the bead; (b) write down the length of a circumferential line at radius  $r$  in the gel; (c) use these results, together with the incompressibility condition, to write down the deformation gradient characterizing the shape change of a material element that has been displaced from  $r=a$  to a general position  $r$ . Assume that the bead is rigid, and that the deformation is spherically symmetric.

- 4.3.5.2. Suppose that new actin polymer is generated at volumetric rate  $\dot{V}$ . Use the incompressibility condition to write down the velocity field in the actin gel in terms of  $\dot{V}$ ,  $a$  and  $r$  (think about the volume of material crossing a radial line per unit time)
- 4.3.5.3. Calculate the velocity gradient  $\mathbf{v} \otimes \nabla$  in the gel (a) by direct differentiation of 5.2 and (b) by using the results of 5.1. Show that the results are consistent.
- 4.3.5.4. Calculate the components of the left Cauchy-Green deformation tensor field and hence write down an expression for the Cauchy stress field in the solid, in terms of an indeterminate hydrostatic pressure.
- 4.3.5.5. Use the equilibrium equations and boundary condition to calculate the full Cauchy stress distribution in the bead. Assume that the outer surface of the gel (at  $r=b$ ) is traction free.

- 4.3.6. A rubber sheet is wrapped around a rigid cylindrical shaft with radius  $a$ . The sheet has thickness  $t$ , and can be idealized as an incompressible neo-Hookean solid. A constant tension  $T$  per unit out-of-plane distance is applied to the sheet during the wrapping process. Calculate the full stress field in the solid rubber, and find an expression for the radial pressure acting on the shaft. Assume that  $t/b \rightarrow 0$  and neglect the shear stress component  $\sigma_{r\theta}$ .

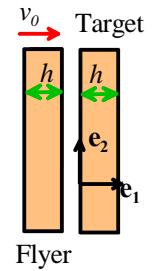


#### 4.4. Solutions to simple dynamic problems involving linear elastic solids

- 4.4.1. Calculate longitudinal and shear wave speeds in (a) Aluminum nitride; (b) Steel; (d) Aluminum and (e) Rubber.
- 4.4.2. A linear elastic half-space with Young's modulus  $E$  and Poisson's ratio  $\nu$  is stress free and stationary at time  $t=0$ , is then subjected to a constant pressure  $p_0$  on its surface for  $t>0$ .
- 4.4.2.1. Calculate the stress, displacement and velocity in the solid as a function of time
- 4.4.2.2. Calculate the total kinetic energy of the half-space as a function of time
- 4.4.2.3. Calculate the total potential energy of the half-space as a function of time
- 4.4.2.4. Verify that the sum of the potential and kinetic energy is equal to the work done by the tractions acting on the surface of the half-space.
- 4.4.3. The surface of an infinite linear elastic half-space with Young's modulus  $E$  and Poisson's ratio  $\nu$  is subjected to a harmonic pressure on its surface, given by  $p(t) = p_0 \sin \omega t$   $t>0$ , with  $p=0$  for  $t<0$ .
- 4.4.3.1. Calculate the distribution of stress, velocity and displacement in the solid.
- 4.4.3.2. What is the phase difference between the displacement and pressure at the surface?
- 4.4.3.3. Calculate the total work done by the applied pressure in one cycle of loading.
- 4.4.4. A linear elastic solid with Young's modulus  $E$  Poisson's ratio  $\nu$  and density  $\rho$  is bonded to a rigid solid at  $x_1 = a$ . Suppose that a plane wave with displacement and stress field

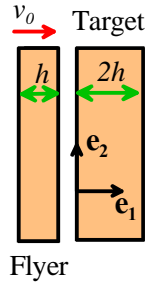
$$u_2(x_1, t) = \begin{cases} \frac{(1-2\nu)(1+\nu)}{(1-\nu)} \frac{\sigma_0}{E} (c_L t - x_1) & x_1 < c_L t \\ 0 & x_1 > c_L t \end{cases} \quad \sigma_{11} = \begin{cases} -\sigma_0 & x_1 < c_L t \\ 0 & x_1 > c_L t \end{cases}$$

is induced in the solid, and at time  $t = x_1/a$  is reflected off the interface. Find the reflected wave, and sketch the variation of stress and velocity in the elastic solid just before and just after the reflection occurs.



4.4.5. Consider the plate impact experiment described in Section 4.4.8

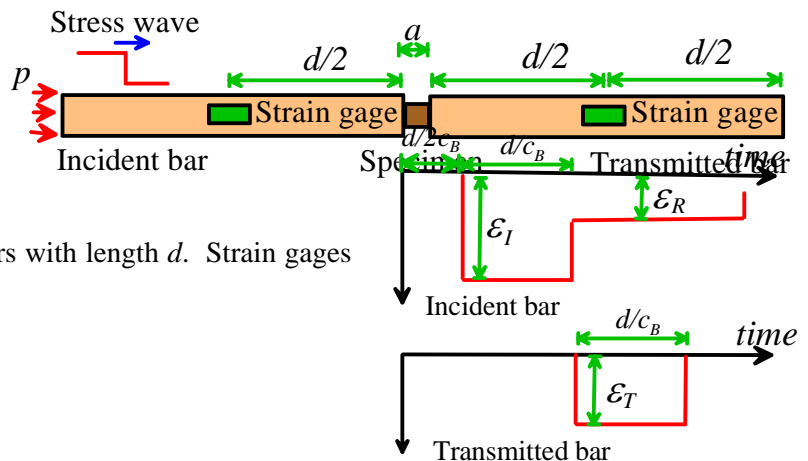
- 4.4.5.1. Draw graphs showing the stress and velocity at the impact face of the flyer plate as a function of time.
- 4.4.5.2. Draw graphs showing the stress and velocity at the rear face of the flyer plate as a function of time
- 4.4.5.3. Draw graphs showing the stress and velocity at the mid-plane of the flyer plate as a function of time
- 4.4.5.4. Draw a graph showing the total strain energy and kinetic energy of the system as a function of time. Verify that total energy is conserved.
- 4.4.5.5. Draw a graph showing the total momentum of the flyer plate and the target plate as a function of time. Verify that momentum is conserved.



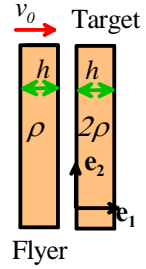
4.4.6. In a plate impact experiment, two identical elastic plates with thickness  $h$ , Young's modulus  $E$ , Poisson's ratio  $\nu$ , density  $\rho$  and longitudinal wave speed  $c_L$  are caused to collide, as shown in the picture. Just prior to impact, the projectile has a uniform velocity  $v_0$ . Draw the  $(x, t)$  diagram for the two solids after impact. Show that the collision is perfectly elastic, in the terminology of rigid body collisions, in the sense that all the energy in the flyer is transferred to the target.

4.4.7. In a plate impact experiment, an elastic plates with thickness  $h$ , Young's modulus  $E$ , Poisson's ratio  $\nu$ , density  $\rho$  and longitudinal wave speed  $c_L$  impacts a second plate with identical elastic properties, but thickness  $2h$ , as shown in the picture. Just prior to impact, the projectile has a uniform velocity  $v_0$ . Draw the  $(x, t)$  diagram for the two solids after impact.

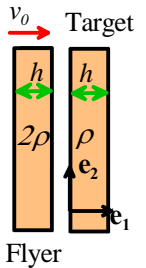
4.4.8. A "Split-Hopkinson bar" or "Kolsky bar" is an apparatus that is used to measure plastic flow in materials at high rates of strain (of order 1000/s). The apparatus is sketched in the figure. A small specimen of the material of interest, with length  $a \ll d$ , is placed between two long slender bars with length  $d$ . Strain gages



are attached near the mid-point of each bar. At time  $t=0$  the system is stress free and at rest. Then, for  $t>0$  a constant pressure  $p$  is applied to the end of the incident bar, sending a plane wave down the bar. This wave eventually reaches the specimen. At this point part of the wave is reflected back up the incident bar, and part of it travels through the specimen and into the second bar (known as the 'transmission bar'). The history of stress and strain in the specimen can be deduced from the history of strain measured by the two strain gages. For example, if the specimen behaves as an elastic-perfectly plastic solid, the incident and reflected gages would record the data shown in the figure. The goal of this problem is to calculate a relationship between the measured strains and the stress and strain rate in the specimen. Assume that the bars are linear elastic with Young's modulus  $E$  and density  $\rho$ , and wave speed  $c_B \approx \sqrt{E/\rho}$ , and that the bars deform in uniaxial compression.



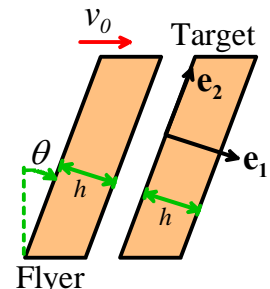
- 4.4.8.1. Write down the stress, strain and velocity field in the incident bar as a function of time and distance down the bar in terms of the applied pressure  $p$  and relevant material and geometric parameters, for  $t < d/c_B$ .
- 4.4.8.2. Assume that the waves reflected from, and transmitted through, the specimen are both plane waves. Let  $\varepsilon_R$  and  $\varepsilon_T$  denote the compressive strains in the regions behind the reflected and transmitted wave fronts, respectively. Write down expressions for the stress and velocity behind the wave fronts in both incident and transmitted bars in terms of  $\varepsilon_R$  and  $\varepsilon_T$ , for  $2d/c_B > t > d/c_B$ .
- 4.4.8.3. The stress behind the reflected and transmitted waves must equal the stress in the specimen. In addition, the strain rate in the specimen can be calculated from the relative velocity of the incident and transmitted bars where they touch the specimen. Show that the strain rate in the specimen can be calculated from the measured strains as  $(\varepsilon_I - \varepsilon_R - \varepsilon_T)c_L/a$ , while the stress in the specimen can be calculated from  $\sigma = E\varepsilon_T$ .



- 4.4.9. In a plate impact experiment, two plates with identical thickness  $h$ , Young's modulus  $E$ , Poisson's ratio  $\nu$  and density  $\rho$  are caused to collide, as shown in the picture. The target plate has twice the mass density of the flyer plate. Find the stress and velocity behind the waves generated by the impact in both target and flyer plate. Hence, draw the  $(x,t)$  diagram for the two solids after impact.

- 4.4.10. In a plate impact experiment, two plates with identical thickness  $h$ , Young's modulus  $E$ , Poisson's ratio  $\nu$ , and density  $\rho$  are caused to collide, as shown in the picture. The flyer plate has twice the mass density of the target plate. Find the stress and velocity behind the waves generated by the impact in both target and flyer plate. Hence, draw the  $(x,t)$  diagram for the two solids after impact.

- 4.4.11. The figure shows a *pressure-shear* plate impact experiment. A flyer plate with speed  $v_0$  impacts a stationary target. Both solids have identical thickness  $h$ , Young's modulus  $E$ , Poisson's ratio  $\nu$ , density  $\rho$  and longitudinal and shear wave speeds  $c_L$  and  $c_S$ . The faces of the plates are inclined at an angle  $\theta$  to the initial velocity, as shown in the figure. Both pressure and shear waves are generated by the impact. Let  $\{\mathbf{e}_1, \mathbf{e}_2\}$  denote unit vectors. Let  $\sigma_{11} = \sigma_0$  denote the (uniform) stress behind the



propagating pressure wave in both solids just after impact, and  $\sigma_{12} = \tau_0$  denote the shear stress behind the shear wave-front. Similarly, let  $\Delta v_1^f, \Delta v_2^f$  denote the change in longitudinal and transverse velocity in the flier across the pressure and shear wave fronts, and let  $\Delta v_1^t, \Delta v_2^t$  denote the corresponding velocity changes in the target plate. Assume that the interface does not slip after impact, so that both velocity and stress must be equal in both flier and target plate at the interface just after impact. Find expressions for  $\sigma_0, \tau_0, \Delta v_1^f, \Delta v_2^f, \Delta v_1^t, \Delta v_2^t$  in terms of  $v_0, \theta$  and relevant material properties.

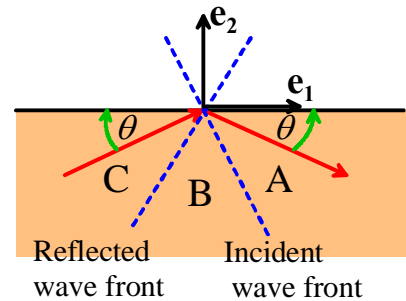
4.4.12. Draw the full  $(x, t)$  diagram for the pressure-shear configuration described in problem 11. Assume that the interface remains perfectly bonded until it separates under the application of a tensile stress. Note that you will have to show  $(x, t)$  diagrams associated with both shear and pressure waves.

4.4.13. Consider an isotropic, linear elastic solid with Young's modulus  $E$ , Poisson's ratio  $\nu$ , density  $\rho$  and shear wave speed  $c_S$ . Suppose that a plane, constant stress shear wave propagates through the solid, which is initially at rest. The wave propagates in a direction  $\mathbf{p} = \cos \theta \mathbf{e}_1 + \sin \theta \mathbf{e}_2$ , and the material has particle velocity  $\mathbf{v} = V \mathbf{e}_3$  behind the wave-front.

4.4.13.1. Calculate the components of stress in the solid behind the wave front.

4.4.13.2. Suppose that the wave front is incident on a flat, stress free surface. Take the origin for the coordinate system at some arbitrary time  $t$  at the point where the propagating wave front just intersects the surface, as shown in the picture. Write down the velocity of this intersection point (relative to a stationary observer) in terms of  $V$  and  $\theta$ .

4.4.13.3. The surface must be free of traction both ahead and behind the wave front. Show that the boundary condition can be satisfied by superposing a second constant stress wave front, which intersects the free surface at the origin of the coordinate system defined in 13.2, and propagates in a direction  $\mathbf{p} = \cos \theta \mathbf{e}_1 - \sin \theta \mathbf{e}_2$ . Hence, write down the stress and particle velocity in each of the three sectors A, B, C shown in the figure. Draw the displacement of the free surface of the half-space.

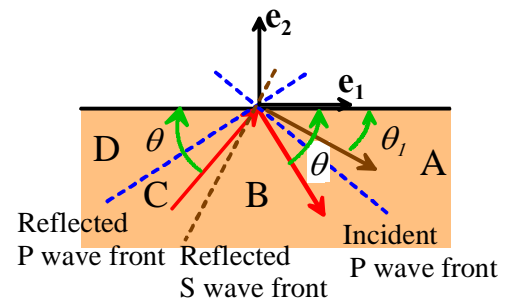


4.4.14. Suppose that a plane, constant stress pressure wave propagates through an isotropic, linear elastic solid that is initially at rest. The wave propagates in a direction  $\mathbf{p} = \cos \theta \mathbf{e}_1 + \sin \theta \mathbf{e}_2$ , and the material has particle velocity  $\mathbf{v} = V \mathbf{p}$  behind the wave-front.

4.4.14.1. Calculate the components of stress in the solid behind the wave front.

4.4.14.2. Suppose that the wave front is incident on a flat, stress free surface. Take the origin for the coordinate system at some arbitrary time  $t$  at the point where the propagating wave front just intersects the surface, as shown in the picture. Write down the velocity of this intersection point (relative to a stationary observer) in terms of  $V$  and  $\theta$ .

4.4.14.3. The pressure wave is reflected as two waves – a reflected pressure wave, which propagates in direction  $\mathbf{p} = \cos \theta \mathbf{e}_1 - \sin \theta \mathbf{e}_2$  and has particle velocity  $v_p \mathbf{p}$  and a reflected shear wave,



which propagates in direction  $\mathbf{p} = \cos \theta_1 \mathbf{e}_1 - \sin \theta_1 \mathbf{e}_2$  and has particle velocity  $v_s (\sin \theta_1 \mathbf{e}_1 + \cos \theta_1 \mathbf{e}_2)$ . Use the condition that the incident wave and the two reflected waves must always intersect at the same point on the surface to write down an equation for  $\theta_1$  in terms of  $\theta$  and Poisson's ratio.

- 4.4.14.4. The surface must be free of traction. Find equations for  $v_p$  and  $v_s$  in terms of  $V$ ,  $\theta$ ,  $\theta_1$  and Poisson's ratio.
- 4.4.14.5. Find the special angles for which the incident wave is reflected *only* as a shear wave (this is called "mode conversion")

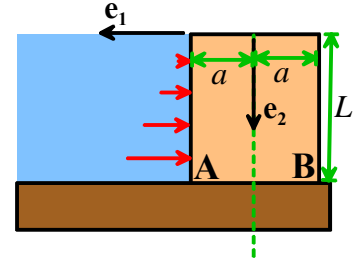


## 5. Chapter 5: Analytical Techniques and Solutions for Linear Elastic Solids

### 5.1. General Principles

### 5.2. Airy Function Solution to Plane Stress and Strain Static Linear Elastic Problems

5.2.1. A rectangular dam is subjected to pressure  $p(x_2) = \rho_w x_2$  on one face, where  $\rho_w$  is the weight density of water. The dam is made from concrete, with weight density  $\rho_c$  (and is therefore subjected to a body force  $\rho_c \mathbf{e}_2$  per unit volume). The goal is to calculate formulas for  $a$  and  $L$  to avoid failure.



5.2.1.1. Write down the boundary conditions on all four sides of the dam.

5.2.1.2. Consider the following approximate state of stress in the dam

$$\sigma_{22} = \frac{\rho_w x_2^3 x_1}{4a^3} + \frac{\rho_w x_2 x_1}{20a^3} (-10x_1^2 + 6a^2) - \rho_c x_2$$

$$\sigma_{11} = -\frac{\rho_w x_2}{2} + \frac{\rho_w x_2 x_1}{4a^3} (x_1^2 - 3a^2)$$

$$\sigma_{12} = \frac{3\rho_w x_2^2}{8a^3} (a^2 - x_1^2) - \frac{\rho_w}{8a^3} (a^4 - x_1^4) + \frac{3\rho_w}{20a} (a^2 - x_1^2)$$

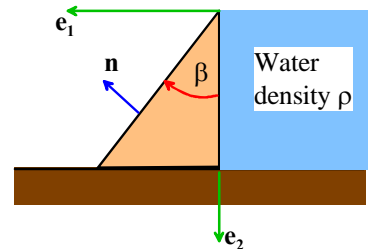
Show that (i) The stress state satisfies the equilibrium equations (ii) the stress state exactly satisfies boundary conditions on the sides  $x_1 = \pm a$ , (iii) The stress does not satisfy the boundary condition on  $x_2 = 0$  exactly.

5.2.1.3. Show, however, that the resultant *force* acting on  $x_2 = 0$  is zero, so by Saint Venant's principle the stress state will be accurate away from the top of the dam.

5.2.1.4. The concrete cannot withstand any tension. Assuming that the greatest principal tensile stress is located at point A ( $x_1 = a, x_2 = L$ ), show that the dam width must satisfy

5.2.1.5. The concrete fails by crushing when the minimum principal stress reaches  $\sigma_{1\min} = -\sigma_c$ . Assuming the greatest principal compressive stress is located at point B, ( $x_1 = -a, x_2 = L$ ) show that the height of the dam cannot exceed

5.2.2. The figure shows a simple design for a dam.



5.2.2.1. Write down an expression for the hydrostatic pressure in the fluid at a depth  $x_2$  below the surface

5.2.2.2. Hence, write down an expression for the traction vector acting on face OA of the dam.

5.2.2.3. Write down an expression for the traction acting on face OB

5.2.2.4. Write down the components of the unit vector normal to face OB in the basis shown



5.2.2.5. Hence write down the boundary conditions for the stress state in the dam on faces OA and OB

5.2.2.6. Consider the candidate Airy function

$$\phi = \frac{C_1}{6} x_1^3 + \frac{C_2}{2} x_1^2 x_2 + \frac{C_3}{2} x_1 x_2^2 + \frac{C_4}{6} x_2^3$$

Is this a valid Airy function? Why?

5.2.2.7. Calculate the stresses generated by the Airy function given in 1.6

5.2.2.8. Use 1.5 and 1.7 to find values for the coefficients in the Airy function, and hence show that the stress field in the dam is

$$\sigma_{11} = -\rho x_2$$

$$\sigma_{22} = \frac{-2\rho}{\tan^3 \beta} x_1 + \frac{\rho}{\tan^2 \beta} x_2$$

$$\sigma_{12} = \frac{-\rho}{\tan^2 \beta} x_1$$

5.2.3. Calculate the stresses generated by the Airy function

$$\phi = -\frac{\sigma_0}{2} \log(r) + \frac{\sigma_0}{4} r^2 + \frac{\sigma_0}{4} \left( 2a^2 - r^2 - \frac{a^4}{r^2} \right) \cos 2\theta$$

Verify that the Airy function satisfies the appropriate governing equation. Show that this stress state represents the solution to a large plate containing a circular hole with radius  $a$  at the origin, which is loaded by a tensile stress  $\sigma_0$  acting parallel to the  $\mathbf{e}_1$  direction. To do this,

5.2.3.1. Show that the surface of the hole is traction free – i.e.  $\sigma_{rr} = \sigma_{r\theta} = 0$  on  $r=a$

5.2.3.2. Show that the stress at  $r/a \rightarrow \infty$  is  $\sigma_{rr} = \sigma_0(1 + \cos 2\theta)/2 = \sigma_0 \cos^2 \theta$ ,  
 $\sigma_{\theta\theta} = 0$   $\sigma_{r\theta} = -\sigma_0 \sin 2\theta$ .

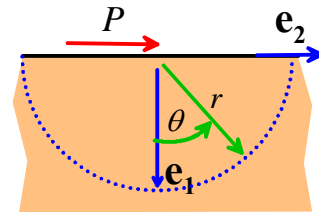
5.2.3.3. Show that the stresses in 6.2 are equivalent to a stress  $\sigma_{11} = \sigma_0$ ,  $\sigma_{22} = \sigma_{12} = 0$ . It is easiest to work backwards – start with the stress components in the  $\{\mathbf{e}_1, \mathbf{e}_2, \mathbf{e}_3\}$  basis and use the basis change formulas to find the stresses in the  $\{\mathbf{e}_r, \mathbf{e}_\theta, \mathbf{e}_z\}$  basis

5.2.3.4. Plot a graph showing the variation of hoop stress  $\sigma_{\theta\theta}/\sigma_0$  with  $\theta$  at  $r=a$  (the surface of the hole). What is the value of the maximum stress, and where does it occur?

5.2.4. The stress due to a line load magnitude  $P$  per unit out-of-plane length acting tangent to the surface of a homogeneous, isotropic half-space can be generated from the Airy function

$$\phi = -\frac{P}{\pi} r \theta \cos \theta$$

Calculate the displacement field in the solid, following the procedure in Section 5.2.6



5.2.5. The stress field in a curved beam subjected to moments acting on its ends can be generated from the stress function

### 5.3. Complex variable Solutions to Static Linear Elasticity Problems

5.3.1. A long cylinder is made from an isotropic, linear elastic solid with shear modulus  $\mu$ . The solid is loaded so

- (i) the resultant forces and moments acting on the ends of the cylinder are zero;
- (ii) the body force  $\mathbf{b} = b(x_1, x_2)\mathbf{e}_3$  in the interior of the solid acts parallel to the axis of the cylinder; and
- (iii) Any tractions  $\mathbf{t} = t(x_1, x_2)\mathbf{e}_3$  or displacements  $\mathbf{u}^* = u^*(x_1, x_2)\mathbf{e}_3$  imposed on the sides of the cylinder are parallel to the axis of the cylinder.

Under these conditions, the displacement field at a point far from the ends of the cylinder has the form  $\mathbf{u} = u(x_1, x_2)\mathbf{e}_3$ , and the solid is said to deform in a state of **anti-plane shear**.

5.3.1.1. Calculate the strain field in the solid in terms of  $u$ .

5.3.1.2. Find an expression for the nonzero stress components in the solid, in terms of  $u$  and material properties.

5.3.1.3. Find the equations of equilibrium for the nonzero stress components.

5.3.1.4. Write down boundary conditions for stress and displacement on the side of the cylinder

5.3.1.5. Hence, show that the governing equations for  $u$  reduce to

$$\frac{\partial^2 u}{\partial x_1^2} + \frac{\partial^2 u}{\partial x_2^2} + b = 0 \quad \left\{ u(\mathbf{x}) = u^*(\mathbf{x}) \quad \mathbf{x} \in S_1 \right\} \quad \left\{ \mu \left( \frac{\partial u(\mathbf{x})}{\partial x_1} n_1(\mathbf{x}) + \frac{\partial u(\mathbf{x})}{\partial x_2} n_2(\mathbf{x}) \right) = t(\mathbf{x}) \quad \mathbf{x} \in S_1 \right\}$$

5.3.2. Let  $\Theta(z)$  be an analytic function of a complex number  $z = x_1 + ix_2$ . Let  $v(x_1, x_2)$ ,  $w(x_1, x_2)$  denote the real and imaginary parts of  $\Theta(z)$ .

5.3.2.1. Since  $\Theta(z)$  is analytic, the real and imaginary parts must satisfy the Cauchy Riemann conditions

$$\frac{\partial v}{\partial x_1} = \frac{\partial w}{\partial x_2} \quad \frac{\partial w}{\partial x_1} = -\frac{\partial v}{\partial x_2}$$

Show that

$$\frac{\partial^2 v}{\partial x_1^2} + \frac{\partial^2 v}{\partial x_2^2} = 0 \quad \frac{\partial^2 w}{\partial x_1^2} + \frac{\partial^2 w}{\partial x_2^2} = 0$$

5.3.2.2. Deduce that the displacement and stress in a solid that is free of body force, and loaded on its boundary so as to induce a state anti-plane shear (see problem 1) can be derived an analytic function  $\Theta(z)$ , using the representation

$$2\mu u(x_1, x_2) = \Theta(z) + \overline{\Theta(z)}$$

$$\sigma_{31} - i\sigma_{32} = \Theta'(z)$$

5.3.3. Calculate the displacements and stresses generated when the complex potential

$$\Theta(z) = -\frac{F}{2\pi} \log(z)$$

is substituted into the representation described in Problem 2. Show that the solution represents the displacement and stress in an infinite solid due to a line force acting in the  $\mathbf{e}_3$  direction at the origin.

5.3.4. Calculate the displacements and stresses generated when the complex potential

$$\Theta(z) = \frac{ib}{2\pi} \log(z)$$

is substituted into the representation described in Problem 2. Show that the solution represents the displacement and stress due to a screw dislocation in an infinite solid, with burgers vector and line direction parallel to  $\mathbf{e}_3$ .

5.3.5. Calculate the displacements and stresses generated when the complex potential

$$\Theta(z) = \tau_0 \left( z - \frac{a^2}{z} \right)$$

is substituted into the representation described in Problem 2. Show that the solution represents the displacement and stress in an infinite solid, which contains a hole with radius  $a$  at the origin, and is subjected to anti-plane shear at infinity

5.3.6. Calculate the displacements and stresses generated when the complex potential

$$\Theta(z) = i\tau_0 \sqrt{z^2 - a^2}$$

is substituted into the representation described in Problem 2. Show that the solution represents the displacement and stress in an infinite solid, which contains a crack with length  $a$  at the origin, and is subjected to a prescribed anti-plane shear stress at infinity. Use the procedure given in Section 5.3.6 to calculate  $\sqrt{z^2 - a^2}$

5.3.7. Consider complex potentials  $\Omega(z) = az + b$ ,  $\omega(z) = cz + d$ , where  $a, b, c, d$  are complex numbers. Let

$$\frac{E}{(1+\nu)} D = (3-4\nu)\Omega(z) - z \overline{\Omega'(z)} - \overline{\omega(z)}$$

$$\sigma_{11} + \sigma_{22} = 2\left(\Omega'(z) + \overline{\Omega'(z)}\right) \quad \sigma_{11} - \sigma_{22} + 2i\sigma_{12} = -2\left(z\overline{\Omega''(z)} + \overline{\omega'(z)}\right)$$

be a displacement and stress field derived from these potentials.

5.3.7.1. Find values of  $a, b, c, d$  that represent a rigid displacement  $u_1 = w_1 + \alpha x_2$ ,  $u_2 = w_2 - \alpha x_1$  where  $w_1, w_2$  are (real) constants representing a translation, and  $\alpha$  is a real constant representing an infinitesimal rotation.

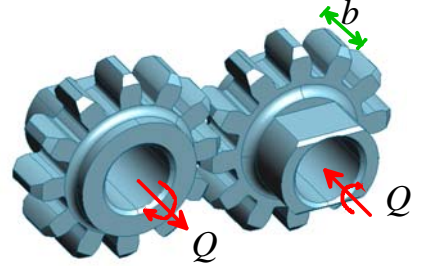
5.3.7.2. Find values of  $a, b, c, d$  that correspond to a state of uniform stress  
Note that the solutions to 7.1 and 7.2 are not unique.

### 5.3.8. The complex potentials

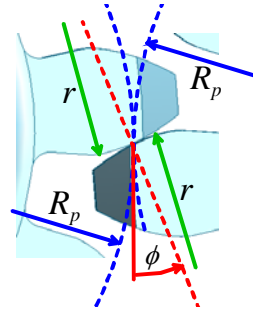
$$\Omega(z) = -i \frac{E(b_1 + ib_2)}{8\pi(1-\nu^2)} \log(z) \quad \omega(z) = i \frac{E(b_1 - ib_2)}{8\pi(1-\nu^2)} \log(z)$$

generate the plane strain solution to an edge dislocation at the origin of an infinite solid. Calculate the displacements and stresses.

- 5.3.9. The figure shows a pair of identical involute spur gears. The contact between the two gears can be idealized as a line contact between two cylindrical surfaces. The goal of this problem is to find an expression for the maximum torque  $Q$  that can be transmitted through the gears. The gears can be idealized as isotropic, linear elastic solids with Young's modulus  $E$  and Poisson's ratio  $\nu$ .



As a representative configuration, consider the instant when a single pair of gear teeth make contact exactly at the pitch point. At this time, the geometry can be idealized as contact between two cylinders, with radius  $r = R_p \sin \phi$ , where  $R_p$  is the pitch circle radius of the gears and  $\phi$  is the pressure angle. The cylinders are pressed into contact by a force  $P = Q / (R_p \cos \phi)$ .



- 5.3.9.1. Find a formula for the area of contact between the two gear teeth, in terms of  $Q$ ,  $R_p$ ,  $\phi$ ,  $b$  and representative material properties.
- 5.3.9.2. Find a formula for the maximum contact pressure acting on the contact area, in terms of  $Q$ ,  $R_p$ ,  $\phi$ ,  $b$  and representative material properties.
- 5.3.9.3. Suppose that the gears have uniaxial tensile yield stress  $Y$ . Find a formula for the critical value of  $Q$  required to initiate yield in the gears.

## 5.4. Solutions to 3D static problems in linear elasticity

- 5.4.1. Consider the Papkovitch-Neuber potentials

$$\Psi_i = \frac{(1-\nu)\sigma_0}{(1+\nu)} x_3 \delta_{i3} \quad \phi = \frac{\nu(1-\nu)\sigma_0}{(1+\nu)} (3x_3^2 - R^2)$$

- 5.4.1.1. Verify that the potentials satisfy the equilibrium equations
- 5.4.1.2. Show that the fields generated from the potentials correspond to a state of uniaxial stress, with magnitude  $\sigma_0$  acting parallel to the  $\mathbf{e}_3$  direction of an infinite solid

- 5.4.2. Show that fields derived from the Papkovitch-Neuber potentials

$$\Psi_i = \frac{(1-\nu)p}{(1+\nu)} x_i \quad \phi = \frac{2\nu(1-\nu)p}{(1+\nu)} R^2$$

- 5.4.2.1. Verify that the potentials satisfy the equilibrium equations
- 5.4.2.2. Show that the fields generated from the potentials correspond to a state of hydrostatic tension  $\sigma_{ij} = p \delta_{ij}$

5.4.3. Consider the Papkovitch-Neuber potentials

$$\Psi_i = \alpha x_i + \beta \frac{x_i}{R^3} \quad \phi = \alpha R^2 - \frac{3\beta}{R}$$

- 5.4.3.1. Verify that the potentials satisfy the governing equations
- 5.4.3.2. Show that the potentials generate a spherically symmetric displacement field
- 5.4.3.3. Calculate values of  $\alpha$  and  $\beta$  that generate the solution to an internally pressurized spherical shell, with pressure  $p$  acting at  $R=a$  and with surface at  $R=b$  traction free.

5.4.4. Verify that the Papkovitch-Neuber potential

$$\Psi_i = \frac{P_i}{4\pi R} \quad \phi = 0$$

generates the fields for a point force  $\mathbf{P} = P_1\mathbf{e}_1 + P_2\mathbf{e}_2 + P_3\mathbf{e}_3$  acting at the origin of a large (infinite) elastic solid with Young's modulus  $E$  and Poisson's ratio  $\nu$ . To this end:

- 5.4.4.1. Verify that the potentials satisfy the governing equation
- 5.4.4.2. Calculate the stresses
- 5.4.4.3. Consider a spherical region with radius  $R$  surrounding the origin. Calculate the resultant force exerted by the stress on the outer surface of this sphere, and show that they are in equilibrium with a force  $\mathbf{P}$ .

5.4.5. Consider an infinite, isotropic, linear elastic solid with Young's modulus  $E$  and Poisson's ratio  $\nu$ . Suppose that the solid contains a rigid spherical particle (an inclusion) with radius  $a$  and center at the origin. The particle is perfectly bonded to the elastic matrix, so that  $u_i = 0$  at the particle/matrix interface. The solid is subjected to a uniaxial tensile stress  $\sigma_{33} = \sigma_0$  at infinity. Calculate the stress field in the elastic solid. To proceed, note that the potentials

$$\Psi_i = \frac{(1-\nu)\sigma_0}{(1+\nu)} x_3 \delta_{i3} \quad \phi = \frac{\nu(1-\nu)\sigma_0}{(1+\nu)} (3x_3^2 - R^2)$$

generate a uniform, uniaxial stress  $\sigma_{33} = \sigma_0$  (see problem 1). The potentials

$$\Psi_i = \frac{a^3 p_{ik}^T x_k}{3R^3} \quad \phi = \frac{a^3 p_{ij}^T}{15R^3} \left( (5R^2 - a^2) \delta_{ij} + 3a^2 \frac{x_i x_j}{R^2} \right)$$

are a special case of the Eshelby problem described in Section 5.4.6, and generate the stresses outside a spherical inclusion, which is subjected to a uniform transformation strain. Let  $p_{ij}^T = A\delta_{ij} + B\delta_{i3}\delta_{j3}$ , where  $A$  and  $B$  are constants to be determined. The two pairs of potentials can be superposed to generate the required solution.

5.4.6. Consider an infinite, isotropic, linear elastic solid with Young's modulus  $E$  and Poisson's ratio  $\nu$ . Suppose that the solid contains a spherical particle (an inclusion) with radius  $a$  and center at the origin. The particle has Young's modulus  $E_p$  and Poisson's ratio  $\nu_p$ , and is perfectly bonded to the matrix, so that the displacement and radial stress are equal in both particle and matrix at the particle/matrix interface. The solid is subjected to a uniaxial tensile stress  $\sigma_{33} = \sigma_0$  at infinity. Calculate the stress field in the elastic solid.

- 5.4.6.1. Assume that the stress field inside the inclusion is given by  $\sigma_{ij} = A\sigma_0\delta_{ij} + B\sigma_0\delta_{i3}\delta_{j3}$ . Calculate the displacement field in the inclusion (assume that the displacement and rotation of the solid vanish at the origin).
- 5.4.6.2. The stress field outside the inclusion can be generated from Papkovitch-Neuber potentials

$$\Psi_i = \frac{(1-\nu)\sigma_0}{(1+\nu)} x_3 \delta_{i3} + \frac{a^3 p_{ik}^T x_k}{3R^3} \quad \phi = \frac{\nu(1-\nu)\sigma_0}{(1+\nu)} (3x_3^2 - R^2) + \frac{a^3 p_{ij}^T}{15R^3} \left( (5R^2 - a^2) \delta_{ij} + 3a^2 \frac{x_i x_j}{R^2} \right)$$

where  $p_{ij}^T = C\sigma_0\delta_{ij} + D\sigma_0\delta_{i3}\delta_{j3}$ , and  $C$  and  $D$  are constants to be determined.

5.4.6.3. Use the conditions at  $r=a$  to find expressions for  $A, B, C, D$  in terms of geometric and material properties.

5.4.7. Consider the Eshelby inclusion problem described in Section 5.4.6. An infinite homogeneous, stress free, linear elastic solid has Young's modulus  $E$  and Poisson's ratio  $\nu$ . The solid is initially stress free. An inelastic strain distribution  $\varepsilon_{ij}^T$  is introduced into an ellipsoidal region of the solid  $B$  (e.g. due to thermal expansion, or a phase transformation). Let  $u_i$  denote the displacement field,  $\varepsilon_{ij} = \varepsilon_{ij}^e + \varepsilon_{ij}^T$  denote the total strain distribution, and let  $\sigma_{ij}$  denote the stress field in the solid.

5.4.7.1. Write down an expression for the total strain energy  $\Phi_I$  within the ellipsoidal region, in terms of  $\sigma_{ij}$ ,  $\varepsilon_{ij}$  and  $\varepsilon_{ij}^T$ .

5.4.7.2. Write down an expression for the total strain energy outside the ellipsoidal region, expressing your answer as a volume integral in terms of  $\varepsilon_{ij}$  and  $\sigma_{ij}$ . Using the divergence theorem, show that the result can also be expressed as

$$\Phi_O = -\frac{1}{2} \int_S \sigma_{ij} n_j u_i dA$$

where  $S$  denotes the surface of the ellipsoid, and  $n_j$  are the components of an outward unit vector normal to  $B$ . Note that, when applying the divergence theorem, you need to show that the integral taken over the (arbitrary) boundary of the solid at infinity does not contribute to the energy – you can do this by using the asymptotic formula given in Section 5.4.6 for the displacements far from an Eshelby inclusion.

5.4.7.3. The Eshelby solution shows that the strain  $\varepsilon_{ij} = \varepsilon_{ij}^e + \varepsilon_{ij}^T$  inside  $B$  is uniform. Write down the displacement field inside the ellipsoidal region, in terms of  $\varepsilon_{ij}$  (take the displacement and rotation of the solid at the origin to be zero). Hence, show that the result of 7.2 can be re-written as

$$\Phi_O = -\frac{1}{2} \int_S \sigma_{ij} \varepsilon_{ik} x_k n_j dA$$

5.4.7.4. Finally, use the results of 7.1 and 7.3, together with the divergence theorem, to show that the total strain energy of the solid can be calculated as

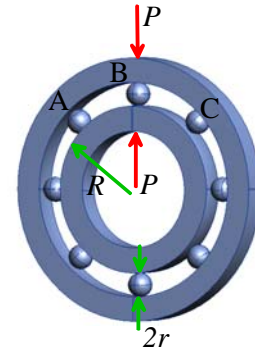
$$\Phi = \Phi_O + \Phi_I = -\frac{1}{2} \int_B \sigma_{ij} \varepsilon_{ij}^T dV$$

5.4.8. Using the solution to Problem 7, calculate the total strain energy of an initially stress-free isotropic, linear elastic solid with Young's modulus  $E$  and Poisson's ratio  $\nu$ , after an inelastic strain  $\varepsilon_{ij}^T$  is introduced into a spherical region with radius  $a$  in the solid.

5.4.9. A steel ball-bearing with radius 1cm is pushed into a flat steel surface by a force  $P$ . Neglect friction between the contacting surfaces. Typical ball-bearing steels have uniaxial tensile yield stress of order

2.8 GPa. Calculate the maximum load that the ball-bearing can withstand without causing yield, and calculate the radius of contact and maximum contact pressure at this load.

- 5.4.10. The figure shows a rolling element bearing. The inner raceway has radius  $R$ , and the balls have radius  $r$ , and both inner and outer raceways are designed so that the area of contact between the ball and the raceway is circular. The balls are equally spaced circumferentially around the ring. The bearing is free of stress when unloaded. The bearing is then subjected to a force  $P$  as shown. This load is transmitted through the bearings at the contacts between the raceways and the balls marked A, B, C in the figure (the remaining balls lose contact with the raceways but are held in place by a cage, which is not shown). Assume that the entire assembly is made from an elastic material with Young's modulus  $E$  and Poisson's ratio  $\nu$



- 5.4.10.1. Assume that the load causes the center of the inner raceway to move vertically upwards by a distance  $\Delta$ , while the outer raceway remains fixed. Write down the change in the gap between inner and outer raceway at A, B, C, in terms of  $\Delta$
- 5.4.10.2. Hence, calculate the resultant contact forces between the balls at A, B, C and the raceways, in terms of  $\Delta$  and relevant geometrical and material properties.
- 5.4.10.3. Finally, calculate the contact forces in terms of  $P$
- 5.4.10.4. If the materials have uniaxial tensile yield stress  $Y$ , find an expression for the maximum force  $P$  that the bearing can withstand before yielding.

- 5.4.11. A rigid, conical indenter with apex angle  $2\beta$  is pressed into the surface of an isotropic, linear elastic solid with Young's modulus  $E$  and Poisson's ratio  $\nu$ .

- 5.4.11.1. Write down the initial gap between the two surfaces  $g(r)$
- 5.4.11.2. Find the relationship between the depth of penetration  $h$  of the indenter and the radius of contact  $a$
- 5.4.11.3. Find the relationship between the force applied to the contact and the radius of contact, and hence deduce the relationship between penetration depth and force. Verify that the contact stiffness is given by  $\frac{dP}{dh} = 2E^*a$
- 5.4.11.4. Calculate the distribution of contact pressure that acts between the contacting surfaces.

- 5.4.12. A sphere, which has radius  $R$ , is dropped from height  $h$  onto the flat surface of a large solid. The sphere has mass density  $\rho$ , and both the sphere and the surface can be idealized as linear elastic solids, with Young's modulus  $E$  and Poisson's ratio  $\nu$ . As a rough approximation, the impact can be idealized as a quasi-static elastic indentation.

- 5.4.12.1. Write down the relationship between the force  $P$  acting on the sphere and the displacement of the center of the sphere below  $x_2 = R$
- 5.4.12.2. Calculate the maximum vertical displacement of the sphere below the point of initial contact.
- 5.4.12.3. Deduce the maximum force and contact pressure acting on the sphere
- 5.4.12.4. Suppose that the two solids have yield stress in uniaxial tension  $Y$ . Find an expression for the critical value of  $h$  which will cause the solids to yield
- 5.4.12.5. Calculate a value of  $h$  if the materials are steel, and the sphere has a 1 cm radius.

## 5.5. Solutions to generalized plane problems for anisotropic linear elastic solids

## 5.6. Solutions to dynamic problems for isotropic linear elastic solids

5.6.1. Consider the Love potentials  $\Psi_i = 0$   $\phi = A \sin(p_i x_i - c_L t)$ , where  $p_i$  is a constant unit vector and  $A$  is a constant.

5.6.1.1. Verify that the potentials satisfy the appropriate governing equations

5.6.1.2. Calculate the stresses and displacements generated from these potentials.

5.6.1.3. Briefly, interpret the wave motion represented by this solution.

5.6.2. Consider the Love potentials  $\Psi_i = U_i \sin(p_k x_k - c_s t)$   $\phi = 0$ , where  $p_i$  is a constant unit vector and  $U_i$  is a constant unit vector.

5.6.2.1. Find a condition relating  $U_i$  and  $p_i$  that must be satisfied for this to be a solution to the governing equations

5.6.2.2. Calculate the stresses and displacements generated from these potentials.

5.6.2.3. Briefly, interpret the wave motion represented by this solution.

5.6.3. Show that  $\Psi_i = 0$   $\phi = \frac{1}{R} f(t - R/c_L)$  satisfy the governing equations for Love potentials. Find expressions for the corresponding displacement and stress fields.

5.6.4. Calculate the radial distribution of Von-Mises effective stress surrounding a spherical cavity of radius  $a$ , which has pressure  $p_0$  suddenly applied to its surface at time  $t=0$ . Hence, find the location in the solid that is subjected to the largest Von-Mises stress, and the time at which the maximum occurs.

5.6.5. Calculate the displacement and stress fields generated by the Love potentials

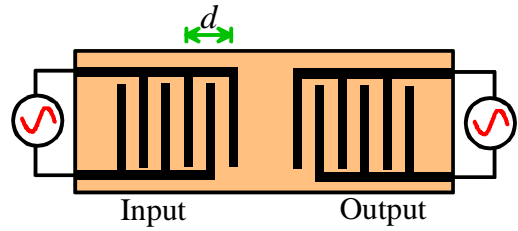
$$\Psi_i = 0 \quad \phi = \frac{A}{R} \sin \left\{ \omega \left( t - (R - a)/c_L \right) + \xi \right\}$$

Calculate the traction acting on the surface at  $r=a$ . Hence, find the Love potential that generates the fields around a spherical cavity with radius  $a$ , which is subjected to a harmonic pressure  $p(t) = p_0 \sin \omega t$ . Plot the amplitude of the surface displacement at  $r=a$  (normalized by  $a$ ) as a function of  $\omega a/c_L$ .

5.6.6. Calculate the distribution of kinetic and potential energy near the surface of a half-space that contains a Rayleigh wave with displacement amplitude  $U_0$  and wave number  $k$ . Take Poisson's ratio  $\nu = 0.3$ . Calculate the total energy per unit area of the wave (find the total energy in one wavelength, then divide by the wavelength). Estimate the energy per unit area in Rayleigh waves associated with earthquakes.



5.6.7. The figure shows a surface-acoustic-wave device that is intended to act as a narrow band-pass filter. A piezoelectric substrate has two transducers attached to its surface – one acts as an “input” transducer and the other as “output.” The transducers are electrodes: a charge can be applied to the input transducer; or detected on the output. Applying a charge to the input transducer induces a strain on the surface of the substrate: at an appropriate frequency, this will excite a Rayleigh wave in the solid. The wave propagates to the “output” electrodes, and the resulting deformation of the substrate induces a charge that can be detected. If the electrodes have spacing  $d$ , calculate the frequency at which the surface will be excited. Estimate the spacing required for a 1GHz filter made from AlN with Young’s modulus 345 GPa and Poisson’s ratio 0.3



5.6.8. In this problem, you will investigate the energy associated with wave propagation down a simple wave guide. Consider an isotropic, linear elastic strip, with thickness  $2H$  as indicated in the figure. The solution for a wave propagating in the  $\mathbf{e}_1$  direction, with particle velocity  $\mathbf{u} = u_3 \mathbf{e}_3$  is given in Section 5.6.6 of the text.

5.6.8.1. The flux of energy associated with wave propagation along a wave-guide can be computed from the work done by the tractions acting on an internal material surface. The work done per cycle is given by

$$\langle P \rangle = \frac{1}{T} \int_0^T \int_{-H}^H \sigma_{ij} n_j \frac{du_i}{dt} dx_2 dt$$

where  $T$  is the period of oscillation and  $n_j = -\delta_{j1}$  is a unit vector normal to an internal plane perpendicular to the direction of wave propagation. Calculate  $\langle P \rangle$  for the  $n$ th wave propagation mode.

5.6.8.2. The average kinetic energy of a generic cross-section of the wave-guide can be calculated from

$$\langle K \rangle = \frac{1}{T} \int_0^T \int_{-H}^H \frac{\rho}{2} \frac{du_i}{dt} \frac{du_i}{dt} dx_2 dt$$

Find  $\langle K \rangle$  for  $n$ th wave propagation mode.

5.6.8.3. The average potential energy of a generic cross-section of the wave-guide can be calculated from

$$\langle \Phi \rangle = \frac{1}{T} \int_0^T \int_{-H}^H \frac{1}{2} \sigma_{ij} \varepsilon_{ij} dx_2 dt$$

Find  $\langle \Phi \rangle$  for  $n$ th wave propagation mode. Check that  $\langle K \rangle = \langle \Phi \rangle$

5.6.8.4. The speed of energy flux down the wave-guide is defined as  $c_e = \langle P \rangle / (\langle K \rangle + \langle \Phi \rangle)$ . Find  $c_e$  for the  $n$ th propagation mode, and compare the solution with the expression for the group velocity of the wave

$$c_g = \frac{d\omega}{dk} = \frac{c_s k H}{\sqrt{(n\pi/2)^2 + k^2 H^2}}$$

## 5.7. Energy methods for solving static linear elasticity problems

5.7.1. A shaft with length  $L$  and square cross section is fixed at one end, and subjected to a twisting moment  $T$  at the other. The shaft is made from a linear elastic solid with Young's modulus  $E$  and Poisson's ratio  $\nu$ . The torque causes the top end of the shaft to rotate through an angle  $\phi$ .

5.7.1.1. Consider the following displacement field

$$v_1 = -\frac{\phi}{L} x_1 x_3 \quad v_2 = \frac{\phi}{L} x_2 x_3 \quad v_3 = 0$$

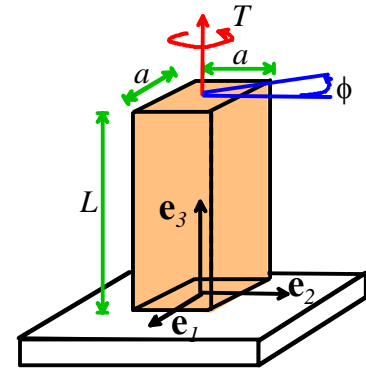
Show that this is a kinematically admissible displacement field for the twisted shaft.

5.7.1.2. Calculate the strains associated with this kinematically admissible displacement field

5.7.1.3. Hence, show that the potential energy of the shaft is

You may assume that the potential energy of the torsional load is  $-T\phi$

5.7.1.4. Find the value of  $\phi$  that minimizes the potential energy, and hence estimate the torsional stiffness of the shaft.



5.7.2. In this problem you will use the principle of minimum potential energy to find an approximate solution to the displacement in a pressurized cylinder. Assume that the cylinder is an isotropic, linear elastic solid with Young's modulus  $E$  and Poisson's ratio  $\nu$ , and subjected to internal pressure  $p$  at  $r=a$ .

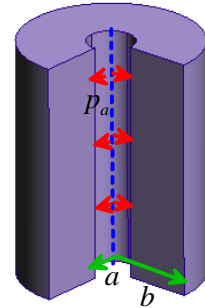
5.7.2.1. Approximate the radial displacement field as  $u_r = C_1 + C_2 r$ , where  $C_1, C_2$  are constants to be determined. Assume all other components of displacement are zero. Calculate the strains in the solid  $\epsilon_{rr}, \epsilon_{\theta\theta}$

5.7.2.2. Find an expression for the total strain energy of the cylinder per unit length, in terms of  $C_1, C_2$  and relevant geometric and material parameters

5.7.2.3. Hence, write down the potential energy (per unit length) of the cylinder.

5.7.2.4. Find the values of  $C_1, C_2$  that minimize the potential energy

5.7.2.5. Plot a graph showing the normalized radial displacement field  $E(b^2 - a^2)u_r(r)/(pab^2)$  as a function of the normalized position  $(r-a)/(b-a)$  in the cylinder, for  $\nu=0.3$ , and  $b/a=1.1$  and  $b/a=2$ . On the same graph, plot the exact solution, given in Section 4.1.9.

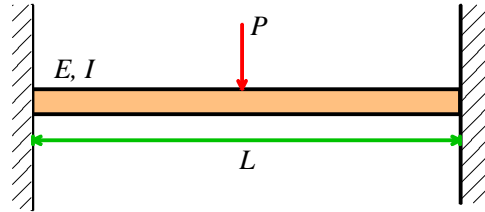


5.7.3. A bi-metallic strip is made by welding together two materials with identical Young's modulus and Poisson's ratio  $E, \nu$ , but with different thermal expansion coefficients  $\alpha_1, \alpha_2$ , as shown in the picture. At some arbitrary temperature  $T_0$  the strip is straight and free of stress. The temperature is then increased to a new value  $T$ , causing the strip to bend. Assume that, after heating, the displacement field in the strip can be approximated as  $u_1 = \lambda x_1 + x_1 x_2 / R$   $u_2 = -x_1^2 / (2R) - \beta x_2$   $u_3 = 0$ , where  $\lambda, R, \beta$  are constants to be determined.

5.7.3.1. Briefly describe the physical significance of the shape changes associated with  $\lambda, R, \beta$ .

- 5.7.3.2. Calculate the distribution of (infinitesimal) strain associated with the kinematically admissible displacement field
- 5.7.3.3. Hence, calculate the strain energy density distribution in the solid. Don't forget to account for the effects of thermal expansion
- 5.7.3.4. Minimize the potential energy to determine values for  $\lambda, R, \beta$  in terms of relevant geometric and material parameters.

- 5.7.4. By guessing the deflected shape, estimate the stiffness of a clamped—clamped beam subjected to a point force at mid-span. Note that your guess for the deflected shape must satisfy  $w(x_1) = \frac{dw}{dx_1} = 0$ , so you



can't assume that it bends into a circular shape as done in class. Instead, try a deflection of the form

$w(x_1) = 1 - \cos(2\pi x_1 / L)$ , or a similar function of your choice (you could try a suitable polynomial, for example). If you try more than one guess and want to know which one gives the best result, remember that energy minimization always overestimates stiffness. The best guess is the one that gives the lowest stiffness.

- 5.7.5. A slender rod with length  $L$  and cross sectional area  $A$  is subjected to an axial body force  $\mathbf{b} = b(x_2)\mathbf{e}_2$ . Our objective is to determine an approximate solution to the displacement field in the rod.

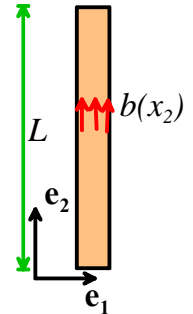
- 5.7.5.1. Assume that the displacement field has the form

$$u_2 = w(x_2) \quad u_1 = u_3 = 0$$

where the function  $w$  is to be determined. Find an expression for the strains in terms of  $w$  and hence deduce the strain energy density.

- 5.7.5.2. Show that the potential energy of the rod is

$$V(w) = EA \frac{1-\nu}{(1-2\nu)(1+\nu)} \int_0^L \frac{1}{2} \left( \frac{dw}{dx_2} \right)^2 dx_2 - A \int_0^L b(x_2) w(x_2) dx_2$$



- 5.7.5.3. To minimize the potential energy, suppose that  $w$  is perturbed from the value the minimizes  $V$  to a value  $w + \delta w$ . Assume that  $\delta w$  is kinematically admissible, which requires that  $\delta w = 0$  at any point on the bar where the value of  $w$  is prescribed. Calculate the potential energy  $V(w + \delta w)$  and show that it can be expressed in the form

$$V(w + \delta w) = V(w) + \delta V + \frac{1}{2} \delta^2 V$$

where  $V$  is a function of  $w$  only,  $\delta V$  is a function of  $w$  and  $\delta w$ , and  $\delta^2 V$  is a function of  $\delta w$  only.

- 5.7.6. As discussed in Section 8 of the online notes (or in class), if  $V$  is stationary at  $\delta w = 0$ , then  $\delta V = 0$ . Show that, to satisfy  $\delta V = 0$ , we must choose  $w$  to satisfy

$$\frac{EA(1-\nu)}{(1-2\nu)(1+\nu)} \int_0^L \frac{dw}{dx_2} \frac{d\delta w}{dx_2} dx_2 - A \int_0^L b \delta w dx_2 = 0$$

- 5.7.6.1. Integrate the first term by parts to deduce that, to minimize,  $V$ ,  $w$  must satisfy

$$\frac{d^2 w}{dx_2^2} + b(x_2) = 0$$

Show that this is equivalent to the equilibrium condition

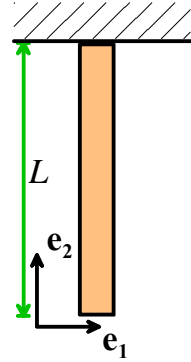
$$\frac{d\sigma_{22}}{dx_2} + b_2 = 0$$

Furthermore, deduce that if  $w$  is not prescribed at either  $x_2 = 0$ ,  $x_2 = L$  or both, then the boundary conditions on the end(s) of the rod must be

$$\frac{dw}{dx_2} = 0$$

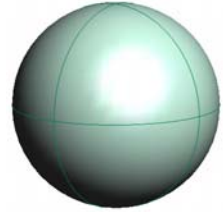
Show that this corresponds to the condition that  $\sigma_{22} = 0$  at a free end.

- 5.7.6.2. Use your results in (2.5) to estimate the displacement field in a bar with mass density  $\rho$ , which is attached to a rigid wall at  $x_2 = L$ , is free at  $x_2 = 0$ , and subjected to the force of gravity (acting vertically downwards...)



## 5.8. The Reciprocal Theorem and applications

- 5.8.1. A planet that deforms under its own gravitational force can be idealized as a linear elastic sphere with radius  $a$ , Young's modulus  $E$  and Poisson's ratio  $\nu$  that is subjected to a radial gravitational force  $\mathbf{b} = -(gR/a)\mathbf{e}_R$ , where  $g$  is the acceleration due to gravity at the surface of the sphere. Use the reciprocal theorem to calculate the change in volume of the sphere, and hence deduce the radial displacement of its surface.



- 5.8.2. Consider an isotropic, linear elastic solid with Young's modulus  $E$ , mass density  $\rho$ , and Poisson's ratio  $\nu$ , which is subjected to a body force distribution  $b_i$  per unit mass, and tractions  $t_i$  on its exterior surface. By using the reciprocal theorem, together with a state of uniform stress  $\sigma_{ij}^*$  as the reference solution, show that the average strains in the solid can be calculated from

$$\frac{1}{V} \int_V \varepsilon_{ij} dV = \frac{1+\nu}{EV} \int_A x_j t_i dA - \frac{\nu}{EV} \int_A \delta_{ij} x_k t_k dA + \frac{1+\nu}{EV} \int_V x_j \rho b_i dV - \frac{\nu}{EV} \int_V \delta_{ij} x_k \rho b_k dV$$

- 5.8.3. A cylinder with arbitrary cross-section rests on a flat surface, and is subjected to a vertical gravitational body force  $\mathbf{b} = -\rho g \mathbf{e}_3$ , where  $\mathbf{e}_3$  is a unit vector normal to the surface. The cylinder is a linear elastic solid with Young's modulus  $E$ , mass density  $\rho$ , and Poisson's ratio  $\nu$ . Define the change in length of the cylinder as

$$\delta L = \frac{1}{A} \int_A u_3(x_1, x_2, L) dA$$

where  $u_3(x_1, x_2, L)$  denotes the displacement of the end  $x_3 = L$  of the cylinder. Show that  $\delta L = W / 2EA$ , where  $W$  is the weight of the cylinder, and  $A$  its cross-sectional area.

5.8.4. In this problem, you will calculate an expression for the change in potential energy that occurs when an inelastic strain  $\varepsilon_{ij}^T$  is introduced into some part  $B$  of an elastic solid. The inelastic strain can be visualized as a generalized version of the Eshelby inclusion problem – it could occur as a result of thermal expansion, a phase transformation in the solid, or plastic flow. Note that  $B$  need not be ellipsoidal.

The figure illustrates the solid of interest. Assume that:

The solid has elastic constants  $C_{ijkl}$

No body forces act on the solid (for simplicity)

Part of the surface of the solid  $S_1$  is subjected to a prescribed displacement  $u_i^*$

The remainder of the surface of the solid  $S_2$  is subjected to a prescribed traction  $t_i^*$

Let  $u_i^0, \varepsilon_{ij}^0, \sigma_{ij}^0$  denote the displacement, strain, and stress in the solid before the inelastic strain is introduced. Let  $V_0$  denote the potential energy of the solid in this state.

Next, suppose that some external process introduces an inelastic strain  $\varepsilon_{ij}^T$  into part of the solid. Let  $\Delta u_i, \Delta \varepsilon_{ij}, \Delta \sigma_{ij}$  denote the change in stress in the solid resulting from the inelastic strain. Note that these fields satisfy

The strain-displacement relation  $\Delta \varepsilon_{ij} = (\partial \Delta u_i / \partial x_j + \partial \Delta u_j / \partial x_i) / 2$

The stress-strain law  $\Delta \sigma_{ij} = C_{ijkl}(\Delta \varepsilon_{kl} - \varepsilon_{kl}^T)$  in  $B$ , and  $\Delta \sigma_{ij} = C_{ijkl} \Delta \varepsilon_{kl}$  outside  $B$

Boundary conditions  $\Delta u_i = 0$  on  $S_1$ , and  $\Delta \sigma_{ij} n_j = 0$  on  $S_2$ .

5.8.4.1. Write down an expressions for  $V_0$  in terms of  $u_i^0, \varepsilon_{ij}^0, \sigma_{ij}^0$

5.8.4.2. Suppose that  $u_i^0, \varepsilon_{ij}^0, \sigma_{ij}^0$  are all zero (i.e. the solid is initially stress free). Write down the potential energy  $V_S$  due to  $\Delta u_i, \Delta \varepsilon_{ij}, \Delta \sigma_{ij}$ . This is called the “self energy” of the eigenstrain – the energy cost of introducing the eigenstrain  $\varepsilon_{ij}^T$  into a stress-free solid.

5.8.4.3. Show that the expression for the self-energy can be simplified to

$$V_S = -\frac{1}{2} \int_B \Delta \sigma_{ij} \varepsilon_{ij}^T dV$$

5.8.4.4. Now suppose that  $u_i^0, \varepsilon_{ij}^0, \sigma_{ij}^0$  are all nonzero. Write down the total potential energy of the system  $V_{TOT}$ , in terms of  $u_i^0, \varepsilon_{ij}^0, \sigma_{ij}^0$  and  $\Delta u_i, \Delta \varepsilon_{ij}, \Delta \sigma_{ij}$ .

5.8.4.5. Finally, show that the total potential energy of the system can be expressed as

$$V_{TOT} = V_0 + V_S - \int_B \sigma_{ij}^0 \varepsilon_{ij}^T dV$$

Here, the last term is called the “interaction energy” of the eigenstrain with the applied load. The steps in this derivation are very similar to the derivation of the reciprocal theorem.

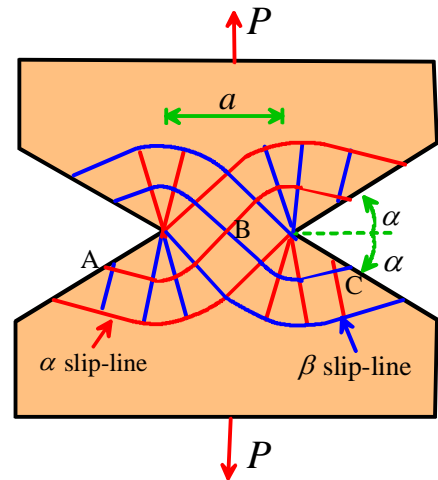
- 5.8.4.6. An infinite, isotropic, linear elastic solid with Young's modulus  $E$  and Poisson's ratio  $\nu$  is subjected to a uniaxial tensile stress  $\sigma_0$ . A uniform dilatational strain  $\varepsilon_{ij}^T = \beta \delta_{ij}$  is then induced in a spherical region of the solid with radius  $a$ .
- 5.8.4.7. Using the solution to problem 1, and the Eshelby solution, find an expression for the change in potential energy of the solid, in terms of  $\beta, \sigma_0$  and relevant geometric and material parameters.
- 5.8.4.8. Find an expression for the critical stress at which the potential energy is decreased as a result of the transformation

## 6. Chapter 6: Analytical Techniques and Solutions for Plastic Solids

### 6.1 Slip-line field theory

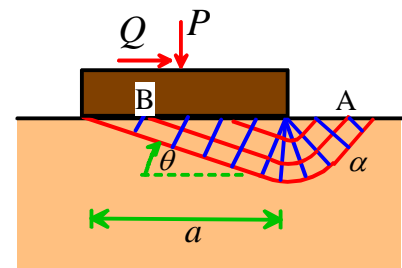
- 6.1.1. The figure shows the slip-line field for a rigid plastic double-notched bar deforming under uniaxial tensile loading. The material has yield stress in shear  $k$

- 6.1.1.1. Draw the Mohr's circle representing the state of stress at A. Write down (i) the value of  $\phi$  at this point, and (ii) the magnitude of the hydrostatic stress  $\bar{\sigma}$  at this point.
- 6.1.1.2. Calculate the value of  $\phi$  at point B, and deduce the magnitude of  $\bar{\sigma}$ . Draw the Mohr's circle of stress at point B, and calculate the horizontal and vertical components of stress
- 6.1.1.3. Repeat 1.1 and 1.2, but trace the  $\beta$  slip-line from point C to point B.



- 6.1.2. The figure shows a slip-line field for oblique indentation of a rigid-plastic surface by a flat punch

- 6.1.2.1. Draw the Mohr's circle representing the state of stress at A. Write down (i) the value of  $\phi$  at this point, and (ii) the magnitude of the hydrostatic stress  $\bar{\sigma}$  at this point.
- 6.1.2.2. Calculate the value of  $\phi$  at point B, and deduce the magnitude of  $\bar{\sigma}$ .
- 6.1.2.3. Draw the Mohr's circle representation for the stress state at B, and hence calculate the tractions acting on the contacting surface, as a function of  $k$  and  $\theta$ .
- 6.1.2.4. Calculate expressions for  $P$  and  $Q$  in terms of  $k, a$  and  $\theta$ , and find an expression for  $Q/P$
- 6.1.2.5. What is the maximum possible value of friction coefficient  $Q/P$ ? What does the slip-line field look like in this limit?



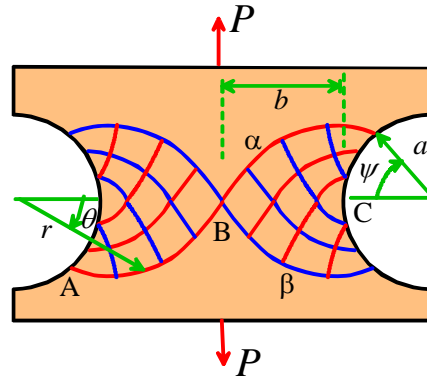
6.1.3. The figure shows the slip-line field for a rigid plastic double-notched bar under uniaxial tension. The material has yield stress in shear  $k$ . The slip-lines are logarithmic spirals, as discussed in Section 6.1.3.

6.1.3.1. Write down a relationship between the angle  $\psi$ , the notch radius  $a$  and the bar width  $b$ .

6.1.3.2. Draw the Mohr's circle representing the state of stress at A. Write down (i) the value of  $\phi$  at this point, and (ii) the magnitude of the hydrostatic stress  $\bar{\sigma}$  at this point.

6.1.3.3. Determine the value of  $\phi$  and the hydrostatic stress at point B, and draw the Mohr's circle representing the stress state at this point.

6.1.3.4. Hence, deduce the distribution of vertical stress along the line BC, and calculate the force  $P$  in terms of  $k$ ,  $a$  and  $b$ .



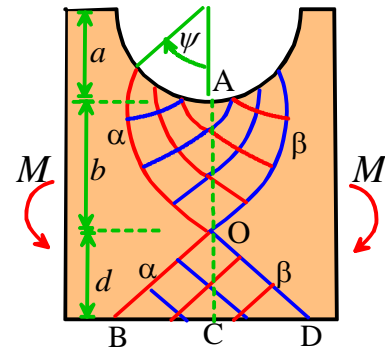
6.1.4. The figure shows the slip-line field for a notched, rigid plastic bar deforming under pure bending (the solution is valid for  $\psi < \pi/2 - 1$ , for reasons discussed in Section 6.1.3). The solid has yield stress in shear  $k$ .

6.1.4.1. Write down the distribution of stress in the triangular region OBD

6.1.4.2. Using the solution to problem 2, write down the stress distribution along the line OA

6.1.4.3. Calculate the resultant force exerted by tractions on the line AOC. Find the ratio of  $d/b$  for the resultant force to vanish, in terms of  $\psi$ , and hence find an equation relating  $a/(b+d)$  and  $\psi$ .

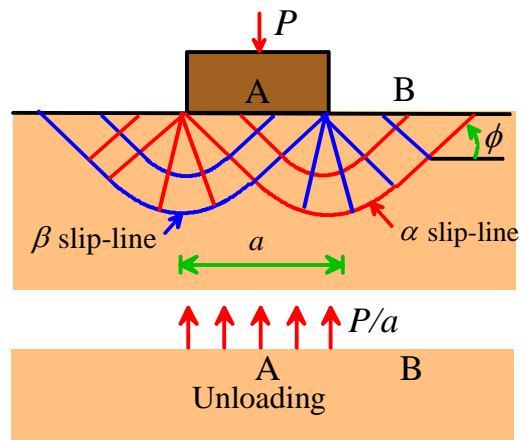
6.1.4.4. Finally, calculate the resultant moment of the tractions about O, and hence find a relationship between  $M$ ,  $a$ ,  $b+d$  and  $\psi$ .



6.1.5. A rigid flat punch is pressed into the surface of an elastic-perfectly plastic half-space, with Young's modulus  $E$ , Poisson's ratio  $\nu$  and shear yield stress  $k$ . The punch is then withdrawn.

6.1.5.1. At maximum load the stress state under the punch can be estimated using the rigid-plastic slip-line field solution (the solution is accurate as long as plastic strains are much greater than elastic strains). Calculate the stress state in this condition (i) just under the contact, and (ii) at the surface just outside the contact.

6.1.5.2. The unloading process can be assumed to be elastic – this means that the *change* in stress during unloading can be calculated using the solution to an elastic half-space subjected to uniform pressure on its surface. Calculate the



change in stress (i) just under the contact, and (ii) just outside the contact, using the solution given in Section 5.2.8.

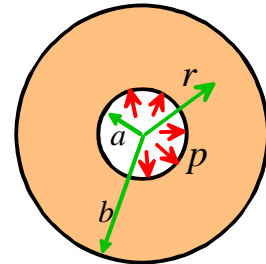
- 6.1.5.3. Calculate the residual stress (i.e. the state of stress that remains in the solid after unloading) at points A and B on the surface

## 6.2. Energy methods in plasticity and their applications: Plastic Limit Analysis

- 6.2.1. The figure shows a pressurized cylindrical cavity. The solid has yield stress in shear  $k$ . The objective of this problem is to calculate an upper bound to the pressure required to cause plastic collapse in the cylinder

6.2.1.1. Take a volume preserving radial distribution of velocity as the collapse mechanism. Calculate the strain rate associated with the collapse mechanism

6.2.1.2. Apply the upper bound theorem to estimate the internal pressure  $p$  at collapse. Compare the result with the exact solution

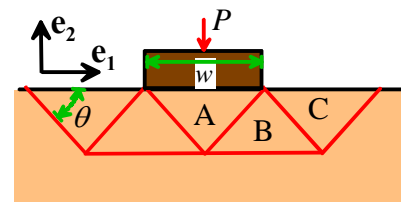


- 6.2.2. The figure shows a proposed collapse mechanism for indentation of a rigid-plastic solid. Each triangle slides as a rigid block, with velocity discontinuities across the edges of the triangles.

6.2.2.1. Assume that triangle A moves vertically downwards. Write down the velocity of triangles B and C

6.2.2.2. Hence, calculate the total internal plastic dissipation, and obtain an upper bound to the force  $P$

6.2.2.3. Select the angle  $\theta$  that minimizes the collapse load.

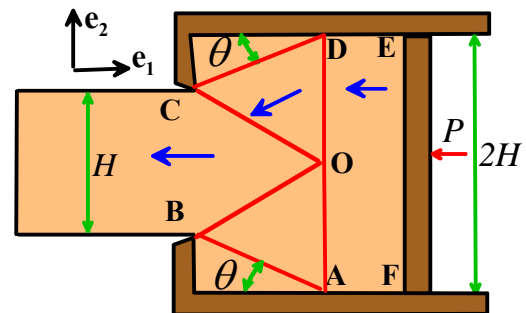


- 6.2.3. The figure shows a kinematically admissible velocity field for an extrusion process. The velocity of the solid is uniform in each sector, with velocity discontinuities across each line. The solid has shear yield stress  $k$ .

6.2.3.1. Assume the ram EF moves to the left at constant speed  $V$ . Calculate the velocity of the solid in each of the three separate regions of the solid, and deduce the magnitude of the velocity discontinuity between neighboring regions

6.2.3.2. Hence, calculate the total plastic dissipation and obtain an upper bound to the extrusion force  $P$  per unit out-of-plane distance

6.2.3.3. Select the angle  $\theta$  that gives the least upper bound.





6.2.4. The figure shows a kinematically admissible velocity field for an extrusion process. Material particles in the annular region ABCD move along radial lines. There are velocity discontinuities across the arcs BC and AD.

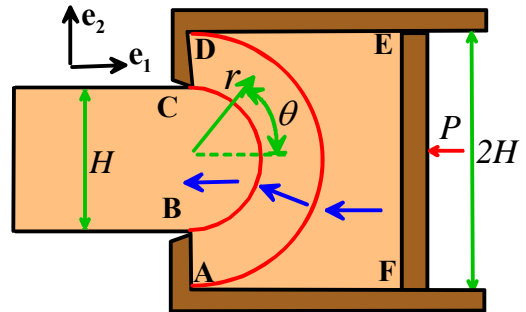
6.2.4.1. Assume the ram EF moves to the left at constant speed  $V$ . Use flow continuity to write down the radial velocity of material particles just inside the arc AD.

6.2.4.2. Use the fact that the solid is incompressible to calculate the velocity distribution in ABCD

6.2.4.3. Calculate the plastic dissipation, and hence obtain an upper bound to the force  $P$ .

6.2.5. The derivation of the upper bound theorem given in Chapter 6 focused on materials with a Von-Mises yield surface. In fact, the theorem is more general than this, and applies to any material that has a constitutive equation satisfying the principle of maximum plastic resistance. In particular, it can be applied to critical state models of soils described in Section 3.11. The goal of this problem is to prove this assertion.

6.3. The first step is to show that

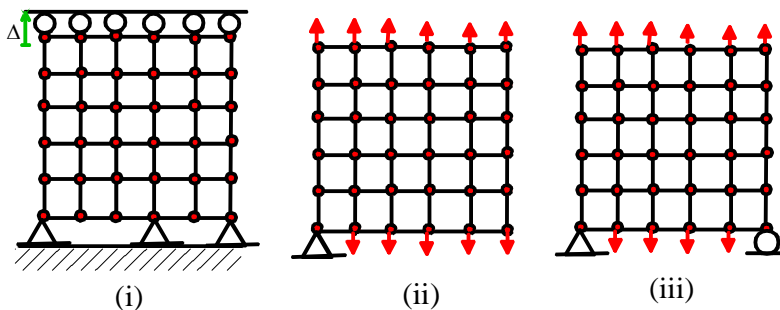


## 7. Chapter 7: Introduction to Finite Element Analysis in Solid Mechanics

### 7.1. A guide to using finite element software

7.1.1. Please answer the following questions

- 7.1.1.1. What is the difference between a static and a dynamic FEA computation (please limit your answer to a sentence!)
- 7.1.1.2. What is the difference between the displacement fields in 8 noded and 20 noded hexahedral elements?
- 7.1.1.3. What is the key difference between the nodes on a beam element and the nodes on a 3D solid element?
- 7.1.1.4. Which of the boundary conditions shown below properly constrain the solid for a plane strain static analysis?



- 7.1.1.5. List three ways that loads can be applied to a finite element mesh
- 7.1.1.6. In a quasi-static analysis of a ceramic cutting tool machining steel, which surface would you choose as the master surface, and which would you choose as the slave surface?

7.1.1.7. Give three reasons why a nonlinear static finite element analysis might not converge.

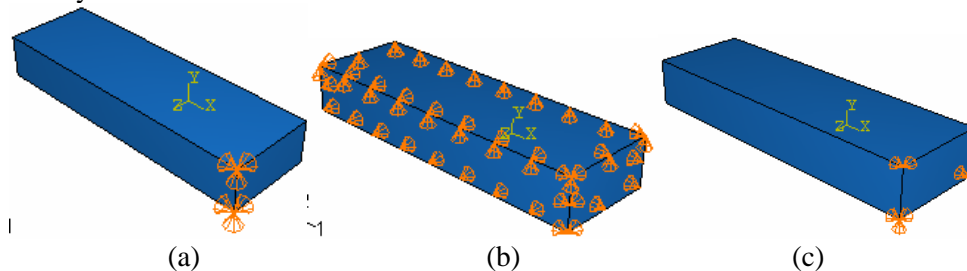
7.1.2. You conduct an FEA computation to calculate the natural frequency of vibration of a beam that is pinned at both ends. You enter as parameters the Young's modulus of the beam  $E$ , its area moment of inertia  $I$ , its mass per unit length  $m$  and its length  $L$ . Work through the dimensional analysis to identify a dimensionless functional relationship between the natural frequency and other parameters.

7.1.3. Please answer the FEA related questions

7.1.3.1. What is the difference between a truss element and a solid element (please limit your answer to a sentence!)

7.1.3.2. What is the difference between the displacement fields in 6 noded and 3 noded triangular elements, and which are generally more accurate?

7.1.3.3. Which of the boundary conditions shown below properly constrain the solid for a static analysis?

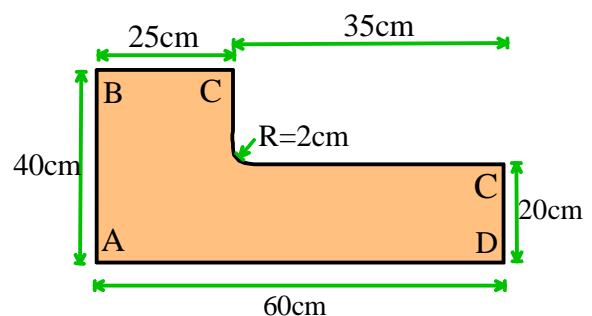


7.1.3.4. A linear elastic FE calculation predicts a maximum Mises stress of 100MPa in a component. The solid is loaded only by prescribing tractions and displacements on its boundary. If the applied loads and prescribed displacements are all doubled, what will be the magnitude of the maximum Mises stress?

7.1.3.5. An FE calculation is conducted on a part. The solid is idealized as an elastic-perfectly plastic solid, with Young's modulus 210 GPa, Poisson ratio  $\nu = 0.3$ . Its plastic properties are idealized with Mises yield surface with yield stress 500MPa. The solid is loaded only by prescribing tractions and displacements on its boundary. The analysis predicts a maximum von-Mises stress of 400MPa in the component. If the applied loads and prescribed displacements are all doubled, what will be the magnitude of the maximum Mises stress?

7.1.4. The objective of this problem is to investigate the influence of element size on the FEA predictions of stresses near a stress concentration.

Set up a finite element model of the 2D (plane strain) part shown below (select the 2D button when creating the part, and make the little rounded radius by creating a fillet radius. Enter a radius of 2cm for the fillet radius). Use SI units in the computation (DO NOT USE cm!)



Use a linear elastic constitutive equation with  $E = 210 \text{ GPa}$ ,  $\nu = 0.3$ . For boundary conditions, use zero horizontal displacement on AB, zero vertical displacement on AD, and apply a uniform horizontal displacement of 0.01 cm on CD. Run a quasi-static computation.

Run computations with the following meshes:

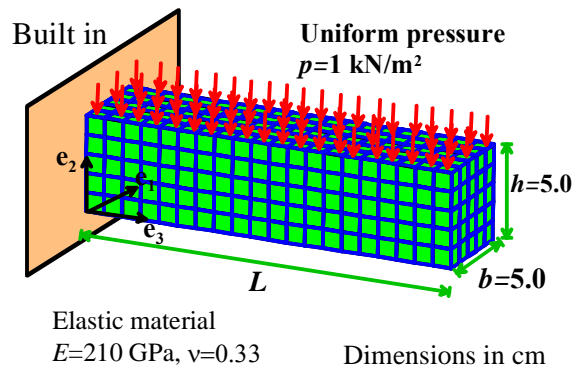
- 7.1.4.1. Linear quadrilateral elements, with a mesh size 0.05 m
- 7.1.4.2. Linear quadrilateral elements, with mesh size 0.01 m
- 7.1.4.3. Linear quadrilateral elements with mesh size 0.005 m
- 7.1.4.4. Linear quadrilateral elements with a mesh size of 0.00125 m (this will have around 100000 elements and may take some time to run)
- 7.1.4.5. 8 noded (quadratic) quadrilateral elements with mesh size 0.005 m.
- 7.1.4.6. 8 noded (quadratic) quadrilateral with mesh size 0.0025 m.

For each mesh, calculate the maximum von Mises stress in the solid (you can just do a contour plot of Mises stress and read off the maximum contour value to do this). Display your results in a table showing the max. stress, element type and mesh size.

Clearly, proper mesh design is critical to get accurate numbers out of FEA computations. As a rough rule of thumb the element size near a geometric feature should be about 1/5 of the characteristic dimension associated with the feature – in this case the radius of the fillet. If there were a sharp corner instead of a fillet radius, you would find that the stresses go on increasing indefinitely as the mesh size is reduced (the stresses are theoretically infinite at a sharp corner in an elastic solid)

- 7.1.5. In this problem, you will run a series of tests to compare the performance of various types of element, and investigate the influence of mesh design on the accuracy of a finite element computation.

We will begin by comparing the behavior of different element types. We will obtain a series of finite element solutions to the problem shown below. A beam of length  $L$  and with square cross section  $b \times b$  is subjected to a uniform distribution of pressure on its top face.



First, recall the beam theory solution to this problem. The vertical deflection of the neutral axis of the beam is given by

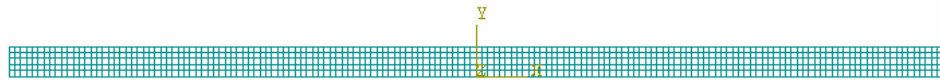
$$u_2(x_3) = -\frac{w}{24EI} \left\{ (L - x_3)^4 + 4L^3x_3 - L^4 \right\}$$

Here,  $w = bp$  is the load per unit length acting on the beam, and  $I = bh^3/12$  is the area moment of inertia of the beam about its neutral axis. Substituting and simplifying, we see that the deflection of the neutral axis at the tip of the beam is

$$u_2(L) = \frac{3}{2} \frac{pL^4}{Eh^3}$$

Observe that this is independent of  $b$ , the thickness of the beam. A thick beam should behave the same way as a thin beam. In fact, we can take  $b \ll h$ , in which case we should approach a state of *plane*

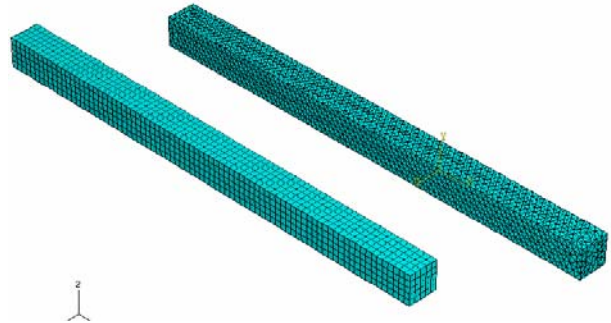
*stress*. We can therefore use this solution as a test case for both plane stress elements, and also plane strain elements.



- 7.1.5.1. First, compare the predictions of beam theory with a finite element solution. Set up a plane stress analysis, with  $L=1.6\text{m}$ ,  $h=5\text{cm}$ ,  $E=210\text{GPa}$ ,  $\nu=0.33$  and  $p=100\text{ kN/m}^2$ . Constrain both  $u_1$  and  $u_2$  at the left hand end of the beam. Generate a mesh of plane stress, 8 noded (quadratic) square elements, with a mesh size of 1cm. Compare the FEM prediction with the beam theory result. You should find excellent agreement.
- 7.1.5.2. Note that beam theory does not give an exact solution to the cantilever beam problem. It is a clever approximate solution, which is valid only for long slender beams. We will check to see where beam theory starts to break down next. Repeat the FEM calculation for  $L=0.8$ ,  $L=0.4$ ,  $L=0.3$ ,  $L=0.2$ ,  $L=0.15$ ,  $L=0.1$ . Keep all the remaining parameters fixed, including the mesh size. Plot a graph of the ratio of the FEM deflection to beam theory deflection as a function of  $L$ .

You should find that as the beam gets shorter, beam theory underestimates the deflection. This is because of *shear deformation* in the beam, which is ignored by simple Euler-Bernoulli beam theory (there is a more complex theory, called Timoshenko beam theory, which works better for short beams. For very short beams, there is no accurate approximate theory).

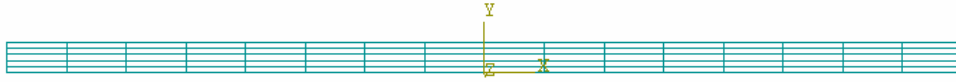
- 7.1.5.3. Now, we will use our beam problem to compare the performance of various other types of element. Generate a plane stress mesh for a beam with  $L=0.8\text{m}$ ,  $h=5\text{cm}$ ,  $E=210\text{GPa}$ ,  $\nu=0.33$ ,  $p=100\text{ kN/m}^2$ , but this time use 4 noded linear elements instead of quadratic 8 noded elements. Keep the mesh size at 0.01m, as before. Compare the tip deflection predicted by ABAQUS with the beam theory result. You should find that the solution is significantly less accurate. This is a general trend – quadratic elements give better results than linear elements, but are slightly more expensive in computer time.
- 7.1.5.4. Run a similar test to investigate the performance of 3D elements. Generate the 3D meshes shown above, using both 4 and 8 noded hexahedral elements, and 4 and 10 noded tetrahedral elements. (Don't attempt to model 2 beams together as shown in the picture; do the computations one at a time otherwise they will take forever).



Prepare a table showing tip deflection for 4 and 8 noded plane stress elements, 8 and 20 noded hexahedral elements, and 4 and 10 noded tetrahedral elements.

Your table should show that quadratic, square elements generally give the best performance. Tetrahedra (and triangles, which we haven't tried ... feel free to do so if you like...) generally give the worst performance. Unfortunately tetrahedral and triangular elements are much easier to generate automatically than hexahedral elements.

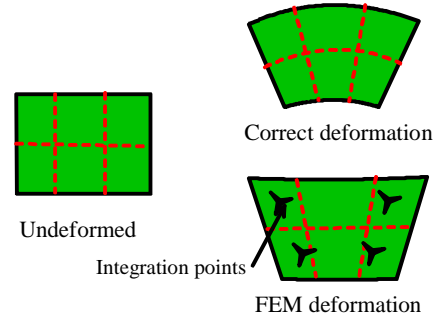
7.1.6. We will continue our comparison of element types. Set up the beam problem again with  $L=1.6\text{m}$ ,  $h=5\text{cm}$ ,  $E=210\text{GPa}$ ,  $\nu=0.33$ ,  $p=100\text{ kN/m}^2$ , but this time use the plane strain mesh shown in the figure.



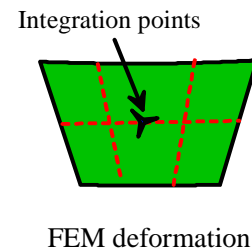
There are 16 elements along the length of the beam and 5 through the thickness. Generate a mesh with fully integrated 4 noded elements.

You should find that the results are highly inaccurate. Similar problems occur in 3d computations if the elements are severely distorted – you can check this out too if you like.

This is due to a phenomenon known as ‘shear locking’: the elements interpolation functions are unable to approximate the displacement field in the beam accurately, and are therefore too stiff. To understand this, visualize the deformation of a material element in pure bending. To approximate the deformation correctly, the sides of the finite elements need to curve, but linear elements cannot do this. Instead, they are distorted as shown. The material near the corners of the element is distorted in shear, so large shear stresses are generated in these regions. These large, incorrect, internal forces make the elements appear too stiff.



There are several ways to avoid this problem. One approach is to use a special type of element, known as a ‘reduced integration’ element. Recall that the finite element program samples stresses at each integration point within an element during its computation. Usually, these points are located near the corners of the elements. In reduced integration elements, fewer integration points are used, and they are located nearer to the center of the element (for a plane stress 4 noded quadrilateral, a single integration point, located at the element center, is used, as shown). There is no shear deformation near the center of the element, so the state of stress is interpreted correctly.

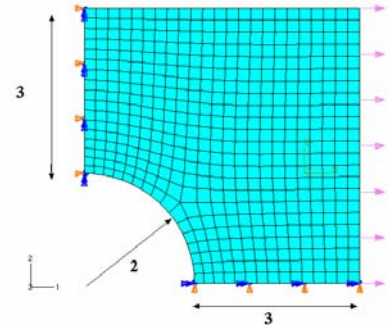
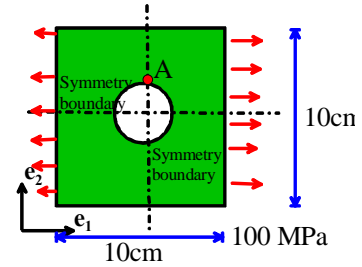


- 7.1.6.1. To test the performance of these reduced integration elements, change the element type in your computation to 4 noded linear quadrilaterals, with reduced integration. You should find much better results, although the linear elements are now a little too flexible.
- 7.1.6.2. Your finite element code may also contain more sophisticated element formulations designed to circumvent shear locking. ‘Incompatible mode’ elements are one example. In these elements, the shape functions are modified to better approximate the bending mode of deformation. If your finite element code has these elements, try them, and compare the finite element solution to the exact solution.

7.1.7. This problem demonstrates a second type of element locking, known as ‘Volumetric locking’. To produce it, set up the boundary value problem illustrated in the figures. Model only one quarter of the plate, applying symmetry boundary conditions as illustrated in the mesh. Assign an elastic material to the plate, with  $E=210\text{GPa}$ ,  $\nu=0.33$ .

Run the following tests:

- 7.1.7.1. Run the problem with fully integrated 8 noded *plane strain* quadrilaterals, and plot contours of horizontal, vertical and Von-Mises equivalent stress.
- 7.1.7.2. Modify to increase Poisson’s ratio to 0.4999 (recall that this makes the elastic material almost incompressible, like a rubber). horizontal, vertical and Von-Mises equivalent stress.. You should find that the mises stress contours look OK, but the horizontal and vertical stresses have weird fluctuations. This is an error – the solution should be independent of Poisson’s ratio, so all the contours should look the way they did in part 1.



The error you observed in part 2 is due to **volumetric locking**. Suppose that an incompressible finite element is subjected to hydrostatic compression. Because the element is incompressible, this loading causes no change in shape. Consequently, the hydrostatic component of stress is independent of the nodal displacements, and cannot be computed. If a material is **nearly incompressible**, then the hydrostatic component of stress is only weakly dependent on displacements, and is difficult to compute accurately. The shear stresses (Mises stress) can be computed without difficulty. This is why the horizontal and vertical stresses in the example were incorrect, but the Mises stress was computed correctly.

You can use two approaches to avoid volumetric locking.

- 7.1.7.3. Use ‘reduced integration’ elements for nearly incompressible materials. Switch the element type to reduced integration 8 noded quads, set Poisson’s ratio to 0.4999 and plot contours of horizontal, vertical and Mises stress. Everything should be fine.
- 7.1.7.4. You can also use a special ‘Hybrid element,’ which computes the hydrostatic stress independently. For fully incompressible materials, you must always use hybrid elements – reduced integration elements will not work. To test the hybrid element, check the ‘Hybrid Element’ box in the ‘Element type...’ menu, set Poisson’s ratio to 0.4999, and plot the same stress contours. As before, everything should work perfectly.

As you see, elements must be selected with care to ensure accurate finite element computations. With more experience, you will develop a feel for the relative merits of the various element types. You should consider the following guidelines for element selection in ABAQUS:

- Avoid using 3 noded triangular elements and 4 noded tetrahedral elements, except for filling in regions that may be difficult to mesh.
- 6 noded triangular elements and 10 noded tetrahedral elements are acceptable, but quadrilateral and brick elements give better performance. (The main advantage of triangles and tetrahedra is that they can be generated easily using automatic mesh generators)
- Fully integrated 4 noded quadrilateral elements and 8 noded bricks in ABAQUS are specially coded to avoid volumetric locking, but are susceptible to shear locking. They can be used for most problems,



although quadratic elements generally give a more accurate solution for the same amount of computer time.

- Use quadratic, reduced integration elements for general analysis work, except for problems involving large strains or complex contact.
- Use quadratic, fully integrated elements in regions where stress concentrations exist. Elements of this type give the best resolution of stress gradients.
- Use a fine mesh of linear, reduced integration elements for simulations with very large strains.

7.1.8. A bar of material with square cross section with base 0.05m and length 0.2m is made from an isotropic, linear elastic solid with Young's Modulus 207 GPa and Poisson's ratio 0.3. Set up your commercial finite element software to compute the deformation of the bar, and use it to plot one or more stress-strain curves that can be compared with the exact solution. Apply a cycle of loading that first loads the solid in tension, then unloads to zero, then loads in compression, and finally unloads to zero again.

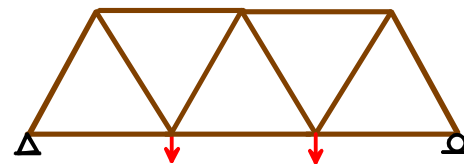
7.1.9. Repeat problem 7, but this time model the constitutive response of the bar as an elastic-plastic solid. Use elastic properties listed in problem 7, and for plastic properties enter the following data

Plastic Strain	Stress/MPa
0	100
0.1	150
0.5	175

Subject the bar to a cycle of axial displacement that will cause it to yield in both tension and compression (subjecting one end to a displacement of  $\pm 0.075\text{m}$  should work). Plot the predicted uniaxial stress-strain curve for the material. Run the following tests:

- 7.1.9.1. A small strain computation using an isotropically hardening solid with Von-Mises yield surface
- 7.1.9.2. A large strain analysis using an isotropically hardening solid with Von-Mises yield surface.
- 7.1.9.3. A small strain computation using a kinematically hardening solid
- 7.1.9.4. A large strain analysis with kinematic hardening

7.1.10. Use your commercial software to set up a model of a 2D truss shown in the figure. Make each member of the truss 2m long, with a  $0.05\text{m}^2$  steel cross section. Give the forces a 1000N magnitude. Mesh the structure using truss elements, and run a static, small-strain computation

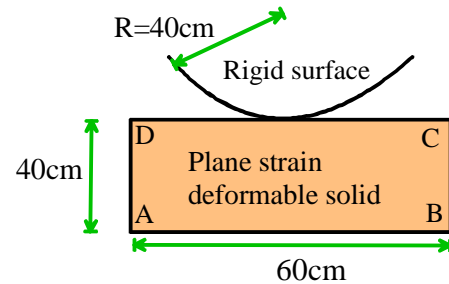


Use the simulation to compute the elastic stress in all the members. Compare the FEA solution with the analytical result.

7.1.11. This problem has several objectives: (i) To demonstrate FEA analysis with contact; (ii) To illustrate *nonlinear* solution procedures and (iii) to demonstrate the effects of convergence problems that frequently arise in nonlinear static FEA analysis.

Set up commercial software to solve the 2D (plane strain) contact problem illustrated in the figure. Use the following procedure

- Create the part ABCD as a 2D deformable solid with a homogeneous section. Make the solid symmetrical about the  $x_2$  axis
- Create the cylindrical indenter as a 2D rigid analytical solid. Make the cylinder symmetrical about the  $x_2$  axis
- Make the block an elastic solid with  $E = 210GNm^{-2}$ ,  $\nu = 0.3$
- Make the rigid surface just touch the block at the start of the analysis.
- Set the properties of the contact between the rigid surface and the block to specify a 'hard,' frictionless contact.
- To set up boundary conditions, (i) Set the vertical displacement of AB to zero; (ii) Set the horizontal displacement of point A to zero; and (iii) Set the horizontal displacement and rotation of the reference point on the cylinder to zero, and assign a vertical displacement of -2cm to the reference point.
- Create a mesh with a mesh size of 1cm with plane strain quadrilateral reduced integration elements.

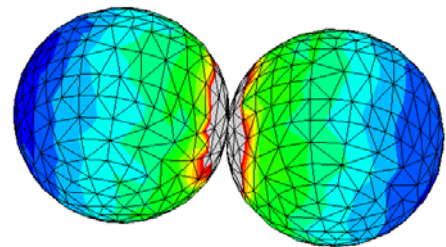


- 7.1.11.1. Begin by running the computation with a perfectly elastic analysis – this should run very quickly. Plot a graph of the force applied to the indenter as a function of its displacement.
- 7.1.11.2. Next, try an elastic-plastic analysis with a solid with yield stress 800MPa. This will run much more slowly. You will see that the nonlinear solution iterations constantly fail to converge – as a result, your code should automatically reduce the time step to a very small value. It will probably take somewhere between 50 and 100 increments to complete the analysis.
- 7.1.11.3. Try the computation one more time with a yield stress of 500MPa. This time the computation will only converge for a very small time-step: the analysis will take at least 150 increments or so.

7.1.12. Set up your commercial finite element software to conduct an explicit dynamic calculation of the impact of two identical spheres, as shown below.

Use the following parameters:

- Sphere radius – 2 cm
- Mass density  $\rho = 1000 \text{ kg/m}^3$
- Young's modulus  $E = 210GNm^{-2}$ , Poisson ratio  $\nu = 0.3$
- First, run an analysis with perfectly elastic spheres. Then repeat the calculation for elastic-plastic spheres, with yield stress  $\sigma_Y = 10000MNm^{-2}$ ,  $\sigma_Y = 5000MNm^{-2}$ ,  $\sigma_Y = 1000MNm^{-2}$ ,  $\sigma_Y = 500MNm^{-2}$ , and again with  $\sigma_Y = 50MNm^{-2}$
- Contact formulation – hard contact, with no friction
- Give one sphere an initial velocity of  $v_0 = 100\text{m/s}$  towards the other sphere.



Estimate a suitable time period for the analysis and step size based on the wave speed, as discussed in Section



Finally, please answer the following questions:

- 7.1.12.1. Suppose that the main objective of the analysis is to compute the restitution coefficient of the spheres, defined as  $e = |\mathbf{v}_{A1} - \mathbf{v}_{B1}| / |\mathbf{v}_{A0} - \mathbf{v}_{B0}|$  where  $\mathbf{v}_{A0}, \mathbf{v}_{A1}$  denote the initial and final velocities of sphere A, and the same convention is used for sphere B. List all the material and geometric parameters that appear in the problem.
- 7.1.12.2. Express the functional relationship governing the restitution coefficient in dimensionless form. Show that for a perfectly elastic material, the restitution coefficient must be a function of a single dimensionless group. Interpret this group physically (hint - it is the ratio of two velocities). For an elastic-plastic material, you should find that the restitution coefficient is a function of two groups.
- 7.1.12.3. If the sphere radius is doubled, what happens to the restitution coefficient? (DON'T DO ANY FEA TO ANSWER THIS!)
- 7.1.12.4. Show that the kinetic energy lost during impact can be expressed in dimensionless form as

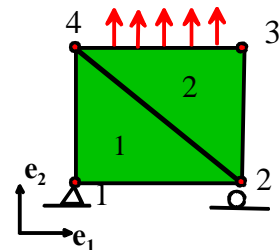
$$\frac{\Delta K}{R^3 \rho v_0^2} = f\left(\frac{\rho v_0^2}{\sigma_Y}, \frac{\rho v_0^2}{E}\right)$$

Note that the second term is very small for any practical application (including our simulation), so in interpreting data we need only to focus on behavior in the limit  $\rho v_0^2 / E \rightarrow 0$ .

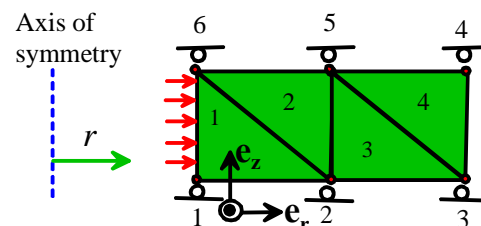
- 7.1.12.5. Use your plots of KE as a function of time to determine the change in KE for each analysis case. Hence, plot a graph showing  $\Delta K / R^3 \rho v_0^2$  as a function of  $\rho v_0^2 / \sigma_Y$
- 7.1.12.6. What is the critical value of  $\rho v_0^2 / \sigma_Y$  where *no* energy is lost? (you may find it helpful to plot  $\Delta K / R^3 \rho v_0^2$  against  $\log(\rho v_0^2 / \sigma_Y)$  to see this more clearly). If no energy is lost, the impact is perfectly elastic.
- 7.1.12.7. Hence, calculate the critical impact velocity for a perfectly elastic collision between two spheres of (a) Alumina; (b) Hardened steel; (c) Aluminum alloy and (d) lead
- 7.1.12.8. The usual assumption in classical mechanics is that restitution coefficient is a material property. Comment briefly on this assumption in light of your simulation results.

## 7.2. A simple Finite Element program

- 7.2.1. Modify the simple FEA code in FEM\_conststrain.mws to solve problems involving *plane stress* deformation instead of plane strain (this should require a change to only one line of the code). Check the modified code by solving the problem shown in the figure. Assume that the block has unit length in both horizontal and vertical directions, use Young's modulus 100 and Poisson's ratio 0.3, and take the magnitude of the distributed load to be 10 (all in arbitrary units). Compare the predictions of the FEA analysis with the exact solution.



- 7.2.2. Modify the simple FEA code in FEM\_conststrain.mws to solve problems involving *axially symmetric* solids. The figure shows a



representative problem to be solved. It represents a slice through an axially symmetric cylinder, which is prevented from stretching vertically, and pressurized on its interior surface. The solid is meshed using triangular elements, and the displacements are interpolated as

$$u_i(x_1, x_2) = u_i^{(a)} N_a(x_1, x_2) + u_i^{(b)} N_b(x_1, x_2) + u_i^{(c)} N_c(x_1, x_2)$$

where

$$N_a(x_1, x_2) = \frac{(x_2 - x_2^{(b)})(x_1^{(c)} - x_1^{(b)}) - (x_1 - x_1^{(b)})(x_2^{(c)} - x_2^{(b)})}{(x_2^{(a)} - x_2^{(b)})(x_1^{(c)} - x_1^{(b)}) - (x_1^{(a)} - x_1^{(b)})(x_2^{(c)} - x_2^{(b)})}$$

$$N_b(x_1, x_2) = \frac{(x_2 - x_2^{(c)})(x_1^{(a)} - x_1^{(c)}) - (x_1 - x_1^{(c)})(x_2^{(a)} - x_2^{(c)})}{(x_2^{(b)} - x_2^{(c)})(x_1^{(a)} - x_1^{(c)}) - (x_1^{(b)} - x_1^{(c)})(x_2^{(a)} - x_2^{(c)})}$$

$$N_c(x_1, x_2) = \frac{(x_2 - x_2^{(a)})(x_1^{(b)} - x_1^{(a)}) - (x_1 - x_1^{(a)})(x_2^{(b)} - x_2^{(a)})}{(x_2^{(c)} - x_2^{(a)})(x_1^{(b)} - x_1^{(a)}) - (x_1^{(c)} - x_1^{(a)})(x_2^{(b)} - x_2^{(a)})}$$

7.2.2.1. Show that the nonzero strain components in the element can be expressed as

$$[\varepsilon] = \begin{bmatrix} \varepsilon_{rr} \\ \varepsilon_{zz} \\ \varepsilon_{\theta\theta} \\ 2\varepsilon_{rz} \end{bmatrix} \quad [u] = \begin{bmatrix} u_r^{(a)} & u_z^{(a)} & u_r^{(b)} & u_z^{(b)} & u_r^{(c)} & u_z^{(c)} & u_r^{(d)} & u_z^{(d)} \end{bmatrix}^T$$

$$[B] = \begin{bmatrix} \frac{\partial N_a}{\partial r} & 0 & \frac{\partial N_b}{\partial r} & 0 & \frac{\partial N_c}{\partial r} & 0 \\ 0 & \frac{\partial N_a}{\partial z} & 0 & \frac{\partial N_b}{\partial z} & 0 & \frac{\partial N_c}{\partial z} \\ \frac{N_a}{r} & 0 & \frac{N_b}{r} & 0 & \frac{N_c}{r} & 0 \\ \frac{\partial N_a}{\partial z} & \frac{\partial N_a}{\partial r} & \frac{\partial N_b}{\partial z} & \frac{\partial N_b}{\partial r} & \frac{\partial N_c}{\partial z} & \frac{\partial N_c}{\partial r} \end{bmatrix}$$

7.2.2.2. Let  $\sigma = [\sigma_{rr} \quad \sigma_{zz} \quad \sigma_{\theta\theta} \quad \sigma_{rz}]$  denote the stress in the element. Find a matrix  $[D]$  that satisfies  $[\sigma] = [D][\varepsilon]$

7.2.2.3. Write down an expression for the strain energy density  $U^{el}$  of the element.

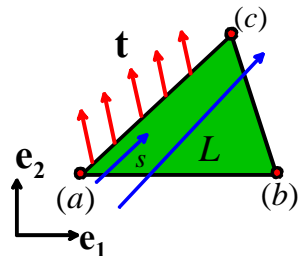
7.2.2.4. The total strain energy of each element must be computed. Note that each element represents a cylindrical region of material around the axis of symmetry. The total strain energy in this material follows as

$$W^{el} = \int_{A_{el}} 2\pi r U^{el} dr dz$$

The energy can be computed with sufficient accuracy by evaluating the integrand at the centroid of the element, and multiplying by the area of the element, with the result

$$W^{el} = 2\pi A_{el} \bar{r} \bar{U}^{el}$$

where  $\bar{r}$  denotes the radial position of the element centroid, and  $\bar{U}^{el}$  is the strain energy density at the element centroid. Use this result to deduce an expression for the element stiffness, and modify the procedure `elstif()` in the MAPLE code to compute the element stiffness.



- 7.2.2.5. The contribution to the potential energy from the pressure acting on element faces must also be computed. Following the procedure described in Chapter 7, the potential energy is

$$P = - \int_0^L 2\pi r t_i u_i ds$$

where

$$u_i = u_i^{(a)} \frac{s}{L} + u_i^{(c)} \left(1 - \frac{s}{L}\right) \quad r = r^{(a)} \frac{s}{L} + r^{(c)} \left(1 - \frac{s}{L}\right)$$

and  $u_i^{(a)}, u_i^{(c)}$  denote the displacements at the ends of the element face, and  $r^{(a)}, r^{(c)}$  denote the radial position of the ends of the element face. Calculate an expression for  $P$  of the form

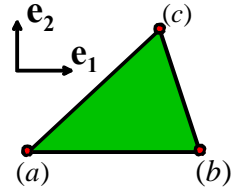
$$P^{\text{element}} = -[t_1 A \quad t_2 A \quad t_1 B \quad t_2 B] \cdot [u_1^{(a)} \quad u_2^{(a)} \quad u_1^{(c)} \quad u_2^{(c)}]$$

where  $A$  and  $B$  are constants that you must determine. Modify the procedure `elresid()` to implement modified element residual.

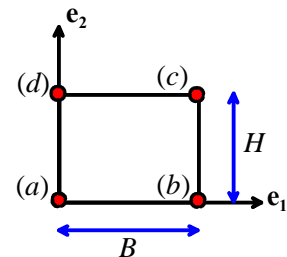
- 7.2.2.6. Test your routine by calculating the stress in a pressurized cylinder, which has inner radius 1, exterior radius 2, and is subjected to pressure  $p=1$  on its internal bore (all in arbitrary units), and deforms under plane strain conditions. Compare the FEA solution for displacements and stresses with the exact solution. Run tests with different mesh densities, and compare the results with the analytical solution.

- 7.2.3. Modify the simple FEA code in `FEM_conststrain.mws` to solve problems which involve thermal expansion. To this end

- 7.2.3.1. Consider a generic element in the mesh. Assume that the material inside the element has a uniform thermal expansion coefficient  $\alpha$ , and its temperature is increased by  $\Delta T$ . Let  $[B]$  and  $[D]$  denote the matrices of shape function derivatives and material properties defined in Sections 7.2.4, and let  $\underline{q} = \alpha \Delta T [1, 1, 0]^T$  denote a thermal strain vector. Write down the strain energy density in the element, in terms of these quantities and the element displacement vector  $\underline{u}^{\text{element}}$ .
- 7.2.3.2. Hence, devise a way to calculate the total potential energy of a finite element mesh, accounting for the effects of thermal expansion.
- 7.2.3.3. Modify the FEA code to read the thermal expansion coefficient and the change in temperature must be read from the input file, and store them as additional material properties.
- 7.2.3.4. Modify the FEA code to add the terms associated with thermal expansion to the system of equations. It is best to do this by writing a procedure that computes the contribution to the equation system from one element, and then add a section to the main analysis procedure to assemble the contributions from all elements into the global system of equations.
- 7.2.3.5. Test your code using the simple test problem



- 7.2.4. Modify the simple FEA code in `FEM_conststrain.mws` to solve plane stress problems using rectangular elements. Use the following procedure. To keep things simple, assume that the sides of each element are parallel to the  $\mathbf{e}_1$  and  $\mathbf{e}_2$  axes, as shown in the picture. Let  $(u_1^{(a)}, u_2^{(a)}), (u_1^{(b)}, u_2^{(b)}), (u_1^{(c)}, u_2^{(c)}), (u_1^{(d)}, u_2^{(d)})$  denote the



components of displacement at nodes  $a, b, c, d$ . The displacement at an arbitrary point within the element can be interpolated between values at the corners, as follows

$$u_1 = (1-\xi)(1-\eta)u_1^{(a)} + \xi(1-\eta)u_1^{(b)} + \xi\eta u_1^{(c)} + (1-\xi)\eta u_1^{(d)}$$

$$u_2 = (1-\xi)(1-\eta)u_2^{(a)} + \xi(1-\eta)u_2^{(b)} + \xi\eta u_2^{(c)} + (1-\xi)\eta u_2^{(d)}$$

where

$$\xi = x_1 / B, \quad \eta = x_2 / H$$

7.2.4.1. Show that the components of nonzero infinitesimal strain at an arbitrary point within the element may be expressed as  $[\varepsilon] = [B][u]$ , where

$$[\varepsilon] = \begin{bmatrix} \varepsilon_{11} \\ \varepsilon_{22} \\ \varepsilon_{12} \end{bmatrix} \quad [u] = \begin{bmatrix} u_1^{(a)} & u_2^{(a)} & u_1^{(b)} & u_2^{(b)} & u_1^{(c)} & u_2^{(c)} & u_1^{(d)} & u_2^{(d)} \end{bmatrix}^T$$

$$[B] = \begin{bmatrix} -\frac{1}{B}\left(1-\frac{x_2}{H}\right) & 0 & \frac{1}{B}\left(1-\frac{x_2}{H}\right) & 0 & \frac{x_2}{BH} & 0 & \frac{-x_2}{BH} & 0 \\ 0 & -\frac{1}{H}\left(1-\frac{x_1}{B}\right) & 0 & \frac{-x_1}{BH} & 0 & \frac{x_1}{BH} & 0 & \frac{1}{H}\left(1-\frac{x_1}{B}\right) \\ -\frac{1}{2H}\left(1-\frac{x_1}{B}\right) & -\frac{1}{2B}\left(1-\frac{x_2}{H}\right) & -\frac{x_1}{2BH} & \frac{1}{2B}\left(1-\frac{x_2}{H}\right) & \frac{x_1}{2BH} & \frac{x_2}{2BH} & \frac{1}{2H}\left(1-\frac{x_1}{B}\right) & \frac{-x_2}{2BH} \end{bmatrix}$$

7.2.4.2. Modify the section of the code which reads the element connectivity, to read an extra node for each element. To do this, you will need to increase the size of the array named connect from connect(1..nelem,1..3) to connect(1..nelem,1..4), and read an extra integer node number for each element.

7.2.4.3. In the procedure named elastif, which defines the element stiffness, you will need to make the following changes. (a) You will need to modify the [B] matrix to look like the one in Problem 11.1. Don't forget to change the size of the [B] array from bmat:=array(1..3,1..6) to bmat:=array(1..3,1..8). Also, note that as long as you calculate the lengths of the element sides  $B$  and  $H$  correctly, you can use the [B] matrix given above even if node  $a$  does not coincide with the origin. This is because the element stiffness only depends on the shape of the element, not on its position. (b) To evaluate the element stiffness, you cannot assume that  $[B]^T [D][B]$  is constant within the element, so instead of multiplying  $[B]^T [D][B]$  by the element area, you will need to integrate over the area of the element

$$[K^{\text{elem}}] = \int_0^H \int_0^B [B]^T [D][B] dx_1 dx_2$$

Note that MAPLE will not automatically integrate each term in a matrix. There are various ways to fix this. One approach is to integrate each term in the matrix separately. Let

$$[A] = [B]^T [D][B]$$

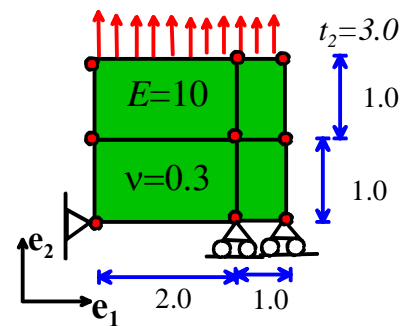
then for  $i=1..8, j=1..8$  let

$$k_{ij}^{\text{elem}} = \int_0^H \int_0^B a_{ij} dx_1 dx_2$$

Use two nested int() statements to do the integrals. Note also that to correctly return a matrix value for elastif, the last line of the procedure must read elastif=k, where  $k$  is the fully assembled stiffness matrix.

7.2.4.4. Just before the call to the elastif procedure, you will need to change the dimensions of the element stiffness matrix from k:=array(1..6,1..6) to k:=array(1..8,1..8).

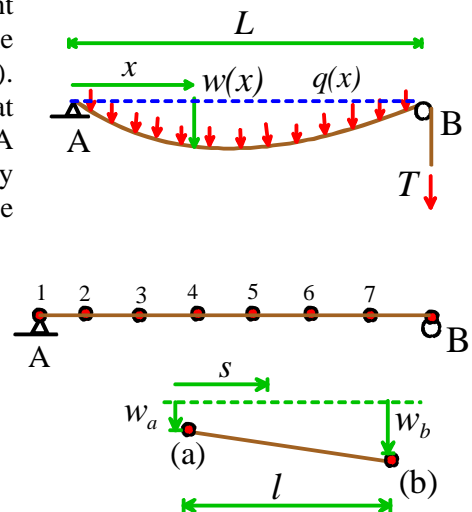
- 7.2.4.5. You will need to modify the loop that assembles the global stiffness matrix to include the fourth node in each element. To do this, you only need to change the lines that read  
 for i from 1 to 3 do  
 to  
 for i from 1 to 4 do  
 and the same for the j loop.
- 7.2.4.6. You will need to modify the part of the routine that calculates the residual forces. The only change required is to replace the line reading  
 >pointer := array(1..3,[2,3,1]):  
 with  
 >pointer:= array(1..4,[2,3,4,1]):
- 7.2.4.7. You will need to modify the procedure that calculates element strains. Now that the strains vary within the element, you need to decide where to calculate the strains. The normal procedure would be to calculate strains at each integration point within the element, but we used MAPLE to evaluate the integrals when assembling the stiffness matrix, so we didn't define any numerical integration points. So, in this case, just calculate the strains at the center of the element.
- 7.2.4.8. To test your routine, solve the problem shown in the figure (dimensions and material properties are in arbitrary units).



- 7.2.5. In this problem you will develop and apply a finite element method to calculate the shape of a tensioned, inextensible cable subjected to transverse loading (e.g. gravity or wind loading). The cable is pinned at A, and passes over a frictionless pulley at B. A tension  $T$  is applied to the end of the cable as shown. A (nonuniform) distributed load  $q(x)$  causes the cable to deflect by a distance  $w(x)$  as shown. For  $w \ll L$ , the potential energy of the system may be approximated as

$$V(w) = \int_0^L \frac{T}{2} \left( \frac{dw}{dx} \right)^2 dx - \int_0^L q w dx$$

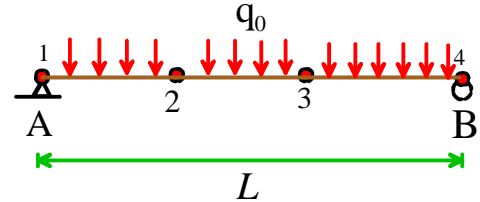
To develop a finite element scheme to calculate  $w$ , divide the cable into a series of 1-D finite elements as shown. Consider a generic element of length  $l$  with nodes  $a, b$  at its ends. Assume that the load  $q$  is uniform over the element, and assume that  $w$  varies linearly between values  $w_a, w_b$  at the two nodes.



- 7.2.5.1. Write down an expression for  $w$  at an arbitrary distance  $s$  from node  $a$ , in terms of  $w_a, w_b, s$  and  $l$ .
- 7.2.5.2. Deduce an expression for  $dw/dx$  within the element, in terms of  $w_a, w_b$  and  $l$ .
- 7.2.5.3. Hence, calculate an expression for the contribution to the potential energy arising from the element shown, and show that element contribution to the potential energy may be expressed as

$$V^{\text{elem}} = \frac{1}{2} [w_a, w_b] \begin{bmatrix} T/l & -T/l \\ -T/l & T/l \end{bmatrix} \begin{bmatrix} w_a \\ w_b \end{bmatrix} - [w_a, w_b] \begin{bmatrix} ql/2 \\ ql/2 \end{bmatrix}$$

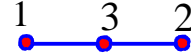
- 7.2.5.4. Write down expressions for the element stiffness matrix and residual vector.
- 7.2.5.5. Consider the finite element mesh shown in the figure. The loading  $q_0$  is uniform, and each element has the same length. The cable tension is  $T$ . Calculate the global stiffness matrix and residual vectors for the mesh, in terms of  $T$ ,  $L$ , and  $q_0$ .
- 7.2.5.6. Show how the global stiffness matrix and residual vectors must be modified to enforce the constraints  $w_1 = w_4 = 0$
- 7.2.5.7. Hence, calculate values of  $w$  at the two intermediate nodes.



## 8. Theory and Implementation of the Finite Element Method

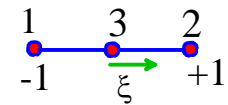
### 8.1. Generalized FEM for static linear elasticity

- 8.1.1. Consider a one-dimensional isoparametric quadratic element, illustrated in the figure, and described in more detail in Section 8.1.5.



- 8.1.1.1. Suppose that the nodes have coordinates  $x_1^1 = 0$ ,  $x_1^2 = 1$ ,  $x_1^3 = 2$ . Using a parametric plot, construct graphs showing the spatial variation of displacement in the element, assuming that the nodal displacements are given by (a)  $u_1^1 = 1$ ,  $u_1^2 = 0$ ,  $u_1^3 = 0$ , (b)  $u_1^1 = 0$ ,  $u_1^2 = 1$ ,  $u_1^3 = 0$ , (c)  $u_1^1 = 0$ ,  $u_1^2 = 0$ ,  $u_1^3 = 1$ , (d)  $u_1^1 = 0$ ,  $u_1^2 = 0.5$ ,  $u_1^3 = 1$
- 8.1.1.2. Suppose that the nodes have coordinates  $x_1^1 = 0$ ,  $x_1^2 = 1.75$ ,  $x_1^3 = 2$ . Plot graphs showing the spatial variation of displacement in the element for each of the four sets of nodal displacements given in 1.1.

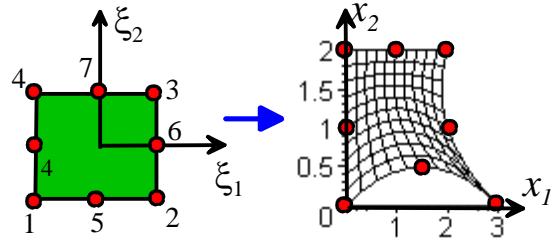
- 8.1.2. Consider the finite element scheme to calculate displacements in an axially loaded 1D bar, described in Section 8.15. Calculate an exact analytical expression for the 3x3 stiffness matrix



$$k_{ab} = \frac{2\mu(1-\nu)}{1-2\nu} h^2 \int_{x_0}^{x_1} \frac{\partial N^a(x_1)}{\partial x_1} \frac{\partial N^b(x_1)}{\partial x_1} dx_1$$

for a quadratic 1-D element illustrated in the figure. Write a simple code to integrate the stiffness matrix numerically, using the procedure described in 8.1.5 and compare the result with the exact solution (for this test, choose material and geometric parameters that give  $2\mu(1-\nu)h^2/(1-2\nu) = 1$ ) Try integration schemes with 1, 2 and 3 integration points.

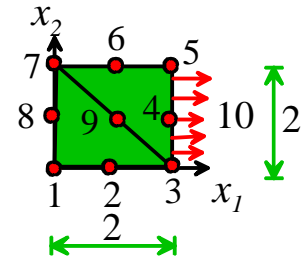
8.1.3. Consider the mapped, 8 noded isoparametric element illustrated in the figure. Write a simple program to plot a grid showing lines of  $\xi_1 = \text{constant}$  and  $\xi_2 = \text{constant}$  in the mapped element, as shown. Plot the grid with the following sets of nodal coordinates



- $x_1^{(1)} = 0, x_2^{(1)} = 0, x_1^{(2)} = 2.0, x_2^{(2)} = 2.0,$   
 $x_1^{(3)} = 2.0, x_2^{(3)} = 6.0, x_1^{(4)} = 0.0, x_2^{(4)} = 4.0,$   
 $x_1^{(5)} = 1.0, x_2^{(5)} = 1.0, x_1^{(6)} = 2.0, x_2^{(6)} = 4.0,$   
 $x_1^{(7)} = 1.0, x_2^{(7)} = 5.0, x_1^{(8)} = 0.0, x_2^{(8)} = 2.0$
- $x_1^{(1)} = 0, x_2^{(1)} = 0, x_1^{(2)} = 2.0, x_2^{(2)} = 0., x_1^{(3)} = 2.0, x_2^{(3)} = 2.0, x_1^{(4)} = 0.0, x_2^{(4)} = 2.0$   
 $x_1^{(5)} = 1.5, x_2^{(5)} = 1.0, x_1^{(6)} = 2.0, x_2^{(6)} = 1.0, x_1^{(7)} = 1.0, x_2^{(7)} = 2.0, x_1^{(8)} = 0.0, x_2^{(8)} = 1.0$

Note that for the latter case, there is a region in the element where  $\det(\partial x_i / \partial \xi_j) < 0$ . This is unphysical. Consequently, if elements with curved sides are used in a mesh, they must be designed carefully to avoid this behavior. In addition, quadratic elements can perform poorly in large displacement analyses.

8.1.4. Set up an input file for the general 2D/3D linear elastic finite element code provided to test the 6 noded triangular elements. Run the test shown in the figure (dimensions and loading are in arbitrary units) and use a Young's modulus and Poissons ratio  $E = 100, \nu = 0.3$ . Compare the FEA solution to the exact solution.

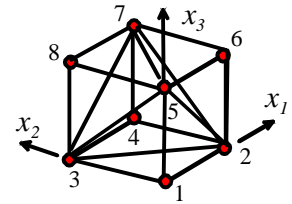


8.1.5. Set up an input file for the general 2D/3D linear elastic finite element code provided to test the 4 noded tetrahedral elements. Run the test shown in the figure. Take the sides of the cube to have length 2 (arbitrary units), and take  $E = 10, \nu = 0.3$ . Run the following boundary conditions:

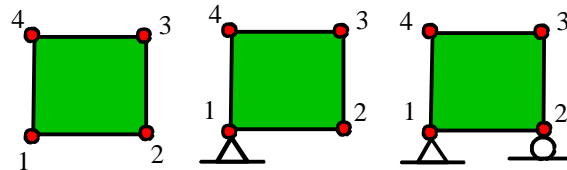
8.1.5.1.  $u_1 = u_2 = u_3 = 0$  at node 1,  $u_2 = u_3 = 0$  at node 2, and  $u_3 = 0$  at nodes 3 and 4. The faces at  $x_3 = 2$  subjected to uniform traction  $t_3 = 2$  (arbitrary units)

8.1.5.2.  $u_1 = u_2 = u_3 = 0$  at node 1,  $u_2 = u_1 = 0$  at node 5, and  $u_2 = 0$  at nodes 3 and 6. The face at  $x_2 = 2$  subjected to uniform traction  $t_2 = 2$  (arbitrary units)

In each case compare the finite element solution with the exact solution (they should be equal)

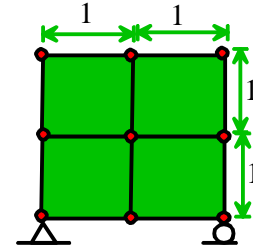


8.1.6. Add lines to the 2D/3D linear elastic finite element code to compute the determinant and the eigenvalues of the global stiffness matrix. Calculate the determinant and eigenvalues for a mesh containing a single 4 noded quadrilateral element, with each of the boundary conditions shown in the figure. Briefly discuss the implications of the results on the nature of solutions to the finite element equations.



8.1.7. Set up an input file for the mesh shown in the figure. Use material properties  $E=100, \nu=0.3$  and assume plane strain deformation. Run the following tests

- 8.1.7.1. Calculate the determinant of the global stiffness matrix
- 8.1.7.2. Change the code so that the element stiffness matrix is computed using only a single integration point. Calculate the determinant and eigenvalues of the global stiffness matrix.



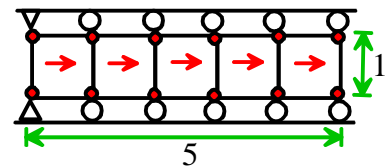
8.1.8. Extend the 2D/3D linear elastic finite element code provided to solve problems involving anisotropic elastic solids with cubic symmetry (see Section 3.2.16 for the constitutive law). This will require the following steps:

- 8.1.8.1. The elastic constants  $E, \nu, \mu$  for the cubic crystal must be read from the input file
- 8.1.8.2. The orientation of the crystal must be read from the input file. The orientation of the crystal can be specified by the components of vectors parallel to the  $[100]$  and  $[010]$  crystallographic directions.
- 8.1.8.3. The parts of the code that compute the element stiffness matrix and stress (for post-processing) will need to be modified to use elastic constants  $C_{ijkl}$  for a cubic crystal. The calculation is complicated by the fact that the components of  $C_{ijkl}$  must be expressed in the *global* coordinate system, instead of a coordinate system aligned with the crystallographic directions. You will need to use the unit vectors in 6.2 to calculate the transformation matrix  $Q_{ij}$  for the basis change, and use the basis change formulas in Section 3.2.11 to calculate  $C_{ijkl}$ .
- 8.1.8.4. Test your code by using it to compute the stresses and strains in a uniaxial tensile specimen made from a cubic crystal, in which the unit vectors parallel to  $[100]$  and  $[010]$  directions have components  $\mathbf{n}_{[100]} = \cos\theta\mathbf{e}_1 + \sin\theta\mathbf{e}_2$  and  $\mathbf{n}_{[010]} = -\sin\theta\mathbf{e}_1 + \cos\theta\mathbf{e}_2$ . Mesh the specimen with a single cubic 8 noded brick element, with side length 0.01m. Apply displacement boundary conditions to one face, and traction boundary conditions on another corresponding to uniaxial tension of 100MPa parallel to the  $\mathbf{e}_1$  axis. Run the following tests: (i) Verify that if  $E, \nu, \mu$  are given values that represent an isotropic material, the stresses and strains the element are independent of  $\theta$ . (ii) Use values for  $E, \nu, \mu$  representing copper (see Section 3.1.17). Define an apparent axial Young's modulus for the specimen as  $E(\theta) = \varepsilon_{11} / \sigma_{11}$ . Plot a graph showing  $E(\theta)$  as a function of  $\theta$ .

8.1.9. Extend the 2D/3D linear elastic finite element code to solve problems involving body forces. This will require the following steps

- 8.1.9.1. You will need to read a list of elements subjected to body forces, and the body force vector for each element. The list can be added to the end of the input file.
- 8.1.9.2. You will need to write a procedure to calculate the contribution from an individual element to the global system of finite element equations. This means evaluating the integral

$$\int_{V_e^{(l)}} b_i N^a(\mathbf{x}) dV$$



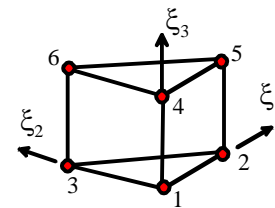


over the volume of the element. The integral should be evaluated using numerical quadrature – the procedure (other than the integrand) is essentially identical to computing the stiffness matrix.

8.1.9.3. You will need to add the contribution from each element to the global force vector. It is simplest to do this by modifying the procedure called `globaltraction()`.

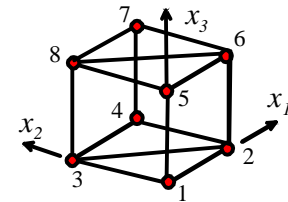
8.1.9.4. Test your code by using it to calculate the stress distribution in a 1D bar which is constrained as shown in the figure, and subjected to a uniform body force. Use 4 noded plane strain quadrilateral elements, and set  $E=10, \nu=0.25$  (arbitrary units) and take the body force to have magnitude 5. Compare the displacements and stresses predicted by the finite element computation with the exact solution.

8.1.10. Implement the linear 3D wedge-shaped element shown in the figure the 2D/3D linear elastic finite element code. To construct the shape functions for the element, use the shape functions for a linear triangle to write down the variation with  $(\xi_1, \xi_2)$ , and use a linear variation with  $\xi_3$ . Assume that  $0 \leq \xi_i \leq 1$ . You will need to add the shape functions and their derivatives to the appropriate procedures in the code. In addition, you will need to modify the procedures that compute the traction vectors associated with pressures acting on the element faces. Test your code by meshing a cube with two wedge-shaped elements as shown in the figure. Take the sides of the cube to have length 2 (arbitrary units), and take  $E=10, \nu=0.3$ . Run the following boundary conditions:



8.1.10.1.  $u_1 = u_2 = u_3 = 0$  at node 1,  $u_2 = u_3 = 0$  at node 2, and  $u_3 = 0$  at nodes 3 and 4. The faces at  $x_3 = 2$  subjected to uniform traction  $t_3 = 2$  (arbitrary units)

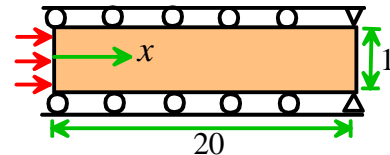
8.1.10.2.  $u_1 = u_2 = u_3 = 0$  at node 1,  $u_2 = u_1 = 0$  at node 5, and  $u_2 = 0$  at nodes 3 and 6. The face at  $x_2 = 2$  subjected to uniform traction  $t_2 = 2$  (arbitrary units)



In each case compare the finite element solution with the exact solution (they should be equal).

## 8.2. The Finite Element Method for dynamic linear elasticity

8.2.1. Set up the general purpose 2D/3D dynamic finite element code to solve the 1D wave propagation problem shown in the figure. Use material properties  $E=10, \nu=0.25, \rho=1$  (arbitrary units). Mesh the bar with square 4 noded quadrilateral plane strain elements. Assume that the left hand end of the bar is subjected to a constant traction with magnitude  $p=5$  at time  $t=0$ .



8.2.1.1. Calculate the maximum time step for a stable explicit computation.

8.2.1.2. Run an explicit dynamics computation (Newmark parameters  $\beta_1 = 1/2, \beta_2 = 0$ ) with a time step equal to half the theoretical stable limit. Use the simulation to plot the time variation of displacement, velocity and acceleration at  $x=0$ . Use at least 160 time steps. Compare the numerical solution with the exact solution.

8.2.1.3. Repeat 1.2 with a time step equal to twice the theoretical stable limit.

8.2.1.4. Repeat 1.2 and 1.3 with Newmark parameters  $\beta_1 = \beta_2 = 1/2$ .

8.2.1.5. Repeat 1.2 and 1.3 with Newmark parameters  $\beta_1 = \beta_2 = 1$ . Try a time step equal to ten times the theoretical stable limit.

8.2.2. The 2D/3D dynamic finite element code uses the row-sum method to compute lumped mass matrices.

- 8.2.2.1. Use the row-sum method to compute lumped mass matrices for linear and quadratic triangular elements with sides of unit length and mass density  $\rho=1$  (you can simply print out the matrix from the code)
- 8.2.2.2. Use the row-sum method to compute lumped mass matrices for linear and quadratic quadrilateral elements with sides of unit length and mass density  $\rho=1$
- 8.2.2.3. Modify the finite element code to compute the lumped mass matrix using the scaled diagonal method instead. Repeat 2.1 and 2.2.
- 8.2.2.4. Repeat problem 1.2 (using Newmark parameters  $\beta_1=1/2, \beta_2=0$ ) using the two versions of the lumped mass matrices, using quadratic quadrilateral elements to mesh the solid. Compare the results with the two versions of the mass matrix.

8.2.3. In this problem you will implement a simple 1D finite element method to calculate the motion of a stretched vibrating string.

The string has mass per unit length  $m$ , and is stretched by applying a tension  $T$  at one end. Assume small deflections. The equation of motion for the string (see Section 10.3.1) is

$$T \frac{d^2 w}{dx^2} = m \frac{d^2 w}{dt^2}$$

and the transverse deflection must satisfy  $w=0$  at  $x=0, x=L$ .

- 8.2.3.1. **Weak form of the equation of motion.** Let  $\delta w$  be a kinematically admissible variation of the deflection, satisfying  $\delta w=0$  at  $x=0, x=L$ . Show that if

$$\int_0^L m \frac{d^2 w}{dt^2} \delta w dx + \int_0^L T \frac{dw}{dx} \frac{d\delta w}{dx} dx = 0$$

for all admissible  $\delta w$ , then  $w$  satisfies the equation of motion.

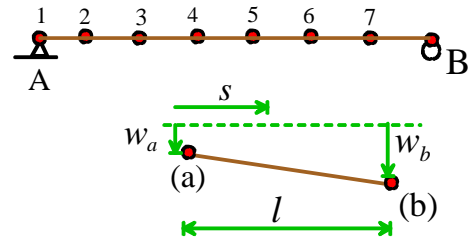
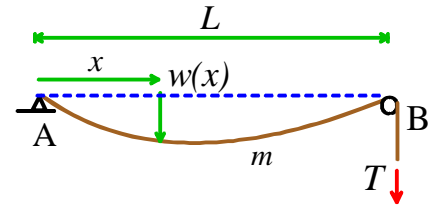
- 8.2.3.2. **Finite element equations** Introduce a linear finite element interpolation as illustrated in the figure. Calculate expressions for the element mass and stiffness matrices (you can calculate analytical expressions for the matrices, or evaluate the integrals numerically)

- 8.2.3.3. **Implementation:** Write a simple code to compute and integrate the equations of motion using the Newmark time integration procedure described in Section 8.2.5.

- 8.2.3.4. **Testing:** Test your code by computing the motion of the string with different initial conditions. Try the following cases:

- $w(x, t=0) = (L/10) \sin(n\pi x/L)$ ,  $n=1, 2, \dots$ . These are the mode shapes for string, so the vibration should be harmonic. You can calculate the corresponding natural frequency by substituting  $w = \cos \omega t \sin(n\pi x/L)$  into the equation of motion and solving for  $\omega$
- $w(x, t=0) = \begin{cases} x/5 & x < L/2 \\ (L-x)/5 & x > L/2 \end{cases}$

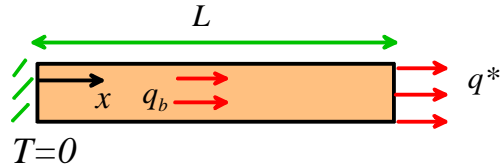
Use geometric and material parameters  $L=10, m=1, T=1$ . Run a series of tests to investigate (i) the effects of mesh size; (ii) the effects of using a lumped or consistent mass matrix; (ii) the



effects of time step size; and (iii) the effects of the Newmark parameters  $\beta_1, \beta_2$  on the accuracy of the solution.

8.2.4. Modify the 1D code described in the preceding problem to calculate the natural frequencies and mode shapes for the stretched string. Calculate the first 5 natural frequencies and mode shapes, and compare the numerical results with the exact solution.

8.2.5. The figure below shows a bar with thermal conductivity  $\kappa$  and heat capacity  $c$ . At time  $t=0$  the bar is at uniform temperature,  $T=0$ . The sides of the bar are insulated to prevent heat loss; the left hand end is held at fixed temperature  $T=0$ , while a flux of heat  $q^*$  is applied into to the right hand end of the bar. In addition, heat is generated inside the bar at rate  $q_b$  per unit length.



The temperature distribution in the bar is governed by the 1-D heat equation

$$c \frac{dT}{dt} = \kappa \frac{d^2T}{dx^2} + q_b$$

and the boundary condition at  $x = L$  is

$$\kappa \frac{dT}{dx} = q^*$$

In this problem, you will (i) set up a finite element method to solve the heat equation; (ii) show that the finite element stiffness and mass matrix for this problem are identical to the 1-D elasticity problem solved in class; (iii) implement a simple stepping procedure to integrate the temperature distribution with respect to time.

8.2.5.1. **Variational statement of the heat equation.** Let  $\delta T$  be an admissible variation of temperature, which must be (a) differentiable and (b) must satisfy  $\delta T = 0$  on the left hand end of the bar. Begin by showing that if the temperature distribution satisfies the heat equation and boundary condition listed above, then

$$\int_0^L c \frac{dT}{dt} \delta T + \int_0^L \kappa \frac{dT}{dx} \frac{d\delta T}{dx} dx - \int_0^L q_b \delta T dx - q^* \delta T(x=0) = 0$$

where  $\delta T(x=0)$  denotes the value of  $\delta T$  at the left hand end of the bar. To show this, use the procedure that was used to derive the principle of virtual work. First, integrate the first integral on the left hand side by parts to turn the  $d\delta T/dx$  into  $\delta T$ , then use the boundary conditions and governing equation to show that the variational statement is true. (Of course we actually rely on the converse – if the variational statement is satisfied for all  $\delta T$  then the field equations are satisfied)

8.2.5.2. **Finite element equations** Now, introduce a linear 1D finite element interpolation scheme as described in Section 8.2.5. Show that the diffusion equation can be expressed in the form

$$C_{ab} \frac{dT^b}{dt} + K_{ab} T^b(t=0) = f_a(t=0) \quad 1 < a \leq N$$

$$T^1 = 0$$

where  $T^b$ ,  $b=1,2,\dots,N$  denotes the unknown nodal values of temperature,  $C_{ab}$  is a heat capacity matrix analogous to the mass matrix defined in 8.2.5, and  $K_{ab}$  is a stiffness

matrix. Derive expressions for the element heat capacity matrix, and the element stiffness matrix, in terms of relevant geometric and material properties.

#### 8.2.5.3.

**Time integration scheme** Finally, we must devise a way to integrate the temperature distribution in the bar with respect to time. Following the usual FEA procedure, we will use a simple Euler-type time stepping scheme. To start the time stepping, we note that  $T^a$  is known at  $t=0$ , and note that we can also compute the rate of change of temperature at time  $t=0$  by solving the FEM equations

$$C_{ab} \frac{dT^b}{dt} + K_{ab} T^b(t=0) = f_a(t=0) \quad 1 < a \leq N$$

$$T^1 = 0$$

For a generic time step, our objective is to compute the temperature  $T^a$  and its time derivative  $\dot{T}^a$  at time  $t + \Delta t$ . To compute the temperature at the end of the step, we write

$$T^a(t + \Delta t) \approx T^a(t) + \Delta t \frac{dT^a}{dt}$$

and estimate  $dT/dt$  based on values at the start and end of the time step as

$$\frac{dT}{dt} = (1 - \beta) \frac{dT(t)}{dt} + \beta \frac{dT(t + \Delta t)}{dt}$$

where  $0 \leq \beta \leq 1$  is an adjustable numerical parameter. The time derivative of temperature at  $t + \Delta t$  must satisfy the FEA equations

$$C_{ab} \frac{dT^b(t + \Delta t)}{dt} + K_{ab} T^b(t + \Delta t) = f_a(t + \Delta t) \quad 1 < a \leq N$$

$$T^1(t + \Delta t) = 0$$

Hence, show that the time derivative of temperature at time  $t + \Delta t$  can be calculated by solving

$$[C_{ab} + \Delta t \beta K_{ab}] \frac{dT^b(t + \Delta t)}{dt} = -K_{ab} \left( T^b(t) + (1 - \beta) \Delta t \frac{dT^b(t)}{dt} \right) + f_a(t + \Delta t) \quad 1 < a \leq N$$

$$T^1(t + \Delta t) = 0$$

whereupon the temperature at  $t + \Delta t$  follows as

$$T^a(t + \Delta t) \approx T^a(t) + \Delta t (1 - \beta) \frac{dT^a(t)}{dt} + \Delta t (1 - \beta) \frac{dT^a(t + \Delta t)}{dt}$$

8.2.5.4. **Implementation.** Modify the 1D dynamic FEA code to calculate the temperature variation in a 1D bar.

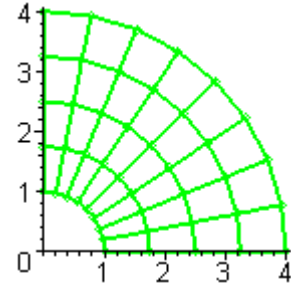
8.2.5.5. **Testing:** Test the code by setting the bar length to 5; x-sect area to 1; heat capacity=100, thermal conductivity=50; set the heat generation in the interior to zero (bodyforce=0) and set the heat input to the right hand end of the bar to 10 (traction=10), then try the following tests:

- To check the code, set the number of elements to  $L=15$ ; set the time step interval to  $dt=0.1$  and the number of steps to  $nstep=1000$ . Also, set up the code to use a lumped mass matrix by setting `lumpedmass=true` and explicit time stepping  $\beta = 0$ . You should find that this case runs quickly, and that the temperature in the bar gradually rises until it reaches the expected linear distribution.
- Show that the explicit time stepping scheme is conditionally stable. Try running with  $dt=0.2$  for just 50 or 100 steps.
- Show that the critical stable time step size reduces with element size. Try running with  $dt=0.1$  with 20 elements in the bar.

- Try running with a fully implicit time stepping scheme with  $\beta = 1$ , 15 elements and  $dt=0.2$ . Use a full consistent mass matrix for this calculation. Show that you can take extremely large time steps with  $\beta = 1$  without instability (eg try  $dt=10$  for 10 or 100 steps) – in fact the algorithm is unconditionally stable for  $\beta = 1$

### 8.3. Finite element method for hypoelastic materials

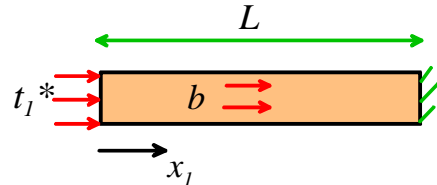
8.3.1. Set up an input file for the example hypoelastic finite element code described in Section 8.3.9 to calculate the deformation and stress in a hypoelastic pressurized cylinder deforming under plane strain conditions. Use the mesh shown in the figure, with appropriate symmetry boundary conditions on  $x_1 = 0$  and  $x_2 = 0$ . Apply a pressure of 50 (arbitrary units) to the internal bore of the cylinder and leave the exterior surface free of traction. Use the following material properties:  $\sigma_0 = 10$ ,  $\varepsilon_0 = 0.001$ ,  $n = 2$ ,  $\nu = 0.3$ . Plot a graph showing the variation of the radial displacement of the inner bore of the cylinder as a function of the internal pressure. **HEALTH WARNING:** The example code uses fully integrated elements and will give very poor results for large values of  $n$ .



8.3.2. Solve the following coupled nonlinear equations for  $x$  and  $y$  using Newton-Raphson iteration.

$$x(x^2 + y^2 + 1)^{1/3} - 5 = 0 \quad y(x^2 + y^2 + 1)^{1/3} + 3 = 0$$

8.3.3. Consider the simple 1D bar shown in the figure. Assume that the boundary conditions imposed on the bar are identical to those for the 1D elastic bar discussed in Section 8.1.5, so that  $u_1(x_1)$  is the only nonzero displacement component in the bar. Assume that the material has a hypoelastic constitutive equation, which has a nonlinear volumetric and deviatoric response, so that the stress-strain relation has the form



$$\sigma_{ij} = S_{ij} + \sigma_{kk} \delta_{ij} / 3 \quad S_{ij} = \frac{2}{3} f(\varepsilon_e) \frac{e_{ij}}{\varepsilon_e} \quad \sigma_{kk} = f(\bar{\varepsilon}) \frac{\varepsilon_{kk}}{\bar{\varepsilon}}$$

where

$$e_{ij} = \varepsilon_{ij} - \frac{1}{3} \varepsilon_{kk} \delta_{ij} \quad \varepsilon_e = \sqrt{\frac{2}{3} e_{ij} e_{ij}} \quad \bar{\varepsilon} = \sqrt{\varepsilon_{ii} \varepsilon_{jj}}$$

$$f(x) = \begin{cases} \sigma_0 \left[ \sqrt{\frac{1+n^2}{(n-1)^2} - \left( \frac{n}{n-1} - \frac{x}{\varepsilon_0} \right)^2} - \frac{1}{n-1} \right] & x \leq \varepsilon_0 \\ \sigma_0 \left( \frac{x}{\varepsilon_0} \right)^{1/n} & x \geq \varepsilon_0 \end{cases}$$

8.3.3.1. Show that the virtual work principle can be reduced to

$$\int_0^L \sigma_{11} \left[ \frac{\partial u_1}{\partial x_1} \right] \frac{\partial \delta v_1}{\partial x_1} dx_1 - \int_0^L b \delta v_1 dx_1 - t^* \delta v_1(0) = 0 \quad \sigma_{11} \left[ \frac{\partial u_1}{\partial x_1} \right] = \begin{cases} f(\partial u_1 / \partial x_1) & \partial u_1 / \partial x_1 > 0 \\ -f(\partial u_1 / \partial x_1) & \partial u_1 / \partial x_1 < 0 \end{cases}$$

- 8.3.3.2. Introduce a 1D finite element interpolation for  $u_1$  and  $\delta v_1$  following the procedure outlined in Section 8.1.5 to obtain a nonlinear system of equations for nodal values of  $u_1^a$ . Show that the nonlinear equations can be solved using a Newton-Raphson procedure, by repeatedly solving a system of linear equations

$$K_{ab}dw_1^b + R^a - F^a = 0$$

where  $dw_1^b$  denotes a correction to the current approximation to  $u_1^a$ . Give expressions for  $K_{ab}$  and  $R^a$ .

- 8.3.3.3. Extend the simple 1D linear elastic finite element code described in Section 8.1.5 to solve the hypoelasticity problem described here.
- 8.3.3.4. Test your code by (i) calculating a numerical solution with material properties  $\sigma_0 = 5$ ,  $n=2$ ,  $\varepsilon_0 = 0.1$  and loading  $b=0$ ,  $t_1^* = 10$ . and (ii) calculating a numerical solution with material properties  $\sigma_0 = 5$ ,  $n=10$ ,  $\varepsilon_0 = 0.1$  and loading  $b=10$ ,  $t_1^* = 0$ . Compare the numerical values of stress and displacement in the bar with the exact solution.

- 8.3.4. Calculate the tangent moduli  $\partial\sigma_{ij}/\partial\varepsilon_{kl}$  for the hypoelastic material described in the preceding problem.

- 8.3.5. In this problem you will develop a finite element code to solve *dynamic* problems involving a hypoelastic material with the constitutive model given in Section . Dynamic problems for nonlinear materials are nearly always solved using explicit Newmark time integration, which is very straightforward to implement. As usual, the method is based on the virtual work principle

$$\int_R \rho \frac{\partial^2 u_i}{\partial t^2} \delta v_i dV + \int_R \sigma_{ij} [\varepsilon_{kl}] \frac{\partial \delta v_i}{\partial x_j} dV - \int_R b_i \delta v_i dV - \int_{\partial_2 R} t_i^* \delta v_i dA = 0$$

$$u_i = u_i^* \quad \text{on } \partial_1 R$$

- 8.3.5.1. By introducing a finite element interpolation, show that the virtual work principle can be reduced to a system of equations of the form

$$(M_{ab} \ddot{u}_i^b + R_i^a - F_i^a) = 0$$

and give expressions for  $M_{ab}, R_i^a, F_i^a$ .

- 8.3.5.2. These equations of motion can be integrated using an explicit Newmark method, using the following expressions for the acceleration, velocity and displacement at the end of a generic time-step

$$u_i^a(t + \Delta t) \approx u_i^a(t) + \Delta t \dot{u}_i^a(t) + \frac{\Delta t^2}{2} \ddot{u}_i^a(t)$$

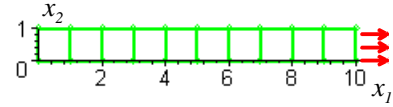
$$\ddot{u}_i^a(t + \Delta t) = M_{ab}^{-1} \left[ -R_i^b[u_i^a(t + \Delta t)] + F_i^b(t) \right]$$

$$\dot{u}_i^a(t + \Delta t) \approx \dot{u}_i^a(t) + \Delta t \left[ (1 - \beta_1) \ddot{u}_i^a(t) + \beta_1 \ddot{u}_i^a(t + \Delta t) \right]$$

A lumped mass matrix should be used to speed up computations. Note that the residual force vector  $R_i^a$  is a function of the displacement field in the solid. It therefore varies with time, and must be re-computed at each time step. Note that this also means that you must apply appropriate constraints to nodes with prescribed accelerations at each step.

Implement this algorithm by combining appropriate routines from the static hypoelastic code and the Newmark elastodynamic code provided.

- 8.3.5.3. Test your code by simulating the behavior of a 1D (plane strain) shown in the figure. Assume that the bar is at rest and stress free at  $t=0$ , and is then subjected to a constant horizontal traction at  $x_1=10$  for  $t>0$ . Fix the displacements for the node at  $x_1=x_2=0$  and apply  $u_1=0$  at  $x_1=0, x_2=1$ . Take the magnitude of the traction to be 2 (arbitrary units) and use material properties  $\sigma_0=1, \varepsilon_0=0.01, n=2, \nu=0.3, \rho=10$ . Take  $\beta_1=0.5$  in the Newmark integration, and use 240 time steps with step size 0.01 units. Plot a graph showing the displacement of the bar at  $x_1=10$  as a function of time. Would you expect the vibration frequency of the end of the bar to increase or decrease with  $n$ ? Test your intuition by running a few simulations.

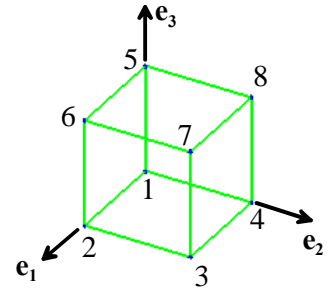


## 8.4. Finite element method for large deformations: hyperelastic materials

- 8.4.1. Write an input file for the demonstration hyperelastic finite element code described in Section 8.4.7 to calculate the stress in a Neo-Hookean tensile specimen subjected to uniaxial tensile stress. It is sufficient to model the specimen using a single 8 noded brick element. Use the code to plot a graph showing the nominal uniaxial stress as a function of the stretch ratio  $\lambda = l/l_0$ . Compare the finite element solution with the exact solution.
- 8.4.2. Extend the hyperelastic finite element code described in Section 8.4.7 to solve problems involving a Mooney-Rivlin material. This will require the following steps:
- 8.4.2.1. Calculate the tangent stiffness  $C_{ijkl}^e$  for the Mooney-Rivlin material
- 8.4.2.2. Modify the procedure called Kirchoffstress(...), which calculates the Kirchoff stress in the material in terms of  $B_{ij}$ , and modify the procedure called materialstiffness(...), which computes the corresponding tangent stiffness. Run the following tests on the code, using an 8 noded brick element to mesh the specimen:
- Subject the specimen to a prescribed change in volume, and calculate the corresponding stress in the element. Compare the FE solution with the exact solution.
  - Subject the specimen to a prescribed uniaxial tensile stress, and compare the FE solution with the exact solution
  - Subject the specimen to a prescribed biaxial tensile stress, and compare the FE solution to the exact solution.
- 8.4.3. Modify the hyperelastic finite element code described in Section 8.4.7 to apply a prescribed *true* traction to the element faces. To do this, you will need to modify the procedure that calculates the element distributed load vector, and you will need to write a new routine to compute the additional term in the stiffness discussed in Section 8.4.6. Test your code by repeating problem 1, but plot a graph showing *true* stress as a function of stretch ratio.

## 8.5. Finite element method for inelastic materials

8.5.1. Set up the demonstration viscoplastic finite element code described in Section 8.5.7 to calculate the stress-strain relation for the viscoplastic material under uniaxial tension. Mesh the specimen with a single 8 noded brick element, using the mesh shown in the figure. Apply the following boundary constraints to the specimen:  $u_1 = u_2 = u_3 = 0$  at node 1;  $u_2 = u_3 = 0$  at node 2,  $u_3 = 0$  at nodes 3 and 4. Apply a uniform traction whose magnitude increases from 0 to 20 (arbitrary units) in time of 2 units on face 2 of the element.



8.5.1.1. Run a simulation with the following material parameters:

$$E = 10000, \quad \nu = 0.3$$

$$Y = 15, \quad \varepsilon_0 = 0.5, \quad n = 10, \quad \dot{\varepsilon}_0 = 0.1, \quad m = 10$$

and plot a graph showing the variation of traction with displacement on the element

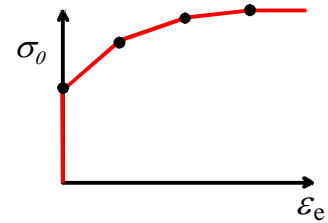
8.5.1.2. Modify the boundary conditions so that only the constraint  $u_3 = 0$  is enforced at node 2.

Run the code to attempt to find a solution (you will have to abort the calculation). Explain why the Newton iterations do not converge.

8.5.1.3. Repeat 1.1 with  $m = 200$ , the correct boundary conditions, and with a maximum traction of 18 units. In this limit the material is essentially rate independent. Compare the predicted traction-displacement curve with the rate independent limit.

8.5.2. Modify the viscoplastic finite element program to apply a constant (nominal) uniaxial strain rate to the specimen described in the preceding problem, by imposing an appropriate history of displacement on the nodes of the mesh. Test the code by plotting a graph showing uniaxial stress- $\nu$ -strain in the specimen, for material parameters  $E = 10000$ ,  $\nu = 0.3$ ,  $Y = 15$ ,  $\varepsilon_0 = 100$ ,  $n = 100$ ,  $\dot{\varepsilon}_0 = 0.1$ ,  $m = 4$  (in this limit the material is essentially a power-law creeping solid with constant flow stress) with an applied strain rate of  $\dot{\varepsilon}_{33} = 0.1$ . Compare the numerical solution with the exact solution.

8.5.3. Modify the viscoplastic finite element program so that instead of using a power-law function to represent the variation of flow-stress  $\sigma_0(\varepsilon_e)$  with accumulated plastic strain  $\varepsilon_e$ , the flow stress is computed by interpolating between a user-defined series of points, as indicated in the figure (the flow stress is constant if the plastic strain exceeds the last point). Test your code by using it to calculate the stress-strain relation for the viscoplastic material under uniaxial tension. Use the mesh described in Problem 1, and use material parameters  $E = 10000$ ,  $\nu = 0.3$ ,  $\dot{\varepsilon}_0 = 0.1$ ,  $m = 150$  (this makes the material essentially rigid and rate independent, so the stress-strain curve should follow the user-supplied data points).



8.5.4. Modify the viscoplastic finite element code described in Section 8.5.7 to solve problems involving a rate independent, power-law isotropic hardening elastic-plastic solid, with incremental stress-strain relations

$$\Delta \dot{\varepsilon}_{ij} = \Delta \dot{\varepsilon}_{ij}^e + \Delta \dot{\varepsilon}_{ij}^p$$



$$\Delta \varepsilon_{ij}^e = \frac{1+\nu}{E} \left( \Delta \sigma_{ij} - \frac{\nu}{1+\nu} \Delta \sigma_{kk} \delta_{ij} \right) \quad \Delta \varepsilon_{ij}^p = \Delta \varepsilon_e \frac{3}{2} \frac{S_{ij}}{\sigma_e}$$

$$S_{ij} = \sigma_{ij} - \sigma_{kk} \delta_{ij} / 3 \quad \sigma_e = \sqrt{\frac{3}{2} S_{ij} S_{ij}} \quad \Delta \varepsilon_e = \sqrt{\frac{2}{3} \Delta \varepsilon_{ij}^p \Delta \varepsilon_{ij}^p}$$

and a yield criterion

$$\sigma_e - Y_0 \left( 1 + \frac{\varepsilon_e}{\varepsilon_0} \right)^{1/n} = 0$$

Your solution should include the following steps:

- 8.5.4.1. Devise a method for calculating the stress  $\sigma_{ij}^{(n+1)}$  at the end of a load increment. Use a fully implicit computation, in which the yield criterion is exactly satisfied at the end of the load increment. Your derivation should follow closely the procedure described in Section 8.5.4, except that the relationship between  $\sigma_e^{(n+1)}$  and  $\Delta \varepsilon_e$  must be calculated using the yield criterion, and you need to add a step to check for elastic unloading.
- 8.5.4.2. Calculate the tangent stiffness  $\partial \sigma_{ij}^{(n+1)} / \partial \Delta \varepsilon_{kl}$  for the rate independent solid, by differentiating the result of 4.1.
- 8.5.4.3. Implement the results of 4.1 and 4.2 in the viscoplastic finite element code.
- 8.5.4.4. Test your code by using it to calculate the stress-strain relation for the viscoplastic material under uniaxial tension. Use the mesh, loading and boundary conditions described in Problem 1, and use material properties  $E = 10000$ ,  $\nu = 0.3$ ,  $Y = 18$ ,  $\varepsilon_0 = 0.5$ ,  $n = 10$

8.5.5. Modify the viscoplastic finite element code described in Section 8.5.7 to solve problems involving a rate independent, linear kinematic hardening elastic-plastic solid, with incremental stress-strain relations

$$\Delta \dot{\varepsilon}_{ij} = \Delta \dot{\varepsilon}_{ij}^e + \Delta \dot{\varepsilon}_{ij}^p$$

$$\Delta \varepsilon_{ij}^e = \frac{1+\nu}{E} \left( \Delta \sigma_{ij} - \frac{\nu}{1+\nu} \Delta \sigma_{kk} \delta_{ij} \right) \quad \Delta \varepsilon_{ij}^p = \Delta \varepsilon_e \frac{3}{2} \frac{S_{ij} - \alpha_{ij}}{Y}$$

$$S_{ij} = \sigma_{ij} - \sigma_{kk} \delta_{ij} / 3 \quad \sigma_e = \sqrt{\frac{3}{2} (S_{ij} - \alpha_{ij})(S_{ij} - \alpha_{ij})} \quad \Delta \varepsilon_e = \sqrt{\frac{2}{3} \Delta \varepsilon_{ij}^p \Delta \varepsilon_{ij}^p}$$

and a yield criterion and hardening law

$$\sigma_e - Y = 0 \quad \Delta \alpha_{ij} = c \Delta \varepsilon_e \frac{(S_{ij} - \alpha_{ij})}{Y}$$

Your solution should include the following steps:

- 8.5.5.1. Devise a method for calculating the stress  $\sigma_{ij}^{(n+1)}$  at the end of a load increment. Use a fully implicit computation, in which the yield criterion is exactly satisfied at the end of the load increment. Your derivation should follow closely the procedure described in Section 8.5.4, except that the relationship between  $\sigma_e^{(n+1)}$  and  $\Delta \varepsilon_e$  must be calculated using the yield criterion and hardening law, and you need to add a step to check for elastic unloading.
- 8.5.5.2. Calculate the tangent stiffness  $\partial \sigma_{ij}^{(n+1)} / \partial \Delta \varepsilon_{kl}$  for the rate independent solid, by differentiating the result of 8.5.5.1.
- 8.5.5.3. Implement the results of 8.5.5.1 and 8.5.5.2 in the viscoplastic finite element code.

- 8.5.5.4. Test your code by using it to calculate the stress-strain relation for the viscoplastic material under uniaxial tension. Use the mesh, loading and boundary conditions described in Problem 1, and use material properties  $E = 10000$ ,  $\nu = 0.3$ ,  $Y = 18$ ,  $c = 100$
- 8.5.6. In this problem you will develop a finite element code to solve *dynamic* problems involving viscoplastic materials. Dynamic problems for nonlinear materials are nearly always solved using explicit Newmark time integration, which is very straightforward to implement. As usual, the method is based on the virtual work principle

$$\int_R \rho \frac{\partial^2 u_i}{\partial t^2} \delta v_i dV + \int_R \sigma_{ij} [\varepsilon_{kl}] \frac{\partial \delta v_i}{\partial x_j} dV - \int_R b_i \delta v_i dV - \int_{\partial_2 R} t_i^* \delta v_i dA = 0$$

$$u_i = u_i^* \quad \text{on } \partial_1 R$$

- 8.5.6.1. By introducing a finite element interpolation, show that the virtual work principle can be reduced to a system of equations of the form

$$(M_{ab} \dot{u}_i^b + R_i^a - F_i^a) = 0$$

and give expressions for  $M_{ab}, R_i^a, F_i^a$ .

- 8.5.6.2. To implement the finite element method, it is necessary to calculate the stress  $\sigma_{ij}$  in the solid. Idealize the solid as a viscoplastic material with constitutive equations described in Section 8.5.1. Since very small time-steps must be used in an explicit dynamic calculation, it is sufficient to integrate the constitutive equations with respect to time using an explicit method, in which the plastic strain rate is computed based on the stress at the start of a time increment. Show that the stress  $\sigma_{ij}^{(n+1)}$  at time  $t + \Delta t$  can be expressed in terms of the stress  $\sigma_{ij}^{(n)}$  at time  $t$ , the increment in total strain  $\Delta \varepsilon_{ij}$  during the time interval  $\Delta t$  and material properties as

$$\sigma_{ij}^{(n+1)} = \sigma_{ij}^{(n)} + \frac{E}{1+\nu} \left( \Delta \varepsilon_{ij} - \Delta t \dot{\varepsilon}_0 \exp(-Q/kT) \left( \frac{\sigma_e^{(n)}}{\sigma_0^{(n)}} \right)^m \frac{3}{2} \frac{S_{ij}^{(n)}}{\sigma_e^{(n)}} \right) + \frac{E}{3(1-2\nu)} \Delta \varepsilon_{kk}$$

- 8.5.6.3. The equations of motion can be integrated using an explicit Newmark method using the following expressions for the acceleration, velocity and displacement at the end of a generic time-step

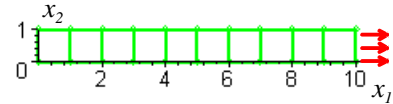
$$u_i^a(t + \Delta t) \approx u_i^a(t) + \Delta t \dot{u}_i^a(t) + \frac{\Delta t^2}{2} \ddot{u}_i^a(t)$$

$$\ddot{u}_i^a(t + \Delta t) = M_{ab}^{-1} \left[ -R_i^b[u_i^a(t + \Delta t)] + F_i^b(t) \right]$$

$$\dot{u}_i^a(t + \Delta t) \approx \dot{u}_i^a(t) + \Delta t \left[ (1 - \beta_1) \ddot{u}_i^a(t) + \beta_1 \ddot{u}_i^a(t + \Delta t) \right]$$

A lumped mass matrix should be used to speed up computations. Note that the residual force vector  $R_i^a$  is a function of the displacement field in the solid. It therefore varies with time, and must be re-computed at each time step. Note that this also means that you must apply appropriate constraints to nodes with prescribed accelerations at each step. Implement this algorithm by combining appropriate routines from the static viscoplastic code and the Newmark elastodynamic code provided.

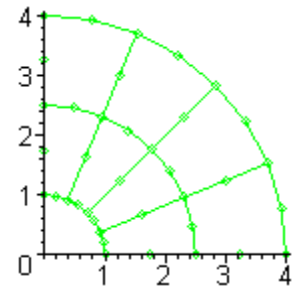
- 8.5.6.4. Test your code by simulating the behavior of a 1D (plane strain) shown in the figure. Assume that the bar is at rest and stress free at  $t=0$ , and is then subjected to a constant horizontal traction at  $x_1=10$  for  $t>0$ . Fix the displacements for the node at  $x_1=x_2=0$  and apply  $u_1=0$  at  $x_1=0, x_2=1$ . Take the magnitude of the traction to be 2 (arbitrary units) and use material properties  $\sigma_0=1, \varepsilon_0=0.01, n=2, \nu=0.3, \rho=10$ . Take  $\beta_1=0.5$  in the Newmark integration, and use 240 time steps with step size 0.01 units. Plot a graph showing the displacement of the bar at  $x_1=10$  as a function of time.



## 8.6. Advanced element formulations – Incompatible modes; reduced integration; and hybrid elements

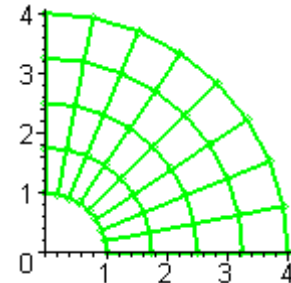
- 8.6.1. Volumetric locking can be a serious problem in computations involving nonlinear materials. In this problem, you will demonstrate, and correct, locking in a finite element simulation of a pressurized hypoelastic cylinder.

- 8.6.1.1. Set up an input file for the example hypoelastic finite element code described in Section 8.3.9 to calculate the deformation and stress in a hypoelastic pressurized cylinder deforming under plane strain conditions. Use the mesh shown in the figure, with appropriate symmetry boundary conditions on  $x_1=0$  and  $x_2=0$ . Apply a pressure of 20 (arbitrary units) to the internal bore of the cylinder and leave the exterior surface free of traction. Use the following material properties:  $\sigma_0=10, \varepsilon_0=0.001, n=2, \nu=0.3$ . Plot a graph of the variation of the radial displacement of the inner bore of the cylinder as a function of the applied pressure. Make a note of the displacement at the maximum pressure.



- 8.6.1.2. Edit the code to reduce the number of integration points used to compute the element stiffness matrix from 9 to 4. (modify the procedure called 'numberofintegrationpoints'). Repeat the calculation in 8.6.1.1. Note the substantial discrepancy between the results of 8.6.1.1 and 8.6.1.2 – this is caused by locking. The solution in 5.2, which uses reduced integration, is the more accurate of the two. Note also that using reduced integration improves the rate of convergence of the Newton-Raphson iterations.

- 8.6.2. Modify the hypoelastic finite element code described in Section 8.3.9 to use selective reduced integration. Check your code by (a) repeating the calculation described in problem 8.6.1; and (b) running a computation with a mesh consisting of 4 noded quadrilateral elements, as shown in the figure. In each case, calculate the variation of the internal radius of the cylinder with the applied pressure, and plot the deformed mesh at maximum pressure to check for hourglassing. Compare the solution obtained using selective reduced integration with the



- 8.6.3. Run the simple demonstration of the B-bar method described in Section 8.6.2 to verify that the method can be used to solve problems involving near-incompressible materials. Check the code with both linear and quadratic quadrilateral elements.

8.6.4. Extend the B-bar method described in Section 8.6.2 to solve problems involving hypoelastic materials subjected to small strains. This will require the following steps:

8.6.4.1. The virtual work principle for the nonlinear material must be expressed in terms of the modified strain measures  $\bar{\varepsilon}_{ij}$  and  $\delta\bar{\varepsilon}_{ij}$  defined in Section 8.6.2. This results in a system of nonlinear equations of the form

$$\int_R \sigma_{ij}[\bar{\varepsilon}_{ij}(u_k)] \delta\bar{\varepsilon}_{ij} dV - \int_R b_i \delta v_i dV - \int_{\partial_2 R} t_i^* \delta v_i dA = 0$$

$$u_i = u_i^* \quad \text{on } \partial_1 R$$

which must be solved using the Newton-Raphson method. Show that the Newton-Raphson procedure involves repeatedly solving the following system of linear equations for corrections to the displacement field  $dw_k^b$

$$K_{aibk} dw_k^b = -R_i^a + F_i^a$$

$$K_{aibk} = \int_R \frac{\partial \sigma_{pq}}{\partial \varepsilon_{kl}} \bar{B}_{pji}^a \bar{B}_{qlj}^b dV \quad R_i^a = \int_R \sigma_{kj} [\bar{\varepsilon}_{kl}(w_i^b)] \bar{B}_{kji}^a dV \quad F_i^a = \int_R b_i N^a dV + \int_{\partial R} t_i^* N^a dA$$

where  $\bar{B}_{ijk}^a$  is defined in Section 8.6.2.

8.6.4.2. Modify the hypoelastic code provided to compute the new form of the stiffness matrix and element residual. You will find that much of the new code can simply be copied from the small strain linear elastic code with the B-bar method

8.6.4.3. Test the code by solving the problems described in 8.6.1 and 8.6.2.

8.6.5. Extend the B-bar method described in Section 8.6.2 to solve problems involving hypoelastic materials subjected to small strains, following the procedure outlined in the preceding problem.

8.6.6. In this problem you will extend the B-bar method to solve problems involving finite deformations, using the hyperelasticity problem described in Section 8.4 as a representative example. The first step is to compute new expressions for the residual vector and the stiffness matrix in the finite element approximation to the field equations. To this end

- New variables are introduced to characterize the volume change, and the rate of volume change in the element. Define

$$\eta = \frac{1}{V_{el}} \int_{V_{el}} \det(\mathbf{F}) dV \quad \dot{\eta} = \frac{1}{V_{el}} \int_{V_{el}} J F_{ji}^{-1} \dot{F}_{ij} dV = \frac{1}{V_{el}} \int_{V_{el}} J L_{kk} dV$$

Here, the integral is taken over the volume of the element in the reference configuration.

- The deformation gradient is replaced by an approximation  $\bar{F}_{ij} = F_{ij} (\eta/J)^{1/n}$ , where  $n=2$  for a 2D problem and  $n=3$  for a 3D problem, while  $J=\det(\mathbf{F})$ .
- The virtual velocity gradient is replaced by the approximation  $\delta\bar{L}_{ij} = \delta L_{ij} + \delta_{ij} (\delta\dot{\eta}/\eta - \delta L_{kk})/n$

The virtual work equation is replaced by

$$\int_{V_0} \tau_{ij} [\bar{F}_{kl}] \delta\bar{L}_{ij} dV_0 - \int_{V_0} \rho_0 b_i \delta v_i dV_0 - \int_{\partial_2 V_0} t_i^* \delta v_i \eta dA_0 = 0$$

8.6.6.1. Verify that  $\bar{L}_{ij} = \bar{F}_{ik} \dot{\bar{F}}_{kj}^{-1}$

8.6.6.2. In calculations to follow it will be necessary to calculate  $\phi_{ij} = \partial\eta/\partial F_{ij}$ . Find an expression for  $\phi_{ij}$ .

- 8.6.6.3. The virtual work equation must be solved for the unknown nodal displacements by Newton-Raphson iteration. Show that, as usual, the Newton-Raphson procedure involves repeatedly solving the following system of linear equations for corrections to the displacement field  $dw_k^b$

$$K_{aibk} dw_k^b = -R_i^a + F_i^a$$

and derive expressions for  $R_i^a$  and  $K_{iakb}$ .

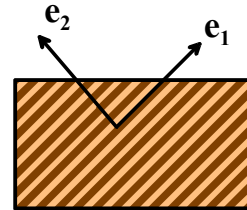
## 9. Modeling Material Failure

### 9.1. Summary of mechanisms of fracture and fatigue under static and cyclic loading

### 9.2. Stress and strain based fracture and fatigue criteria

- 9.2.1. A flat specimen of glass with fracture strength  $\sigma_{TS}$ , Young's modulus  $E$  and Poisson's ratio  $\nu$  is indented by a hard metal sphere with radius  $R$ ,  $E_2$  and Poisson's ratio  $\nu_2$ . Using solutions for contact stress fields given in Chapter 5, calculate a formula for the load  $P$  that will cause the glass to fracture, in terms of geometric and material parameters. You can assume that the critical stress occurs on the surface of the glass.

- 9.2.2. The figure shows a fiber reinforced composite laminate.
- (i) When loaded in uniaxial tension parallel to the fibers, it fails at a stress of 500MPa.
  - (ii) When loaded in uniaxial tension transverse to the fibers, it fails at a stress of 250 MPa.
  - (iii) When loaded at 45 degrees to the fibers, it fails at a stress of 223.6 MPa



The laminate is then loaded in uniaxial tension at 30 degrees to the fibers. Calculate the expected failure stress under this loading, assuming that the material can be characterized using the Tsai-Hill failure criterion.

- 9.2.3. A number of cylindrical specimens of a brittle material with a 1cm radius and length 4cm are tested in uniaxial tension. It is found 60% of the specimens withstand a 150MPa stress without failure; while 30% withstand a 170 MPa stress without failure.

9.2.3.1. Calculate values for the Weibull parameters  $\sigma_0$  and  $m$  for the specimens

9.2.3.2. Suppose that a second set of specimens is made from the same material, with length 8cm and radius 1cm. Calculate the stress level that will cause 50% of these specimens to fail.

- 9.2.4. A beam with length  $L$ , and rectangular cross-section  $b \times h$  is made from a brittle material with Young's modulus  $E$ , Poisson's ratio  $\nu$ , and the failure probability distribution of a volume  $V_0$  is characterized by Weibull parameters  $\sigma_0$  and  $m$ .

9.2.4.1. Suppose that the beam is loaded in uniaxial tension parallel to its length. Calculate the stress level  $\sigma_0$  corresponding to 63% failure, in terms of geometric and material parameters.

- 9.2.4.2. Suppose that the beam is loaded in 3 point bending. Let  $\sigma_R = 3PL/(bh^2)$  denote the maximum value of stress in the beam (predicted by beam theory). Find an expression for the stress distribution in the beam in terms of  $\sigma_R$
- 9.2.4.3. Hence, find an expression for the value of  $\sigma_R$  that corresponds to 63% probability of failure in the beam. Calculate the ratio  $\sigma_R/\sigma_0$ .
- 9.2.5. A glass shelf with length  $L$  and rectangular cross-section  $b \times h$  is subjected to a uniform load  $w$  on its surface. As received, the shelf has a tensile strength  $\sigma_{TS0}$
- 9.2.6. A cylindrical concrete column with radius  $R$ , cross-sectional radius  $R$ , and length  $L$  is subjected to a monotonically increasing compressive axial load  $P$ . Assume that the material can be idealized using the constitutive law given in Section 9.2.4, with the compressive yield stress-v-plastic strain of the form
- $$Y(\bar{\varepsilon}^P) = \sigma_0 \left( \frac{\bar{\varepsilon}^P}{\varepsilon_0} \right)^{1/m}$$
- where  $\sigma_0, \varepsilon_0$  and  $m$  are material properties. Assume small strains, and a homogeneous state of stress and strain in the column. Neglect elastic deformation, for simplicity.
- 9.2.6.1. Calculate the relationship between the axial stress  $P/A$  and strain  $\delta/L$ , in terms of the plastic properties  $c$ ,  $\sigma_0, \varepsilon_0$  and  $m$
- 9.2.6.2. Calculate the volume change of the column, in terms of  $P/A$ ,  $c$ ,  $\sigma_0, \varepsilon_0$  and  $m$
- 9.2.6.3. Suppose that the sides of the column are subjected to a uniform traction  $q$ . Repeat the calculations in parts 9.2.6.1 and 9.2.6.2.
- 9.2.7. Suppose that the column described in the previous problem is encased in a steel tube, with (small) wall thickness  $t$ . The steel can be idealized as a rigid perfectly plastic material with yield stress  $Y$ . Calculate the relationship between the axial stress  $P/A$  and strain  $\delta/L$ , in terms of geometric and material properties.
- 9.2.8. Extend the viscoplastic finite element program described in Section 8.5 to model the behavior of a porous plastic material with constitutive equations given in Section 9.2.5. This will involve the following steps:
- 9.2.8.1. Develop a procedure to calculate the stress  $\sigma_{ij}^{(n+1)}$ , the void volume fraction  $V_f^{(n+1)}$ , the effective strain measures  $\bar{\varepsilon}_m^{(n+1)}, \bar{\varepsilon}_e^{(n+1)}$  at the end of the time increment, given their values at the start of the increment and given an increment in plastic strain  $\Delta\varepsilon_{ij}$ . You should use a fully implicit update, as discussed in Section 8.5. The simplest approach is to set up, and solve, three simultaneous nonlinear equations for  $(V_f^{(n+1)}, \bar{\varepsilon}_m^{(n+1)}, \bar{\varepsilon}_e^{(n+1)})$  using Newton-Raphson iteration, and subsequently compute the stress distribution.
- 9.2.8.2. Calculate the tangent stiffness  $\partial\sigma_{ij}^{(n+1)}/\partial\Delta\varepsilon_{ij}$  for the material
- 9.2.8.3. Implement the new constitutive equations in the viscoplastic finite element program
- 9.2.8.4. Test your code by simulating the behavior of a uniaxial tensile specimen

- 9.2.9. A specimen of steel has a yield stress of 500MPa. Under cyclic loading at a stress amplitude of 200 MPa it is found to fail after  $10^4$  cycles, while at a stress amplitude of 100MPa it fails after  $10^5$  cycles. This material is to be used to fabricate a plate, with thickness  $h$ , containing circular holes with radius  $a < h$ . The plate will be subjected to constant amplitude cyclic uniaxial stress far from the holes, and must have a life of at least  $10^5$  cycles. What is the maximum stress amplitude that the plate can withstand?
- 9.2.10. A spherical pressure vessel with internal radius  $a$  and external radius  $b=1.5a$  is repeatedly pressurized from zero internal pressure to a maximum value  $p$ . The sphere has yield stress  $Y$ , and its fatigue behavior of the vessel (under fully reversed uniaxial tension) can be characterized by Basquin's law  $\sigma_a N^b = C$ .
- 9.2.10.1. Find an expression for the fatigue life of the vessel in terms of  $p$ , and relevant geometric and material properties. Assume that the effects of mean stress can be approximated using Goodman's rule. Assume that  $p/Y < 2(1 - a^3/b^3)/3$
- 9.2.10.2. Suppose that the vessel is first pressurized to its collapse load and then unloaded, so as to induce a distribution of residual stress in the cylinder. It is subsequently subjected to a cyclic pressure with magnitude  $p$ . Calculate the mean stress and stress amplitude as a function of position in the vessel wall, and hence deduce an expression for its fatigue life.
- 9.2.11. A specimen of steel is tested under cyclic loading. It is found to have a fatigue threshold  $\sigma_0 = 75\text{MPa}$ , and fails after  $10^3$  cycles when tested at a stress amplitude  $\sigma_a = 1.5\sigma_0$ . Suppose that, in service, the material spends 80% of its life subjected to stress amplitudes  $\sigma_a < \sigma_0$ , 10% of its life at  $\sigma_a = 1.1\sigma_0$ , and the remainder at  $\sigma_a = 1.2\sigma_0$ . Calculate the life of the component during service (assume that the mean stress  $\sigma_m = 0$  during both testing and service).
- 9.2.12. The figure shows a solder joint on a printed circuit board. The printed circuit board can be idealized as a pinned-pinned beam with thickness  $h$ , length  $L$ , Young's modulus  $E$  and mass density  $\rho$ . The board vibrates in its fundamental mode with a frequency  $\omega = (\pi h/L)\sqrt{E/12\rho}$  and mode shape  $u_3 = A\sin(\pi x_1/L)$ . The yield stress of solder is so low it can be neglected. The fatigue life of solder can be characterized by a Coffin-Manson law  $\Delta\epsilon^p N^b = C$ . Find an expression for the time to failure of the solder joint, in terms of relevant geometric and material parameters.

### 9.3. Modeling failure by crack growth – linear elastic fracture mechanics

- 9.3.1. Using the equations for the crack tip fields find an expression for the maximum shear stress distribution around the tip of a plane-strain Mode I crack. Hence, plot approximate contours of successive yield zones
- 9.3.2. Briefly describe the way in which the concept of stress intensity factor can be used as a fracture criterion.
- 9.3.3. A welded plate with fracture toughness  $K_{IC}$  contains a residual stress distribution

$$\sigma_{22} = \sigma_R a / \left( \sqrt{x_1^2 + a^2} \right)$$

A crack with length  $2a$  lies on the weld line. The solid is subjected to a uniaxial tensile stress  $\sigma_{22} = \sigma_0$ . Find an expression for the critical value of  $\sigma_0$  that will cause the weld to fracture, in terms of  $K_{IC}$ ,  $\sigma_R$  and  $a$ .

9.3.4. Hard, polycrystalline materials such as ceramics often contain a distribution of inter-granular residual stress. The objective of this problem is to estimate the influence of this stress distribution on crack propagation through the material. Assume that

- The solid has mode I fracture toughness  $K_{IC}$
- As a rough estimate, the residual stress distribution can be idealized as  $\sigma_{22} = \sigma_R \sin(\pi x_1 / L)$ , where  $L$  is of the order of the grain size of the solid and  $\sigma_R$  is the magnitude of the stress.
- A long (semi-infinite) crack propagates through the solid – at some time  $t$ , the crack tip is located at  $x_1 = c$
- The solid is subjected to a remote stress, which induces a mode I stress intensity factor  $K_I^\infty$  at the crack tip

9.3.4.1. If the solid is free of residual stress, what value of  $K_I^\infty$  that causes fracture.

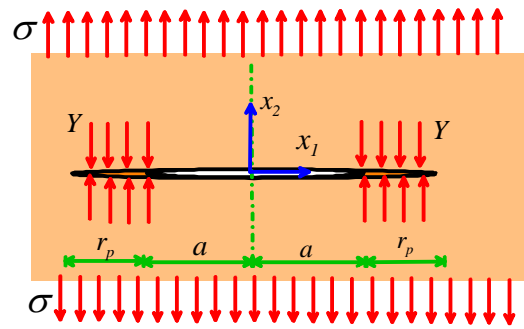
9.3.4.2. Calculate the stress intensity factor induced by the residual stress distribution, as a function of  $c$ .

9.3.4.3. What value of  $K_I^\infty$  is necessary to cause crack propagation through the residual stress field? What is the maximum value of  $K_I^\infty$ , and for what crack tip position  $c$  does it occur?

9.3.5. A dislocation, with burgers vector  $\mathbf{b} = b_1 \mathbf{e}_1 + b_2 \mathbf{e}_2$  and line direction  $\mathbf{e}_3$  lies a distance  $d$  ahead of a semi-infinite crack. Calculate the crack tip stress intensity factors.

9.3.6. The figure shows a simple model that is used to estimate the size of the plastic zone at a crack tip. The crack, with length  $2a$ , together with the plastic zones with length  $r_p$ , are considered together to be a crack with length  $2(a + r_p)$ . The solid is loaded by uniform stress  $\sigma$  at infinity. The region with length  $r_p$  near each crack tip is subjected to traction  $Y$  acting to close the crack. Using the solutions in Section 9.3.3, calculate an expression for the Mode I crack tip stress intensity factor.

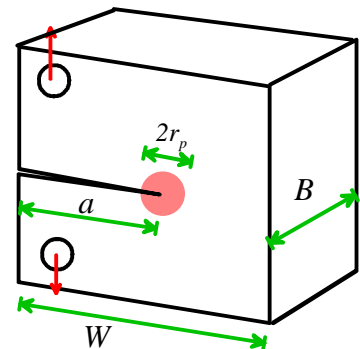
Show that  $K_I = 0$  if  $\frac{r_p}{a} = \sec\left(\frac{\pi\sigma}{2Y}\right) - 1$



9.3.7. Suppose that an ASTM compact tension specimen is used to measure the fracture toughness of a steel. The specimen has dimensions  $W = 40\text{mm}$  and  $B = 20\text{mm}$ . The crack length was  $18.5\text{mm}$ , and the fracture load was  $15\text{kN}$ .

9.3.7.1. Calculate the fracture toughness of the steel.

9.3.7.2. If the steel has yield stress  $800\text{MPa}$ , was this a valid measurement?



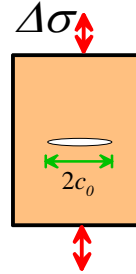


9.3.8. Find expressions for the Mode I and II stress intensity factors for the angled crack shown. If  $\alpha = 45^\circ$ , what is the initial direction of crack propagation? Confirm your prediction experimentally, using a center-cracked specimen of paper.

9.3.9. A large solid contains a crack with initial length  $2c_0$ . The solid has plane-strain fracture toughness  $K_{IC}$ , and under cyclic loading the crack growth rate obeys Paris law

$$\frac{da}{dN} = C(\Delta K_I)^n$$

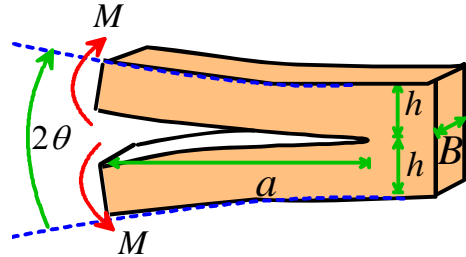
- 9.3.9.1. Suppose that the material is subjected to a cyclic uniaxial stress with amplitude  $\Delta\sigma$  and mean stress  $\Delta\sigma$  (so the stress varies between 0 and  $2\Delta\sigma$ ). Calculate the critical crack length that will cause fracture, in terms of  $K_{IC}$  and  $\Delta\sigma$
- 9.3.9.2. Calculate an expression for the number of cycles of loading that are necessary to cause a crack to grow from an initial length  $2c_0$  to fracture under the loading described in 7.1
- 9.3.9.3. Show that the number of cycles to failure can be expressed in the form of Basquin's law (discussed in Section 9.2.7) as  $N(\Delta\sigma)^b = D$ , where  $b$  and  $D$  are constants. Give expressions for  $b$  and  $D$  in terms of the initial crack length, the fracture toughness, and the material properties in Paris law



#### 9.4. Energy methods in fracture mechanics

9.4.1. The figure shows a double-cantilever beam fracture specimen that is loaded by applying moments to the ends of the beams. Define the compliance of the solid as  $C = 2\theta / M$

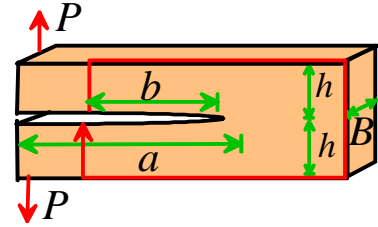
- 9.4.1.1. Derive an expression relating the crack tip energy release rate to compliance and dimensions of the specimen.
- 9.4.1.2. Use the result of 9.4.1.1 to calculate the crack tip stress intensity factors for the specimen in terms of  $M$  and relevant geometric and material properties.



9.4.2. The figure shows a thin rectangular strip of material with height  $2h$  and out-of-plane thickness  $B$ . The material can be idealized as a linear elastic solid with Young's modulus  $E$  and Poisson's ratio  $\nu$ . The strip is damaged by an array of widely-spaced cracks with length  $2a$  and spacing  $L \gg a$ . It is loaded by a uniform tensile traction  $t$  acting on the top and bottom surface, which induces a displacement  $\Delta$ .

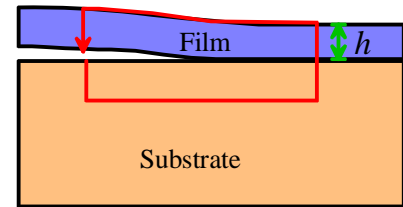
- 9.4.2.1. Write down an expression for the compliance  $\Delta/t$  of the undamaged strip (i.e. with no cracks)
- 9.4.2.2. Write down a relationship between the compliance of the strip and the crack tip energy release rate.
- 9.4.2.3. Estimate the crack tip using the energy release rate for an isolated crack in an infinite solid. Hence, estimate the compliance of the cracked strip.

- 9.4.3. The figure shows a double cantilever beam specimen that is loaded by forces applied to the ends of the beams. Evaluate the  $J$  integral around the path shown to calculate the crack tip energy release rate. You can use elementary beam theory to estimate the strain energy density, stress, and displacement in the two cantilevers. The solution must, of course, be independent of  $b$ .



- 9.4.4. Use the  $J$  integral, together with the solution for the stress and displacement field near the tip of a crack given in Section 9.3.1, to calculate the relationship between the crack tip energy release rate and the stress intensity factor for a Mode I crack.

- 9.4.5. The figure shows a thin film with thickness  $h$ , thermal expansion coefficient  $\alpha_f$ , Young's modulus  $E$  and Poisson's ratio  $\nu$  on a large substrate with thermal expansion coefficient  $\alpha_s$ . The film is initially perfectly bonded to the substrate and stress free. The system is then heated, inducing a thermal stress in the film. As a result, the film delaminates from the substrate, as shown in the figure.

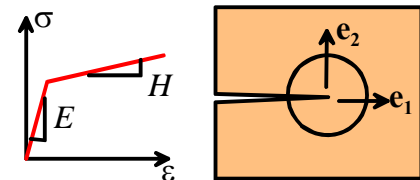


- 9.4.5.1. Calculate the state of stress a distance  $d \gg h$  ahead of the advancing crack tip
- 9.4.5.2. Assume that the film is stress free a distance  $d \gg h$  behind the crack tip. By directly calculating the change in energy of the system as the crack advances, find an expression for the crack tip energy release rate
- 9.4.5.3. Check your answer to 9.4.5.2 by evaluating the  $J$  integral around the path indicated in the figure.

## 9.5. Plastic fracture mechanics

- 9.5.1. Explain briefly the main concepts underlying the use of the  $J$  integral as a fracture criterion in components experiencing large-scale plastic deformation.

- 9.5.2. The figure shows the tip of a semi-infinite crack in an elastic-plastic material with a bi-linear uniaxial stress-strain curve, as indicated in the figure. To provide some insight into the nature of the crack tip fields, the constitutive behavior can be approximated as a hypoelastic material, characterized by a strain energy density  $W$  such that  $\sigma_{ij} = \partial W / \partial \varepsilon_{ij}$ . Suppose that the solid is subjected to remote mode I loading (so that the shear stresses  $\sigma_{12} = \sigma_{13} = 0$  on  $x_2 = 0$ ).



- 9.5.2.1. Construct the full stress-strain equations for the hypoelastic material, using the approach described in Section 3.3
- 9.5.2.2. Consider a material point that is very far from the crack tip, and so is subjected to a very low stress. Write down the asymptotic stress field in this region, in terms of an arbitrary constant  $K_I^\infty$  that characterizes the magnitude of the remote mode I loading

- 9.5.2.3. Consider a material point that is very close to the crack tip, and so is subjected to a very large stress. Write down the asymptotic stress field in this region, in terms of an arbitrary constant  $K_I^{tip}$  that characterizes the magnitude of the near tip stresses.
- 9.5.2.4. Using the path independence of the J integral, find a relationship between  $K_I^\infty$ ,  $K_I^{tip}$ , and the slopes  $E, H$  of the uniaxial stress-strain curve
- 9.5.2.5. Suppose that the material fractures when the stress at a small distance  $d$  ahead of the crack tip reaches a critical magnitude  $\sigma_0$ . Assume that the critical distance is much smaller than the region of high stress considered in 2.4. Calculate the critical value of  $K_I^\infty$  that will cause the crack to grow, in terms of relevant material parameters.
- 9.5.2.6. Consider a finite sized crack with length  $a$  in the hypoelastic material. Assume that the solid is subjected to a remote uniaxial stress far from the crack. Discuss qualitatively how the stress field around the crack evolves as the remote stress is increased. Discuss the implications of this behavior on the validity of the fracture criterion derived in 2.5.

## 9.6 Linear Elastic Fracture mechanics of interfaces

1. Calculate values for the elastic constants  $\alpha$ ,  $\beta$  and the crack tip singularity parameter  $\varepsilon$  for the following bi-material interfaces:
  - 1.1. Aluminum on glass
  - 1.2. A glass fiber in a PVC matrix
  - 1.3. Nickel on titanium carbide
  - 1.4. Copper on Silicon

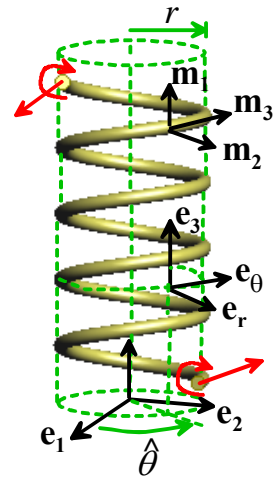
## 10. Approximate theories for solids with special shapes: rods, beams, membranes, plates and shells

### 10.1. Preliminaries: Dyadic notation for vectors and tensors

### 10.2. Motion and Deformation of slender rods

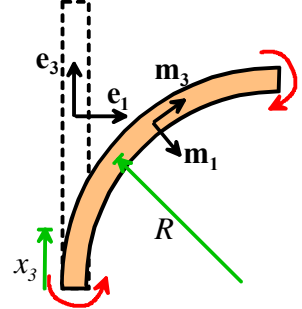
- 10.2.1. The figure shows an inextensible rod that is bent into a helical shape. The shape of the helix can be characterized by the radius  $r$  of the generating cylinder, and the number of turns  $n$  in the helix per unit axial length. Consider a point on the axis of the rod specified by the polar coordinates  $(r, \hat{\theta}, z)$ .

- 10.2.1.1. Write down an expression for  $z$  in terms of  $r$ ,  $n$  and  $\theta$ .
- 10.2.1.2. Write down the position vector of the point as components in the  $\{\mathbf{e}_1, \mathbf{e}_2, \mathbf{e}_3\}$  basis.
- 10.2.1.3. Calculate an expression for the unit vector  $\mathbf{m}_3$  that is tangent to the rod, in terms of the basis vectors  $\{\mathbf{e}_1, \mathbf{e}_2, \mathbf{e}_3\}$  and appropriate coordinates.
- 10.2.1.4. Assume that  $\mathbf{m}_2$  is perpendicular to the axis of the cylinder. Use this and the solution to 1.3 to find expressions for the basis vectors  $\mathbf{m}_1, \mathbf{m}_2$  in terms of  $\{\mathbf{e}_1, \mathbf{e}_2, \mathbf{e}_3\}$ .



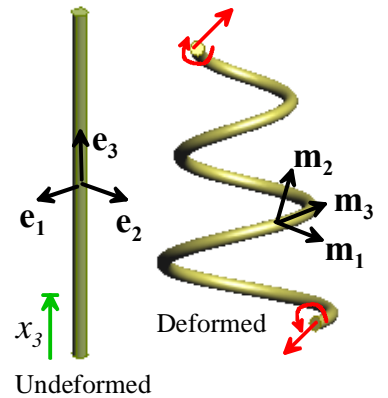
- 10.2.1.5. Calculate the normal and binormal vectors to the curve and hence deduce an expression for the torsion of the curve.
- 10.2.1.6. Deduce an expression for the curvature vector of the rod.
- 10.2.1.7. Suppose that the stress state in the deformed rod is a simple axial distribution  $\sigma \mathbf{m}_3 \otimes \mathbf{m}_3$ . Calculate the stress components in the  $\{\mathbf{e}_1, \mathbf{e}_2, \mathbf{e}_3\}$  basis.

10.2.2. An initially straight, inextensible slender bar with length  $L$  and circular cross-section with radius  $a$  is bent into a circle with radius  $R$  by terminal couples, as shown in the figure. Assume that cross-sections of the rod remain circles with radius  $a$  and remain transverse to the axis of the rod after deformation.



- 10.2.2.1. Write down an expression for the position vector  $\mathbf{r}(x_3)$  of a position vector on the axis of the deformed rod, expressing your answer as components in the  $\{\mathbf{e}_1, \mathbf{e}_2, \mathbf{e}_3\}$  basis
- 10.2.2.2. Find an expression for the basis vectors  $\{\mathbf{m}_1, \mathbf{m}_2, \mathbf{m}_3\}$  as a function of arc-length  $s$ , expressing each unit vector as components in  $\{\mathbf{e}_1, \mathbf{e}_2, \mathbf{e}_3\}$ . Hence find an expression for the orthogonal tensor  $\mathbf{R}$  that maps  $\{\mathbf{e}_1, \mathbf{e}_2, \mathbf{e}_3\}$  onto  $\{\mathbf{m}_1, \mathbf{m}_2, \mathbf{m}_3\}$ .
- 10.2.2.3. Write down the curvature vector for the deformed rod, and verify that
- $$\frac{d\mathbf{m}_1}{ds} = -\kappa_2 \mathbf{m}_3 + \kappa_3 \mathbf{m}_2 \quad \frac{d\mathbf{m}_2}{ds} = \kappa_1 \mathbf{m}_3 - \kappa_3 \mathbf{m}_1 \quad \frac{d\mathbf{m}_3}{ds} = -\kappa_1 \mathbf{m}_2 + \kappa_2 \mathbf{m}_1$$
- 10.2.2.4. Write down expressions for the deformation gradient in the rod, expressing your answer as both components in  $\{\mathbf{e}_1, \mathbf{e}_2, \mathbf{e}_3\}$  and  $\{\mathbf{m}_1, \mathbf{m}_2, \mathbf{m}_3\}$
- 10.2.2.5. Find an expression for the Lagrange strain tensor in the rod, expressing your answer as both components in  $\{\mathbf{e}_1, \mathbf{e}_2, \mathbf{e}_3\}$  and  $\{\mathbf{m}_1, \mathbf{m}_2, \mathbf{m}_3\}$ . Neglect second-order terms.
- 10.2.2.6. Hence deduce expressions for the Material stress and Cauchy stress in the rod.
- 10.2.2.7. Calculate the resultant internal moment and force acting on a generic internal cross-section of the rod.
- 10.2.2.8. Show that the internal moment satisfies the equations of equilibrium.

10.2.3. Consider a deformable rod, as shown in the figure. Let  $x_3$  denote the arc-length of a point on the axis un-deformed rod from some arbitrary origin, and let  $\psi$  denote the twist of the rod, as defined in Section 10.2.2. In addition, let  $\mathbf{r}(x_3)$  and  $\mathbf{v} = d\mathbf{r}/dt = v_i \mathbf{m}_i$  denote the position vector and velocity of this point on the deformed rod, let  $s$  denote its arc-length after deformation, and let  $\boldsymbol{\kappa} = \kappa_i \mathbf{m}_i$  denote the curvature vector of the rod, where  $\mathbf{m}_i$  are basis vectors aligned with the deformed rod as discussed in Section 10.2.2. Show that



- 10.2.3.1. The time derivative of a unit vector tangent to the rod can be computed as

$$\frac{d\mathbf{t}}{dt} \equiv \frac{d\mathbf{m}_3}{dt} = \frac{d}{ds} \left( \frac{d\mathbf{r}}{dt} \right) - \frac{d\mathbf{r}}{ds} \left[ \frac{d\mathbf{r}}{ds} \cdot \frac{d}{ds} \left( \frac{d\mathbf{r}}{dt} \right) \right] = \left( \frac{dv_1}{ds} - v_2 \kappa_3 + v_3 \kappa_2 \right) \mathbf{m}_1 + \left( \frac{dv_2}{ds} + v_1 \kappa_3 - v_3 \kappa_1 \right) \mathbf{m}_2$$

- 10.2.3.2. The time derivative of the rate of stretching of the rod's centerline is related to its velocity by

$$\frac{d}{dt} \left( \frac{ds}{dx_3} \right) = \mathbf{m}_3 \cdot \frac{ds}{dx_3} \frac{d}{ds} \left( \frac{d\mathbf{r}}{dt} \right) = \frac{ds}{dx_3} \left( \frac{dv_3}{ds} - v_1 \kappa_2 + v_2 \kappa_1 \right)$$

10.2.3.3. The angular velocity of the basis vectors can be calculated as

$$\boldsymbol{\omega} = \mathbf{m}_3 \times \frac{d\mathbf{v}}{ds} + \dot{\psi} \mathbf{m}_3 = - \left( \frac{dv_2}{ds} + v_1 \kappa_3 - v_3 \kappa_1 \right) \mathbf{m}_1 + \left( \frac{dv_1}{ds} - v_2 \kappa_3 + v_3 \kappa_2 \right) \mathbf{m}_2 + \dot{\psi} \mathbf{m}_3$$

10.2.3.4. The angular acceleration of the basis vectors can be calculated as

$$\boldsymbol{\alpha} = \frac{d\boldsymbol{\omega}}{dt} = \mathbf{m}_3 \times \frac{d\mathbf{a}}{ds} - 2 \left( \frac{d\mathbf{v}}{ds} \cdot \mathbf{m}_3 \right) \mathbf{m}_3 \times \frac{d\mathbf{v}}{ds} + \frac{d\psi}{dt} \left\{ \frac{d\mathbf{v}}{ds} - \left( \frac{d\mathbf{v}}{ds} \cdot \mathbf{m}_3 \right) \mathbf{m}_3 \right\} + \frac{d^2\psi}{dt^2} \mathbf{m}_3$$

### 10.3. Simplified versions of the general theory of deformable rods

#### 10.4. Exact solutions to problems involving slender rods

10.4.1. A slender, linear elastic rod has shear modulus  $\mu$  and an elliptical cross-section, as illustrated in the figure. It is subjected to equal and opposite axial couples with magnitude  $Q$  on its ends. Using the general theory of slender rods, and assuming that the rod remains straight:

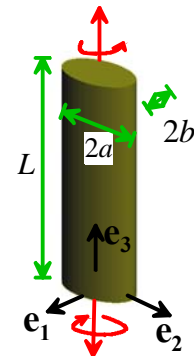
10.4.1.1. Write down the internal force and moment distribution in the rod

10.4.1.2. Calculate the twist per unit length of the shaft  $\psi$

10.4.1.3. Find an expression for the displacement field in the shaft

10.4.1.4. Find an expression for the stress distribution in the shaft

10.4.1.5. Find an expression for the critical couple  $Q$  that will cause the shaft to yield



10.4.2. A slender, linear elastic rod has shear modulus  $\mu$  and an equilateral triangular cross-section, as illustrated in the figure. It is subjected to equal and opposite axial couples with magnitude  $Q$  on its ends. Using the general theory of slender rods, and assuming that the rod remains straight:

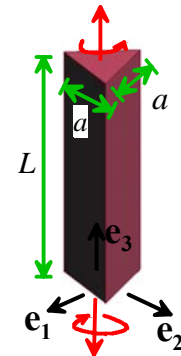
10.4.2.1. Write down the internal force and moment distribution in the rod

10.4.2.2. Calculate the twist per unit length of the shaft  $\psi$

10.4.2.3. Find an expression for the displacement field in the shaft

10.4.2.4. Find an expression for the stress distribution in the shaft

10.4.2.5. Find an expression for the critical couple  $Q$  that will cause the shaft to yield

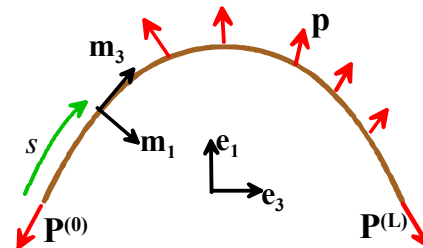


10.4.3. The figure shows a flexible cable, subjected to a transverse force per unit length  $\mathbf{p} = p_i \mathbf{m}_i$  and forces

$\mathbf{P}^{(0)} = P_i^{(0)} \mathbf{m}_i$  and  $\mathbf{P}^{(L)} = P_i^{(L)} \mathbf{m}_i$  acting at its ends. In a

flexible cable, the area moments of inertia can be neglected, so that the internal moments  $M_i \approx 0$ . In addition, the axial tension

$T_3 = \int_A \sigma_{33} dA$  is the only nonzero internal force. Show that

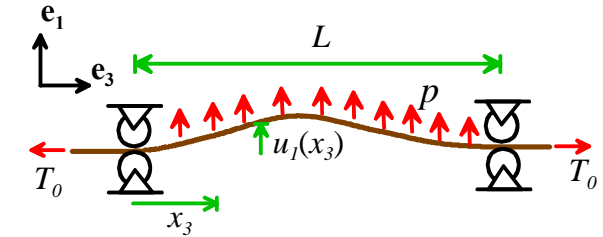


under these conditions the virtual work equation reduces to

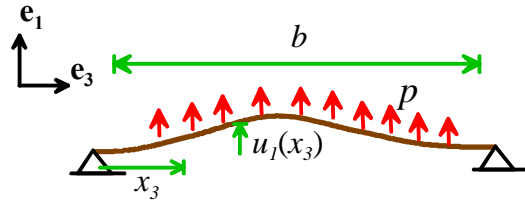
$$\int_0^{L_0} \frac{d\delta s}{dx_3} T_3 dx_3 + \int_0^L \rho A a_i \delta v_i ds - \int_0^L (p_i \delta v_i) ds - \left[ P_i^{(0)} \delta v_i \right]_{x_3=0} - \left[ P_i^{(L)} \delta v_i \right]_{x_3=L} = 0$$

where  $\delta v_i$  is the virtual velocity of the cable, and  $\delta \dot{s}$  is the corresponding rate of change of arc-length along the cable. Show that if the virtual work equation is satisfied for all  $\delta v_i$  and compatible  $\delta \dot{s}$ , the internal force and curvature of the cable must satisfy

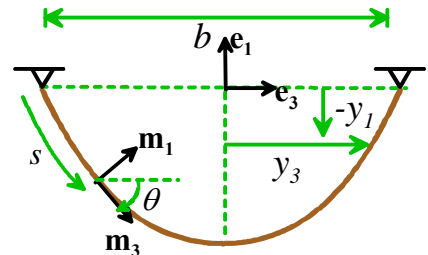
- 10.4.4. The figure shows a flexible string, which is supported at both ends and subjected to a tensile force  $T_0$ . The string is subjected to a uniform transverse for  $p$  per unit length. Calculate the deflection  $u_1(x_3)$  of the string, assuming small deflections.



- 10.4.5. The figure shows a flexible string with length  $L$ , which is pinned at both ends. The string is subjected to a uniform transverse for  $p$  per unit length. Calculate the deflection  $u_1(x_3)$  of the string, assuming small deflections.



- 10.4.6. The figure shows a flexible cable with length  $L$  and weight  $m$  per unit length hanging between two supports under uniform vertical gravitational loading. In a flexible cable, the area moments of inertia can be neglected, so that the internal moments  $M_i \approx 0$

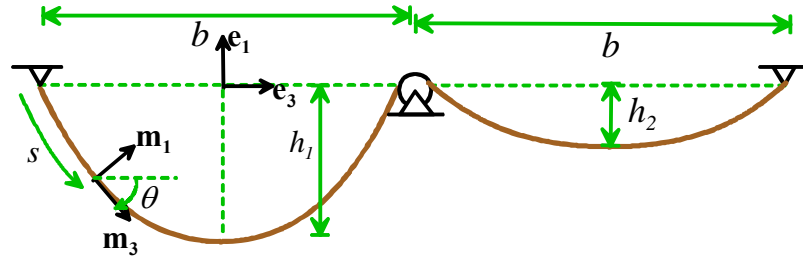


- 10.4.6.1. Write down the curvature vector of the cable in terms of the angle  $\theta(s)$  shown in the figure
- 10.4.6.2. Hence, show that the equations of equilibrium for the cable reduce to

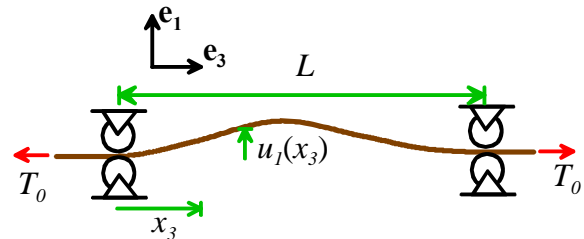
$$\frac{dT_3}{ds} + m \sin \theta = 0 \quad T_3 \frac{d\theta}{ds} + m \cos \theta = 0$$

- 10.4.6.3. Hence, show that  $T_3 \cos \theta = H$ , where  $H$  is a constant. Interpret the equation physically.
- 10.4.6.4. Deduce that  $w(y_3) = \tan \theta = -ms/H \Rightarrow dw/dy_3 = -m\sqrt{1+w^2}/H$
- 10.4.6.5. Hence, deduce that  $w(y_3) = dy_1/dy_3 = -\sinh(my_3/H)$  and calculate  $y_1$  as a function of  $y_3$
- 10.4.6.6. Finally, calculate the internal forces in the cable.
- 10.4.6.7. Show that, as  $L \rightarrow b$  the full solution approaches the small deflection solution calculated in Problem 5. Find the value of  $L/b$  for which the discrepancy between the full solution and the small deflection solution is 10%.

- 10.4.7. The figure shows an inextensible cable with weight per unit length  $m$ , and length  $2L$  that is pinned at both ends. The cable is supported by a frictionless pulley midway between the two ends. Find all the possible equilibrium values of the sags  $h_1, h_2$  of the cable. Display your results by plotting a graph showing the equilibrium values of  $h_1/b$  as a function of  $L/b$ . You will need to solve problem 6 before attempting this one.

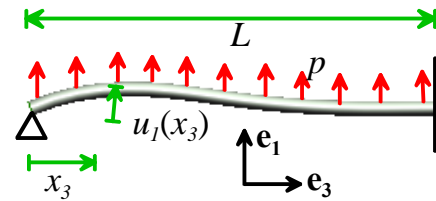


- 10.4.8. The figure shows a flexible string, which is supported at both ends and subjected to a tensile force  $T_0$ . The string has mass per unit length  $m$  and can be approximated as inextensible. Calculate the natural frequencies of vibration and the corresponding mode shapes, assuming small transverse deflections.

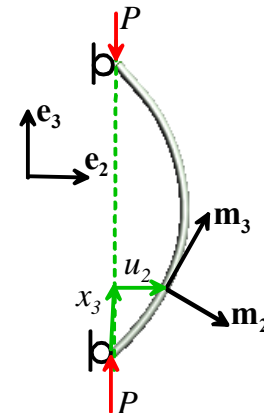


- 10.4.9. Estimate the fundamental frequency of vibration for the stretched string described in the preceding problem, using the Rayleigh-Ritz method. Use the approximation  $u_1(x_3) = Ax_3(L - x_3)$  for the mode shape. Compare the estimate with the exact solution derived in problem 8.2.11.

- 10.4.10. The figure shows an Euler-Bernoulli beam with Young's modulus  $E$ , area moments of inertia  $I_1, I_2$  and length  $L$ , which is clamped at  $x_3 = L$  and pinned at  $x_3 = 0$ . It is subjected to a uniform load  $p$  per unit length. Calculate the internal moment and shear force in the beam, and calculate the transverse deflection.

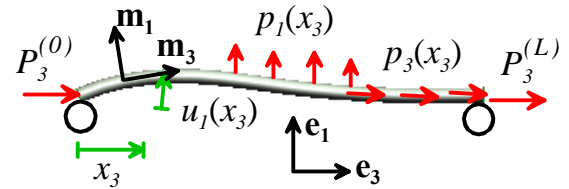


- 10.4.11. The figure shows an initially straight, inextensible elastic rod, with Young's modulus  $E$ , length  $L$  and principal in-plane moments of area  $I_1 = I_2 = I$ , which is subjected to end thrust. The ends of the rod are constrained to travel along a line that is parallel to the undeformed rod, but the ends are free to rotate. Use the small-deflection solution for beams subjected to significant axial force given in Section 10.3.3 to calculate the value of  $P$  required to hold the rod in equilibrium with a small nonzero deflection, and find an expression for the deflected shape. Compare the predicted deflection with the exact post-buckling solution given in Section 10.4.3.





10.4.12. The theory describing small-deflections of beams subjected to significant axial force given in Section 10.3.3 can be extended to obtain an approximate large deflection solution. Consider the beam shown in the figure. The beam has Young's modulus  $E$ , cross-sectional area  $A$ , and principal transverse moments of inertia  $I_1, I_2$ . The bar is subjected to load per unit



length  $\mathbf{p} = p_1 \mathbf{e}_1 + p_3 \mathbf{e}_3$ , and axial forces  $\mathbf{P}^{(0)} = P_3^{(0)} \mathbf{e}_3$ ,  $\mathbf{P}^{(L)} = P_3^{(L)} \mathbf{e}_3$  at its two ends. Assume that the displacement field can be described as  $\mathbf{u} = u_1(x_3) \mathbf{e}_1 + u_3(x_3) \mathbf{e}_3$ . Deformation measures are to be expanded up to second order in transverse deflection, so that

- The axial stretch can be approximated as

$$\frac{ds}{dx_3} \approx \left(1 + \frac{\partial u_3}{\partial x_3}\right) \sqrt{1 + \left(\frac{\partial u_1}{\partial x_3}\right)^2} \approx 1 + \frac{\partial u_3}{\partial x_3} + \frac{1}{2} \left(\frac{\partial u_1}{\partial x_3}\right)^2$$

- The curvature can be approximated as  $\boldsymbol{\kappa} \approx \frac{d^2 u_1}{dx_3^2} \mathbf{e}_2$

10.4.12.1. Show that the static equilibrium equations for the displacement components can be reduced to

$$EI_2 \frac{d^4 u_1}{dx_3^4} + EA \left( \frac{\partial u_3}{\partial x_3} + \frac{1}{2} \left( \frac{\partial u_1}{\partial x_3} \right)^2 \right) \frac{d^2 u_1}{dx_3^2} - p_3 \frac{du_1}{dx_3} + p_1 \left( 1 - \frac{1}{2} \left( \frac{\partial u_1}{\partial x_3} \right)^2 \right) = 0$$

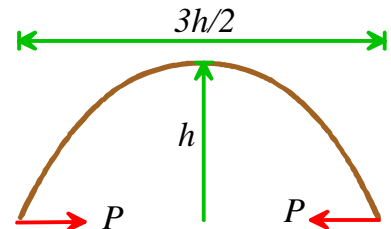
$$EA \frac{d}{dx_3} \left( \frac{\partial u_3}{\partial x_3} + \frac{1}{2} \left( \frac{\partial u_1}{\partial x_3} \right)^2 \right) + p_3 \left( 1 - \frac{1}{2} \left( \frac{\partial u_1}{\partial x_3} \right)^2 \right) = 0$$

and list the boundary conditions on the ends of the beam.

10.4.12.2. Solve the governing equations for the beam problem described in Problem 14. Compare the predicted deflection with the exact post-buckling solution given in Section 10.4.3, for the limiting case of an inextensible beam.

10.4.13. An initially straight tent-pole with Young's modulus  $E$  and hollow circular cross-section with external radius  $a$ , moment of inertia  $I$  is to be bent into an arc with height  $h$  and base  $3h/2$  as shown in the figure. Calculate expressions for

- 10.4.13.1. The force  $P$  required to bend the pole into shape
- 10.4.13.2. The total length of the pole
- 10.4.13.3. The maximum stress in the pole



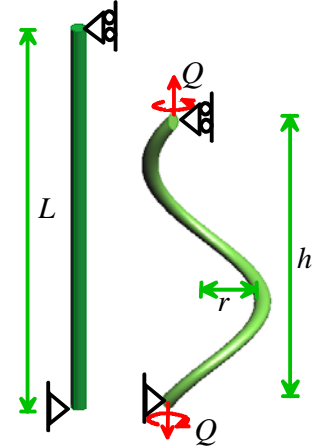


10.4.14. An initially straight, elastic rod with Young's modulus  $E$ , area moments of inertia  $I_1 = I_2 = I$  and axial effective inertia  $J_3$  is subjected to an axial couple  $\mathbf{Q} = Q\mathbf{e}_3$ , which remains fixed in direction as the rod deforms.

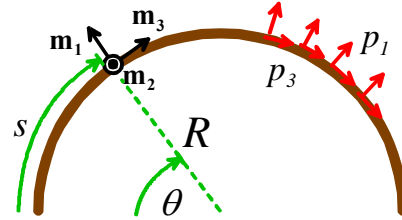
10.4.14.1. Show that the straight rod, with an appropriate twist is a possible equilibrium configuration for all values of  $Q$ , and calculate the value of twist

10.4.14.2. Show that, for a critical value of  $Q$ , the rod may adopt a helical shape, with one complete turn and arbitrary height  $h$  and radius  $r$ . Calculate the critical value of  $Q$

10.4.14.3. What can you infer about the stability of a straight rod subjected to end couples?



10.4.15. The figure shows a rod, which is a circular arc with radius  $R$  in its stress free configuration, and is subjected to load per unit length  $\mathbf{p} = p_1\mathbf{m}_1 + p_3\mathbf{m}_3$  and forces  $\mathbf{P}^{(0)}$ ,  $\mathbf{P}^{(L)}$  on its ends that cause a small change in its shape. In this problem, we shall neglect out-of-plane deformation and twisting of the rod, for simplicity. Let  $\bar{s} = R\theta$  denote the arc length measured along the undeformed rod, and let  $\mathbf{u} = u_1(\theta)\mathbf{m}_1 + u_3(\theta)\mathbf{m}_3$  the displacement of the rod's centerline.



10.4.15.1. Note that approximate expressions for the resulting (small) change in arc length and curvature of the rod can be calculated using the time derivatives given in Section 10.2.3. Hence, show that

- The derivative of the change in arc-length of the deformed rod is  $\frac{d\delta s}{d\bar{s}} = \frac{1}{R} \left( \frac{du_3}{d\theta} + u_1(\theta) \right)$
- The change in curvature vector is  $\delta\boldsymbol{\kappa} = \frac{1}{R^2} \left( \frac{d^2 u_1}{d\theta^2} - \frac{du_3}{d\theta} \right) \mathbf{m}_2$

10.4.15.2. The geometric terms in the equilibrium equations listed in Section 10.2.9 can be approximated using the geometry of the undeformed rod. Show that internal forces  $\mathbf{T} = T_1\mathbf{m}_1 + T_3\mathbf{m}_3$  and internal moment  $\mathbf{M} = M_2\mathbf{m}_2$  must satisfy the following static equilibrium equations

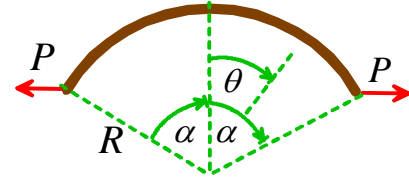
$$\frac{dT_1}{d\theta} - T_3 + R p_1 = 0 \quad \frac{dT_3}{d\theta} + T_1 + R p_3 = 0 \quad \frac{dM_2}{d\theta} + R T_1 = 0$$

10.4.15.3. Assume that the rod is elastic, with Young's modulus  $E$  and area moment of inertia  $I_1 = I_2 = I$ , and can be idealized as inextensible. Show that under these conditions the axial displacement  $u_3$  must satisfy

$$\frac{EI}{R^4} \left( \frac{d^6 u_3}{d\theta^6} + 2 \frac{d^4 u_3}{d\theta^4} + \frac{d^2 u_3}{d\theta^2} \right) + \frac{dp_1}{d\theta} + p_3 = 0$$

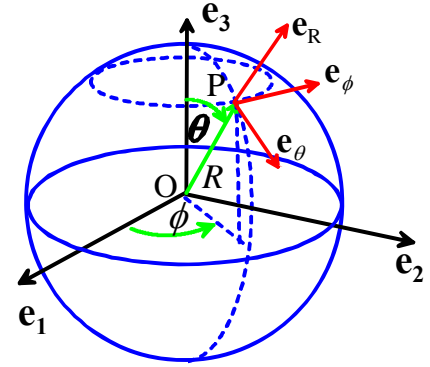
and write down expressions for the boundary conditions at the ends of the rod.

- 10.4.15.4. As a particular example, consider a rod which is a semicircular arc between  $\theta = \pm\alpha$ , subjected to equal and opposite forces acting on its ends, as shown in the figure. Assume that the displacement and rotation of the rod vanish at  $\theta = 0$ , for simplicity. Calculate  $u_1(\theta)$  and  $u_3(\theta)$  for the rod.



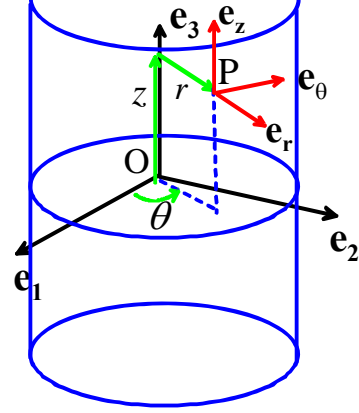
## 10.5. Motion and Deformation of thin shells

- 10.5.1. A spherical-polar coordinate system is to be used to describe the deformation of a spherical shell with radius  $R$ . The two angles  $(\phi, \theta)$  illustrated in the figure are to be used as the coordinate system  $(\xi_1, \xi_2)$  for this geometry.



- 10.5.1.1. Write down the position vector  $\bar{\mathbf{r}}$  in terms of  $(\phi, \theta)$ , expressing your answer as components in the basis  $\{\mathbf{e}_1, \mathbf{e}_2, \mathbf{e}_3\}$  shown in the figure.
- 10.5.1.2. Calculate the covariant basis vectors  $(\bar{\mathbf{m}}_1, \bar{\mathbf{m}}_2, \bar{\mathbf{m}}_3)$  in terms of  $\{\mathbf{e}_1, \mathbf{e}_2, \mathbf{e}_3\}$  and  $(\phi, \theta)$
- 10.5.1.3. Calculate the contravariant basis vectors  $(\bar{\mathbf{m}}^1, \bar{\mathbf{m}}^2, \bar{\mathbf{m}}^3)$  in terms of  $\{\mathbf{e}_1, \mathbf{e}_2, \mathbf{e}_3\}$  and  $(\phi, \theta)$
- 10.5.1.4. Calculate the covariant, contravariant and mixed components of the metric tensor  $\bar{\mathbf{g}}$
- 10.5.1.5. Calculate the covariant, contravariant and mixed components of the curvature tensor  $\bar{\mathbf{\kappa}}$  for the shell
- 10.5.1.6. Find the components of the Christoffel symbol  $\Gamma_{\alpha\beta}^i$  for the coordinate system
- 10.5.1.7. Suppose that under loading the shell simply expands radially to a new radius  $r$ . Find the components of the mid-plane Lagrange strain tensor
- $$\boldsymbol{\gamma} = \gamma_{\alpha\beta} \bar{\mathbf{m}}^\alpha \otimes \bar{\mathbf{m}}^\beta = \frac{1}{2} (g_{\alpha\beta} - \bar{g}_{\alpha\beta}) \bar{\mathbf{m}}^\alpha \otimes \bar{\mathbf{m}}^\beta$$
- and the components of the curvature change tensor  $\Delta\boldsymbol{\kappa} = (\kappa_\beta^\alpha - \bar{\kappa}_\beta^\alpha) g_{\lambda\alpha} \bar{\mathbf{m}}^\lambda \otimes \bar{\mathbf{m}}^\beta$
- 10.5.1.8. Suppose that the shell is elastic, with Young's modulus  $E$  and Poisson's ratio  $\nu$ . Calculate the contravariant components of the internal force  $T^{\alpha\beta}$  and internal moment  $M^{\alpha\beta}$
- 10.5.1.9. Find the physical components of the internal force and moment, expressing your answer as components in the spherical-polar basis of unit vectors  $\{\mathbf{e}_R, \mathbf{e}_\theta, \mathbf{e}_\phi\}$

10.5.2. A cylindrical-polar coordinate system is to be used to describe the deformation of a cylindrical shell with radius  $r$ . The angles and axial distance  $(\theta, z)$  illustrated in the figure are to be used as the coordinate system  $(\xi_1, \xi_2)$  for this geometry.



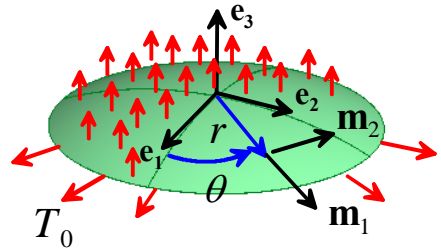
- 10.5.2.1. Write down the position vector  $\bar{\mathbf{r}}$  in terms of  $(\theta, z)$ , expressing your answer as components in the basis  $\{\mathbf{e}_1, \mathbf{e}_2, \mathbf{e}_3\}$  shown in the figure.
- 10.5.2.2. Calculate the covariant basis vectors  $(\bar{\mathbf{m}}_1, \bar{\mathbf{m}}_2, \bar{\mathbf{m}}_3)$  in terms of  $\{\mathbf{e}_1, \mathbf{e}_2, \mathbf{e}_3\}$  and  $(\theta, z)$
- 10.5.2.3. Calculate the contravariant basis vectors  $(\bar{\mathbf{m}}^1, \bar{\mathbf{m}}^2, \bar{\mathbf{m}}^3)$  in terms of  $\{\mathbf{e}_1, \mathbf{e}_2, \mathbf{e}_3\}$  and  $(\theta, z)$
- 10.5.2.4. Calculate the covariant, contravariant and mixed components of the metric tensor  $\bar{\mathbf{g}}$
- 10.5.2.5. Calculate the covariant, contravariant and mixed components of the curvature tensor  $\bar{\mathbf{\kappa}}$  for the shell
- 10.5.2.6. Find the components of the Christoffel symbol  $\bar{\Gamma}_{\alpha\beta}^i$  for the undeformed shell
- 10.5.2.7. Suppose that under loading the shell simply expands radially to a new radius  $\rho$ , without axial stretch. Find the covariant components of the mid-plane Lagrange strain tensor  $\gamma$  and the covariant components of the curvature change tensor  $\Delta\mathbf{\kappa}$
- 10.5.2.8. Suppose that the shell is elastic, with Young's modulus  $E$  and Poisson's ratio  $\nu$ . Calculate the contravariant components of the internal force  $T^{\alpha\beta}$  and internal moment  $M^{\alpha\beta}$ .
- 10.5.2.9. Find the physical components of the internal force and moment, expressing your answer as components in the spherical-polar basis of unit vectors  $\{\mathbf{e}_r, \mathbf{e}_\theta, \mathbf{e}_z\}$

10.5.3. The figure illustrates a triangular plate, whose geometry can be described by two vectors  $\mathbf{a}$  and  $\mathbf{b}$  parallel to two sides of the triangle. The position vector of a point is to be characterized using a coordinate system  $(\xi_1, \xi_2)$  by setting  $\bar{\mathbf{r}} = \xi_1\mathbf{a} + \xi_2\mathbf{b}$  where  $0 \leq \xi_1 \leq 1$ ,  $0 \leq \xi_2 \leq 1$ .

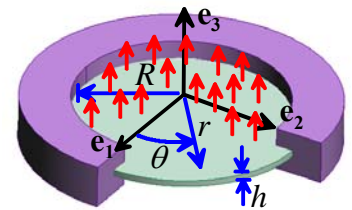
- 10.5.3.1. Calculate the covariant basis vectors  $(\bar{\mathbf{m}}_1, \bar{\mathbf{m}}_2, \bar{\mathbf{m}}_3)$  in terms of  $\mathbf{a}$  and  $\mathbf{b}$
- 10.5.3.2. Calculate the contravariant basis vectors  $(\bar{\mathbf{m}}^1, \bar{\mathbf{m}}^2, \bar{\mathbf{m}}^3)$  in terms of  $\mathbf{a}$  and  $\mathbf{b}$
- 10.5.3.3. Calculate the covariant, contravariant and mixed components of the metric tensor  $\bar{\mathbf{g}}$
- 10.5.3.4. Suppose that the plate is subjected to a homogeneous deformation, so that after deformation its sides lie parallel to vectors  $\mathbf{c}$  and  $\mathbf{d}$ . Find the mid-plane Lagrange strain tensor 
$$\gamma = \gamma_{\alpha\beta} \bar{\mathbf{m}}^\alpha \otimes \bar{\mathbf{m}}^\beta = \frac{1}{2} (g_{\alpha\beta} - \bar{g}_{\alpha\beta}) \bar{\mathbf{m}}^\alpha \otimes \bar{\mathbf{m}}^\beta$$
, in terms of  $\mathbf{a}, \mathbf{b}, \mathbf{c}$  and  $\mathbf{d}$
- 10.5.3.5. Suppose that the plate is elastic, with Young's modulus  $E$  and Poisson's ratio  $\nu$ . Calculate the contravariant components of the internal force  $T^{\alpha\beta}$

- 10.5.4. The figure illustrates a triangular plate. The position points in the plate is to be characterized using the height  $z$  and angle  $\theta$  as the coordinate system  $(\xi_1, \xi_2)$ .
- 10.5.4.1. Calculate the covariant basis vectors  $(\bar{\mathbf{m}}_1, \bar{\mathbf{m}}_2, \bar{\mathbf{m}}_3)$  expressing your answer as components in the basis  $\{\mathbf{e}_1, \mathbf{e}_2, \mathbf{e}_3\}$  shown in the figure.
- 10.5.4.2. Calculate the contravariant basis vectors  $(\bar{\mathbf{m}}^1, \bar{\mathbf{m}}^2, \bar{\mathbf{m}}^3)$  as components in  $\{\mathbf{e}_1, \mathbf{e}_2, \mathbf{e}_3\}$
- 10.5.4.3. Calculate the covariant, contravariant and mixed components of the metric tensor  $\bar{\mathbf{g}}$
- 10.5.4.4. Find the components of the Christoffel symbol  $\bar{\Gamma}_{\alpha\beta}^i$  for the undeformed plate
- 10.5.4.5. Suppose that the plate is subjected to a homogeneous deformation, so that the position vector of a point that lies at  $(z, \theta)$  in the undeformed shell has position vector  $\mathbf{r} = z \tan(\theta + \alpha) \mathbf{e}_1 + z \mathbf{e}_2$  after deformation Find the mid-plane Lagrange strain tensor  $\gamma = \gamma_{\alpha\beta} \bar{\mathbf{m}}^\alpha \otimes \bar{\mathbf{m}}^\beta$ , in terms of  $z, \theta, \alpha$
- 10.5.4.6. Suppose that the plate is elastic, with Young's modulus  $E$  and Poisson's ratio  $\nu$ . Calculate the contravariant components of the internal force  $T^{\alpha\beta}$
- 10.5.4.7. Find the physical components of the internal force  $\mathbf{T}$  as components in the  $\{\mathbf{e}_1, \mathbf{e}_2, \mathbf{e}_3\}$  basis.

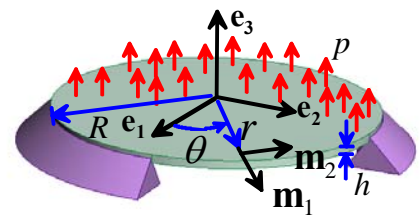
- 10.5.5. A thin circular membrane with radius  $R$  is subjected to in-plane boundary loading that induces a uniform biaxial membrane tension with magnitude  $T_0$ . Vertical displacement of the membrane is prevented at  $r = R$ . The membrane is subjected to a uniform out-of-plane pressure with magnitude  $p$  on its surface. Calculate the displacement field in the membrane, assuming small deflections. This problem can be solved quite easily using Cartesian coordinates.



- 10.5.6. The figure shows a thin circular plate with thickness  $h$ , Young's modulus  $E$  and Poisson's ratio  $\nu$ . The edge of the plate is clamped, and its surface is subjected to a uniform out-of-plane pressure with magnitude  $p$ . Calculate the displacement field and internal moment and shear force in the plate, assuming small deflections. This problem can easily be solved using Cartesian coordinates.



- 10.5.7. The figure shows a thin circular plate with thickness  $h$ , mass density  $\rho$ , Young's modulus  $E$  and Poisson's ratio  $\nu$  that is simply supported at its edge and is subjected to a pressure distribution acting perpendicular to its surface. The goal of this problem is to derive the equations governing the transverse deflection of the plate in terms of the cylindrical-polar coordinate  $(r, \theta)$  system shown in the figure.



- 10.5.7.1. Write down the position vector of a point on the mid-plane of the undeformed plate in terms of

$(r, \theta)$ , expressing your answer as components in the  $\{\mathbf{e}_1, \mathbf{e}_2, \mathbf{e}_3\}$  basis.

10.5.7.2. Calculate the basis vectors  $(\bar{\mathbf{m}}_1, \bar{\mathbf{m}}_2, \bar{\mathbf{m}}_3)$  and  $(\bar{\mathbf{m}}^1, \bar{\mathbf{m}}^2, \bar{\mathbf{m}}^3)$ , expressing your answer as components in the basis  $\{\mathbf{e}_1, \mathbf{e}_2, \mathbf{e}_3\}$  shown in the figure.

10.5.7.3. Find the components of the Christoffel symbol  $\bar{\Gamma}_{\alpha\beta}^i$  for the undeformed plate;

10.5.7.4. Calculate the contravariant components of the metric tensor  $\bar{\mathbf{g}}$

10.5.7.5. Find the basis vectors  $(\mathbf{m}_1, \mathbf{m}_2, \mathbf{m}_3)$  for the deformed plate, neglecting terms of order  $(\partial u_3 / \partial r)^2, (\partial u_3 / \partial \theta)^2$ , etc

10.5.7.6. Show that the curvature tensor has components

$$\kappa_{11} = -\frac{\partial^2 u_3}{\partial r^2} \quad \kappa_{12} = \kappa_{21} = \frac{1}{r} \frac{\partial u_3}{\partial \theta} - \frac{\partial^2 u_3}{\partial r \partial \theta} \quad \kappa_{22} = -r \frac{\partial u_3}{\partial r} - \frac{\partial^2 u_3}{\partial \theta^2}$$

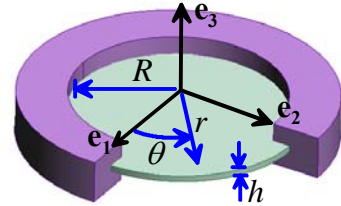
10.5.7.7. Express the internal moments  $M^{\alpha\beta}$  in the plate in terms of  $E, \nu$  and  $u_3$  and its derivatives.

10.5.7.8. Write down the equations of motion for the plate in terms of  $M^{\alpha\beta}$  and  $V^\alpha$

10.5.7.9. Hence, show that the transverse displacement must satisfy the following governing equation

$$\frac{Eh^3}{12(1-\nu^2)} \left( \frac{\partial^2}{\partial r^2} + \frac{1}{r} \frac{\partial}{\partial r} + \frac{1}{r^2} \frac{\partial^2}{\partial \theta^2} \right) \left( \frac{\partial^2 u_3}{\partial r^2} + \frac{1}{r} \frac{\partial u_3}{\partial r} + \frac{1}{r^2} \frac{\partial^2 u_3}{\partial \theta^2} \right) + \rho h \frac{\partial^2 u_3}{\partial t^2} = p_3$$

10.5.8. The figure shows a circular elastic plate with Young's modulus  $E$ , Poissons ratio  $\nu$ . The plate has thickness  $h$  and radius  $R$ , and is clamped at its edge. The goal of this problem is to calculate the mode shapes and natural frequencies of vibration of the plate.



10.5.8.1. Show that the general solution to the equation of motion for the freely vibrating plate is given by

$$u_3(r, \theta) = \left( A J_n(k_{(m,n)} r) \sin(n\theta + \theta_0) + B Y_n(k_{(m,n)} r) \sin(n\theta + \theta_1) \right. \\ \left. + C I_n(k_{(m,n)} r) \sin(n\theta + \theta_2) + B K_n(k_{(m,n)} r) \sin(n\theta + \theta_3) \right) \cos(\omega_{(m,n)} t + \phi)$$

where  $A, B, C, D, \phi, \theta_0, \dots, \theta_3$  are arbitrary constants,  $J_n, Y_n$  are Bessel functions of the first and second kinds, and  $I_n, K_n$  are modified Bessel functions of the first and second kinds, with order  $n$ , while  $k_{(m,n)}$  and  $\omega_{(m,n)}$  are a wave number and vibration frequency that are related by

$$k_{(m,n)}^2 = \omega_{(m,n)} \sqrt{12(1-\nu) \rho / Eh^2}$$

10.5.8.2. Show that most general solution with bounded displacements at  $r=0$  has the form

$$u_3(r, \theta) = \left( \left[ A_1 J_n(k_{(m,n)} r) + B_1 I_n(k_{(m,n)} r) \right] \sin(n\theta) \right. \\ \left. + \left[ A_2 J_n(k_{(m,n)} r) + B_2 I_n(k_{(m,n)} r) \right] \cos(n\theta) \right) \cos(\omega_{(m,n)} t + \phi)$$

- 10.5.8.3. Write down the boundary conditions for  $u_3$  at  $r=R$ , and hence show that the wave numbers  $k_{(m,n)}$  are roots of the equation

$$J_n(k_{(m,n)}R)I_{n+1}(k_{(m,n)}R) + I_n(k_{(m,n)}R)J_{n+1}(k_{(m,n)}R) = 0$$

- 10.5.8.4. Show that the corresponding mode shapes are given by

$$U_{(m,n)}(r, \theta) = A \left[ I_n(k_{(m,n)}R)J_n(k_{(m,n)}r) - J_n(k_{(m,n)}R)I_n(k_{(m,n)}r) \right] \sin(n\theta + \theta_1)$$

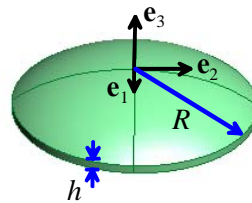
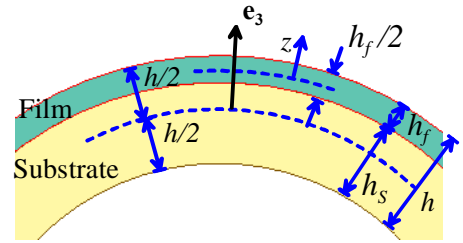
- 10.5.8.5. Calculate  $k_{(m,n)}$  for  $0 < n < 3$ ,  $1 < m < 3$  and tabulate your results. Compare the solution to the corresponding membrane problem solved in Section 10.7.2.
- 10.5.8.6. Plot contours showing the mode shapes for the modes with the lowest four frequencies.

- 10.5.9. Repeat the preceding problem for a plate with a simply supported edge. You should find that the wave numbers  $k_{(m,n)}$  are the roots of the equation

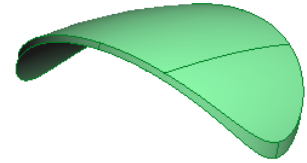
$$(1 - \nu) \left[ k_{(m,n)} R J_n(k_{(m,n)}R) I_{n+1}(k_{(m,n)}R) + I_n(k_{(m,n)}R) J_{n+1}(k_{(m,n)}R) \right] - 2 \left( k_{(m,n)} R \right)^2 I_n(k_{(m,n)}R) J_n(k_{(m,n)}R) = 0$$

Calculate the natural frequencies for  $\nu = 0.3$ .

- 10.5.10. A thin film with thickness  $h_f$  is deposited on the surface of a circular wafer with radius  $R$  and thickness  $h$ . Both film and substrate have Young's modulus  $E$ , and Poisson's ratio  $\nu$ . An inelastic strain  $\varepsilon_{11}^p = \varepsilon_{22}^p = \varepsilon_0$  is introduced into the film by some external process (e.g. thermal expansion), which generates stresses in the film, and also causes the substrate to bend. In Section 10.7.3, expressions were derived relating the substrate curvature to the mismatch strain in the film. These expressions are only valid if the substrate curvature is small. For mismatch strains, the wafer buckles, as shown in the figure. The goal of this problem is to estimate the critical value of mismatch strain that will cause the wafer to buckle.



Deformed shape for low mismatch



Deformed shape for high mismatch

- 10.5.10.1. Assume that the displacement of the mid-plane of the wafer-film system is

$$u_3 = \kappa_1 x_1^2 / 2 + \kappa_2 x_2^2 / 2 \quad u_1 = A_1 x_1 + A_2 x_1^3 + A_3 x_1 x_2^2 \quad u_2 = B_1 x_1 + B_2 x_2^3 + B_3 x_2 x_1^2$$

Calculate the distribution of strain in the film and substrate, and hence deduce the total strain energy density of the system. It is best to do this calculation using a symbolic manipulation program.

- 10.5.10.2. Calculate the values of  $A_i, B_i$  that minimize the potential energy of the plate, and hence show that the two curvatures satisfy

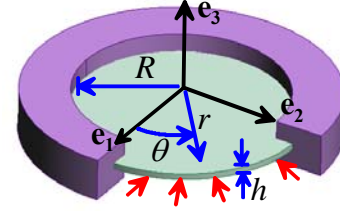
$$\kappa_1 \kappa_2^2 (1 - \nu^2) R^4 + 16 h^2 \kappa_1 + 16 h^2 \nu \kappa_2 - C \varepsilon_0 = 0$$

$$\kappa_2 \kappa_1^2 (1 - \nu^2) R^4 + 16 h^2 \kappa_2 + 16 h^2 \nu \kappa_1 - C \varepsilon_0 = 0$$

and find a formula for the constant  $C$ .

- 10.5.10.3. Hence, plot a graph showing the equilibrium values of the normalized curvature  $\kappa_1 R^2 \sqrt{1+\nu}/(4h)$  as a function of a suitably normalized measure of mismatch strain, for a Poisson's ratio  $\nu = 0.3$ .

- 10.5.11. The figure shows an elastic plate with Young's modulus  $E$ , Poisson's ratio  $\nu$  and thermal expansion coefficient  $\alpha$ . The plate is circular, with radius  $R$  and its edge is clamped. The plate is initially stress free and is then heated to raise its temperature by  $\Delta T$ , inducing a uniform internal force  $T_{\alpha\beta} = -Eh\alpha\Delta T\delta_{\alpha\beta}/(1-\nu)$  in the plate. The goal of this problem is to calculate the critical temperature that will cause the plate to buckle, using the governing equations listed in Section 10.6.2.



- 10.5.11.1. Assume an axially symmetric buckling mode, so that

$u_3 = w(r)$  with  $r = \sqrt{x_\alpha x_\alpha}$ . Show that  $w$  satisfies the governing equation

$$\frac{Eh^3}{12(1-\nu^2)} \left( \frac{d^4 w}{dr^4} + \frac{2}{r} \frac{d^3 w}{dr^3} - \frac{1}{r^2} \frac{d^2 w}{dr^2} + \frac{1}{r^3} \frac{dw}{dr} \right) + \frac{Eh\alpha\Delta T}{(1-\nu)} \left( \frac{\partial^2 w}{\partial r^2} + \frac{1}{r} \frac{\partial w}{\partial r} \right) = 0$$

- 10.5.11.2. Show that the general solution to this equation is

$$w(r) = A + B \log(r) + C J_0(k_n r) + D Y_0(k_n r)$$

where  $A, B, C, D$ , are arbitrary constants,  $J_0, Y_0$  are Bessel functions of the first and second kind of order zero, and  $k_n$  is the wave number for the  $n$ th buckling mode. Find an expression for  $k_n$  in terms of  $\Delta T$  and relevant geometric and material properties.

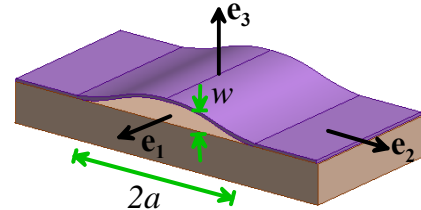
- 10.5.11.3. Show that the wave number  $k_n$  satisfies  $J_1(k_n R) = 0$ , and deduce an expression for the critical temperature change at which the plate can first buckle.
- 10.5.11.4. Plot the buckling mode associated with this temperature.

- 10.5.12. Repeat the preceding problem for a plate with a simply supported edge. You should find that the wave numbers  $k_n$  are the roots of the equation

$$(1-\nu)J_1(k_n R) - k_n R J_0(k_n R) = 0$$

Calculate the critical buckling temperature and plot the corresponding buckling mode for  $\nu = 0.3$ .

- 10.5.13. The interface between a thin film and its substrate contains a tunnel crack with length  $2a$ . The film is initially stress free, then heated to raise its temperature by  $\Delta T$ , inducing a uniform biaxial stress field  $\sigma_{\alpha\beta} = -E\alpha\Delta T\delta_{\alpha\beta}/(1-\nu)$  in the film. At a critical temperature, the film buckles as shown in the figure. For  $R \gg h$  the buckled film can be modeled as a plate with clamped edge. The goal of this problem is to calculate the critical temperature required to cause the film to buckle, and to calculate the crack tip energy release rate as the buckled film delaminates from the substrate. Assume that the displacement of the mid-plane of the film has the form  $\mathbf{u} = u(x_2)\mathbf{e}_2 + w(x_2)\mathbf{e}_3$ , and use the Von-Karman plate bending theory of Section 10.6.3.





10.5.13.1. Write down expressions for the mid-plane strain  $\gamma_{\alpha\beta}$  and the curvature change tensor  $\Delta\kappa_{\alpha\beta}$  for the film in terms of  $u$  and  $w$ , and hence find a formula for the internal force  $T_{\alpha\beta}$  and moment  $M_{\alpha\beta}$  in terms of  $u$ ,  $w$ ,  $\Delta T$  and material properties.

10.5.13.2. Hence, show that the equations of equilibrium in terms of  $u$  and  $w$  reduce to

$$\frac{dT_{22}}{dx_2} = 0 \quad \frac{d^4w}{dx_2^4} - \frac{12(1-\nu^2)}{Eh^3} T_{22} \frac{d^2w}{dx_2^2} = 0 \quad T_{22} = \frac{Eh}{12(1-\nu^2)} \left[ -(1+\nu)\alpha\Delta T + \frac{du}{dx_2} + \frac{1}{2} \left( \frac{dw}{dx_2} \right)^2 \right]$$

10.5.13.3. Assume that  $w = dw/dx_2 = 0$  at  $x_2 = \mp a$ . Hence, calculate the smallest value of  $T_{22}$  for which a solution with nonzero  $w$  exists.

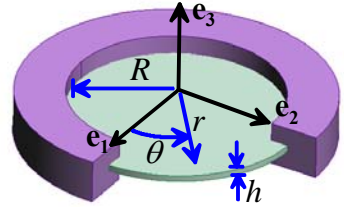
10.5.13.4. Deduce an expression for the critical temperature required to cause the film to buckle

10.5.13.5. Assume that  $\Delta T$  exceeds the critical value. Calculate the resulting displacement field

10.5.13.6. Hence calculate the decrease in energy of the film during the buckling

10.5.13.7. Use the preceding result to deduce the crack tip energy release rate during delamination.

10.5.14. Consider a thin circular plate with thickness  $h$ , Young's modulus  $E$ , Poisson's ratio  $\nu$  and thermal expansion coefficient  $\alpha$ . Let  $(r, \theta)$  be a cylindrical-polar coordinate system and let  $\{\mathbf{e}_r, \mathbf{e}_\theta, \mathbf{e}_z\}$  be a triad of unit vectors parallel to the natural (covariant) basis vectors for the coordinate system. Assume that the deformation of the plate is axially symmetric, so that the displacement field can be expressed as  $\mathbf{u} = u(r)\mathbf{e}_r + w(r)\mathbf{e}_z$ . Show that the Von-Karman equations governing the motion of the plate can be reduced to the following form



10.5.14.1. Mid-plane strain-deflection relation  $\gamma_{rr} = \frac{du}{dr} + \frac{1}{2} \left( \frac{dw}{dr} \right)^2$   $\gamma_{\theta\theta} = \frac{u}{r}$

10.5.14.2. Displacement-curvature relation  $\Delta\kappa_{rr} = -\frac{d^2w}{dr^2}$   $\Delta\kappa_{\theta\theta} = -\frac{1}{r} \frac{dw}{dr}$

10.5.14.3. Membrane stress-strain relation  $T_{rr} = \frac{Eh}{(1-\nu^2)} (\gamma_{rr} + \nu\gamma_{\theta\theta})$   $T_{\theta\theta} = \frac{Eh}{(1-\nu^2)} (\gamma_{\theta\theta} + \nu\gamma_{rr})$

10.5.14.4. Moment-curvature relations

$$M_{rr} = \frac{Eh^3}{12(1-\nu^2)} (\Delta\kappa_{rr} + \nu\Delta\kappa_{\theta\theta}) \quad M_{\theta\theta} = \frac{Eh^3}{12(1-\nu^2)} (\Delta\kappa_{\theta\theta} + \nu\Delta\kappa_{rr})$$

10.5.14.5. Equations of motion

$$\frac{dT_{rr}}{dr} + \frac{1}{r}(T_{rr} - T_{\theta\theta}) = \rho h \frac{d^2u}{dt^2} \quad \frac{dM_{rr}}{dr} + \frac{1}{r}(M_{rr} - M_{\theta\theta}) - V_r = 0$$

$$\frac{dV_r}{dr} + \frac{V_r}{r} - T_{rr}\Delta\kappa_{rr} - T_{\theta\theta}\Delta\kappa_{\theta\theta} + p_3 = \rho h \frac{d^2w}{dt^2}$$

10.5.15. The Von-Karman equations for a circular plate cannot be solved analytically, even for the case of axially symmetric deformations. However, it is very straightforward to set up a simple spreadsheet to calculate the potential energy of the plate, and find a numerical solution by using the spreadsheet's solver function to minimize the potential energy. To this end, consider a circular plate with radius  $R$ ,



thickness  $h$ , Young's modulus  $E$ , Poisson's ratio  $\nu$  and thermal expansion coefficient  $\alpha$ . Assume that the plate is initially stress free, and is then heated to increase its temperature uniformly by  $\Delta T$ . At the same time, the surface of the plate is subjected to a uniform pressure  $p$  acting perpendicular to its surface. Assume that the deformation of the plate is axially symmetric, so that the displacement field can be expressed as  $\mathbf{u} = u(r)\mathbf{e}_r + w(r)\mathbf{e}_z$ .

10.5.15.1. Show that the potential energy of the plate can be expressed as

$$U = \frac{\pi E h}{(1-\nu^2)} \left\{ \int_0^R \left( (\gamma_{rr} - \alpha \Delta T)^2 + (\gamma_{\theta\theta} - \alpha \Delta T)^2 + 2\nu(\gamma_{\theta\theta} - \alpha \Delta T)(\gamma_{rr} - \alpha \Delta T) \right) r dr \right. \\ \left. + \frac{h^2}{12} \int_0^R \left( \Delta \kappa_{rr}^2 + \Delta \kappa_{\theta\theta}^2 + 2\nu \Delta \kappa_{rr} \Delta \kappa_{\theta\theta} \right) r dr \right\} - 2\pi p \int_0^R w(r) r dr$$

where  $\gamma_{rr}, \gamma_{\theta\theta}$  and  $\Delta \kappa_{rr}, \Delta \kappa_{\theta\theta}$  are related to the displacements by the equations listed in the preceding problem.

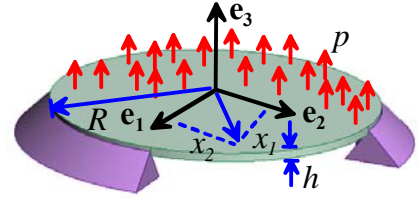
10.5.15.2. To obtain a numerical solution, let  $r_i = i\Delta r$ ,  $u_i, w_i$ , with  $i=0, 1, 2, \dots, N$  and  $\Delta r = R/N$ , denote the position and displacements of a set of  $N+1$  equally spaced points along a radius of the disk. The derivatives of  $u$  and  $w$  can be approximated using simple difference formulas. For example, define  $u'_i \approx du/dr = (u_i - u_{i-1})/\Delta r$ ,  $w'_i \approx dw/dr = (w_i - w_{i-1})/(r_i - r_{i-1})$ ,  $i=1, 2, \dots, N$  to be the derivatives of  $u$  and  $w$  at  $r = (r_i + r_{i-1})/2$ ; similarly, approximate the second derivative of  $w$  as  $w''_i \approx d^2w/dr^2 = (w'_{i+1} - w'_i)/\Delta r$  at each  $i=1, 2, \dots, N-1$ . The value of  $d^2w/dr^2$  at  $r=R$  can be estimated by extrapolation as  $w''_N \approx (2w''_{N-1} - w''_N)$ . The integrals in the expression for the potential energy can be evaluated using a simple piecewise-constant approximation (or if you prefer piecewise linear) to the integrand. Use this approach to set up an EXCEL spreadsheet to calculate the total potential energy of the plate. You should find  $N=40$  sufficient for most practical purposes.

10.5.15.3. Check your spreadsheet by calculating the potential energy of a heated flat plate with  $w = u = 0$ , and compare the prediction with the exact solution.

10.5.15.4. The deflection of the plate under loading can be calculated by using the solver feature of EXCEL to determine the values of  $u_i$  and  $w_i$  that minimize the potential energy. To test your spreadsheet, use it to calculate the deflection of a circular plate with thickness  $h/R=0.02$ , with a clamped boundary, which is subjected to a pressure  $pR^3(1-\nu^2)/Eh^3 = 0.0025$ . You will need to enforce the clamped boundary condition using a constraint. You can set  $w'_N = 0$  but you will find that this makes the plate slightly too stiff. A better result is obtained by extrapolating the slope of the plate to  $r=R$  based on the slope of the last two segments, and enforcing the constraint  $(3w'_N - w'_{N-1})/2 = 0$ . Show that, for this pressure, the numerical solution agrees with the predictions of the exact small-deflection solution.

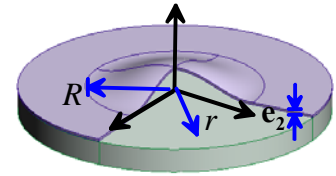
10.5.15.5. Show that if the deflection of the center of the plate is comparable to the plate thickness, the small deflection solution predicts deflections that are substantially greater than the numerical solution of the Von-Karman equations. This is because the in-plane strains begin to significantly stiffen the plate. Plot a graph showing the deflection of the center of the plate (normalized by plate thickness) as a function of normalized pressure  $pR^3(1-\nu^2)/Eh^3$ .

10.5.16. Use the spreadsheet developed in Problem 10.5.15 to calculate the deflection of a flat circular plate elastic plate with simply supported boundary that subjected to uniform pressure on its surface. Use  $h/R=0.02$  and  $\nu=0.3$ . Plot a graph showing the deflection of the center of the plate (normalized by plate thickness) as a function of the dimensionless pressure  $pR^3(1-\nu^2)/Eh^3$ . Show that, for small pressures, the



numerical solution agrees with the exact (small deflection) solution given in Section 10.7.1. The discrepancy for large strains is due to the constraining effect of the in-plane strains induced by the transverse deflection.

10.5.17. The interface between a thin film and its substrate contains a circular crack with radius  $R$ . The film has Young's modulus  $E$ , Poisson's ratio  $\nu$  and thermal expansion coefficient  $\alpha$ . The substrate can be idealized as rigid. The film is initially stress free, then heated to raise its temperature by  $\Delta T$ , inducing a uniform biaxial stress field  $\sigma_{\alpha\beta} = -E\alpha\Delta T\delta_{\alpha\beta}/(1-\nu)$  in the film. At a critical temperature, the film buckles as shown in the figure. For  $R \gg h$  the buckled film can be modeled as a plate with clamped edge, so that the critical buckling temperature is given by the solution to problem 9. When the film buckles, some of the strain energy in the film is relaxed. This relaxation in energy can cause the film to delaminate from the substrate.



For  $R \gg h$  the buckled film can be modeled as a plate with clamped edge, so that the critical buckling temperature is given by the solution to problem 9. When the film buckles, some of the strain energy in the film is relaxed. This relaxation in energy can cause the film to delaminate from the substrate.

10.5.17.1. Show that the change in strain energy of the system during the formation of the buckle can be expressed in dimensionless form by defining dimensionless measures of displacement, position and strain as

$$\hat{u} = u / R\sqrt{\alpha\Delta T} \quad \hat{w} = w / R \quad \hat{r} = r\sqrt{\alpha\Delta T} / R$$

$$\hat{\gamma}_{rr} = \frac{d\hat{u}}{d\hat{r}} + \frac{1}{2} \left( \frac{d\hat{w}}{d\hat{r}} \right)^2 \quad \hat{\gamma}_{\theta\theta} = \frac{\hat{u}}{\hat{r}} \quad \Delta\hat{\kappa}_{rr} = -\frac{d^2\hat{w}}{d\hat{r}^2} \quad \Delta\hat{\kappa}_{\theta\theta} = -\frac{1}{\hat{r}} \frac{d\hat{w}}{d\hat{r}}$$

so that

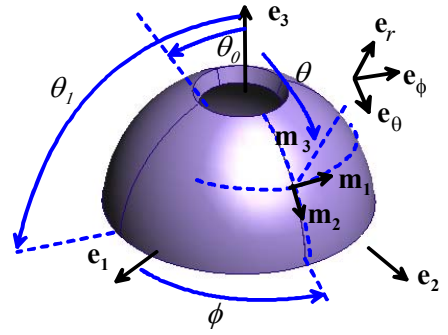
$$\frac{(1+\nu)\Delta U}{U_0} = -\int_0^1 \left( \hat{\gamma}_{rr}^2 + \hat{\gamma}_{\theta\theta}^2 + 2\nu\hat{\gamma}_{rr}\hat{\gamma}_{\theta\theta} + \frac{\beta^2}{12} \left[ \Delta\hat{\kappa}_{rr}^2 + \Delta\hat{\kappa}_{\theta\theta}^2 + 2\nu\Delta\hat{\kappa}_{rr}\Delta\hat{\kappa}_{\theta\theta} \right] \right) \xi d\xi + 2 \int_0^1 \left( \hat{\gamma}_{rr} + \hat{\gamma}_{\theta\theta} \right) \xi d\xi$$

where  $\beta = h / R\sqrt{\alpha\Delta T}$  and  $U_0 = \pi R^2 h E (\alpha\Delta T)^2 / (1-\nu)$  is the total strain energy of the circular portion of the film before buckling.

10.5.17.2. The implication of 10.5.17.1 is that the change in strain energy (and hence the normalized displacement field which minimizes the potential energy) is a function only of Poisson's ratio  $\nu$  and the dimensionless parameter  $\beta$ . Use the spreadsheet developed in problem 10.5.15 to plot a graph showing  $(1+\nu)\Delta U / U_0$  as a function of  $\beta$  for a film with  $\nu=0.3$ . Verify that the critical value of  $\beta$  corresponding to  $\Delta U = 0$  is consistent with the solution to problem 9.

10.5.17.3. Find an expression for the crack tip energy release rate  $G = -(\partial\Delta U / \partial R) / (2\pi R)$  and the dimensionless function  $(1+\nu)\Delta U / U_0 = f(\beta, \nu)$ . Hence, use the results of 10.5.17.2 to plot a graph showing the crack tip energy release rate (suitably normalized) as a function of  $\beta$ , for a film with  $\nu=0.3$ .

- 10.5.18. The figure shows a thin-walled, spherical dome with radius  $R$ , thickness  $h$  and mass density  $\rho$ . The dome is open at its top, so that the shell is bounded by spherical polar angles  $\theta_0 < \theta < \theta_1$ . Calculate the internal forces induced by gravitational loading of the structure, using the membrane theory of shells in Section 10.7.7.



- 10.5.19. The figure shows a thin-walled conical shell with thickness  $h$  and mass density  $\rho$ . Calculate the internal forces induced by gravitational loading of the structure, using the membrane theory of shells in Section 10.7.7. Use the cylindrical-polar coordinates  $(z, \theta)$  as the coordinate system.

